

# Plastic Catalytic Degradation Study of the role of external catalytic surface, Catalytic Reusability and Temperature Effects

By

**Toju S. Kpere-Daibo**

**April 2009**

**A Thesis submitted for the degree of Doctor of Philosophy of  
the University of London**

Department of Chemical Engineering

University College London,

London, WC1E 7JE

# Abstract

Technological advancements over the last century have lead large and continuous growth in the output of plastic materials. This exponential growth has created public concern over the environmental impact caused by the polymeric waste produced. These have acted as driving forces for a lot of current research aimed at the development of plastic recycle processes. As a result, the conversion of plastic waste to useful products is gaining increasing attention.

The aim of this work was to study aspects of polymer catalytic degradation using zeolite based catalysts. More specifically the study focused on identifying the role of the external catalytic surface on overall polymer decomposition reactions, the reusability of the catalysts as well as temperature and acidity effects.

The first stage of this investigation aimed to explore the premise behind the assumption that polymer catalytic degradation takes place initially on the external catalytic surface by selectively poisoning the external sites of a zeolite catalyst (ZSM-5). Degradation results in a semi-batch reactor as well as thermogravimetric analysis demonstrated that the activity of poisoned catalyst samples was indeed lower than that of fresh catalyst.

The next stage of the study involved an investigation of the extent of catalytic reusability of four zeolite catalysts - HZSM-5, USY and two commercial cracking catalysts containing 20 % and 40 % USY respectively. While the performance of USY showed deterioration with each cycle, ZSM-5 and both commercial cracking catalysts retained consistent levels of activity that enabled full polymer conversion in each cycle.

Finally, the temperature effect on catalytic reactions was studied as well as the effect of catalyst acidity. While temperature effects were not conclusive regarding selectivity towards gas or liquid products prompting the suggestion of further work using a continuous flow reactor system, the formation of liquid products showed a maximum with the acidity content.

# Acknowledgements

I wish to thank my supervisor, Dr George Manos, all his patience and guidance throughout the entire course of this work. His contribution to my academic progress is immensely significant.

The many sacrifices made by all members of my family, particularly my Mum and Dad cannot be overemphasised enough. I am so grateful for all the love and support you have given me throughout this period. I am especially grateful for the unfaltering belief and confidence you held in me. And the constant prayers and encouragement you continue to give me.

I would also like to acknowledge the support from my friends and would like to thank you all for your devotion and loyalty towards me. I would like to say that even when you haven't known it you have all been there for me and given me that extra support when I have needed it at difficult moments.

Finally I am thankful to God for all his blessings and for everything bestowed upon me.

# Dedication

*Dedicated to the loving memory of my wonderful sister Mojirin*

# Table of Contents

---

<b>Abstract</b> .....	2
<b>List of Figures</b> .....	10
<b>List of Tables</b> .....	14
<b>Chapter One</b> .....	<b>15</b>
<b>Introduction</b> .....	15
1.1 Background .....	15
1.2 Motivations and Objectives of this Work .....	16
1.3 Outline of this Thesis .....	17
<b>Chapter Two</b> .....	<b>19</b>
<b>Literature Survey</b> .....	19
2.1 Plastics .....	19
2.2 Basics of Polymers.....	21
2.2.1 Polyethylene (PE) .....	21
2.2.2 Polypropylene (PP) .....	22
2.2.3 The plastic-linear low-density polyethylene (LLDPE).....	22
2.3 Classification of Plastic Recycling .....	22
2.3.1 Primary recycling.....	23
2.3.2 Secondary Recycling .....	24
2.3.3 Tertiary Recycling .....	24
2.3.4 Quaternary Recycling .....	25
2.4 Thermal and Catalytic Degradation .....	25

2.5 Mechanism of the Degradation Process.....	28
2.5.1 Mechanism of Polymer Thermal Degradation.....	29
2.5.2 Mechanism of Catalytic Cracking Reactions.....	30
2.5.2.1 Cracking of a Carbon-Carbon Bond .....	32
2.5.2.2 Isomerization.....	32
2.5.2.3 Hydrogen Transfer .....	33
2.6 Past Work Involving Methods of Recycling Plastic Waste .....	34
2.7 Catalysis .....	37
2.7.1 Basics of Catalysis .....	37
2.7.2 Different Types of Catalysts .....	39
2.8 Zeolite based catalysts .....	40
2.8.1 Silicalite and ZSM-5 .....	43
2.8.2 Ultrastable Y Zeolite (US-Y).....	45
2.8.3 Commercial Cracking Catalysts .....	46
2.8.4 Secondary Reactions and Over-Cracking .....	48
2.9 Silylation (Poisoning) .....	50
2.10 Temperature Programme Desorption (TPD) .....	52
2.11 Thermo-Gravimetric Analysis (TGA) .....	54
2.12 Deactivation of Catalysts by Coking .....	55
<b>Chapter Three .....</b>	<b>57</b>
<b>Experimental .....</b>	<b>57</b>
3.1 Introduction.....	57
3.2 Materials .....	58
3.3 Semi Batch Reactor.....	59
3.3.1 Equipment .....	59

3.3.2 Experimental procedure .....	60
3.3.3 Experimental Calculations .....	64
3.3.4 Boiling Point Distribution.....	67
3.4 Thermo-gravimetric Analysis Equipment (TGA).....	72
3.5 Temperature Programmed Desorption (TPD) .....	73
3.6 Chemical Liquid Deposition (CLD) .....	74
<b>Chapter Four .....</b>	<b>75</b>
<b>Role of external sites on catalytic polymer degradation performance.....</b>	<b>75</b>
4.1 Introduction.....	75
4.2 Acid Site Distribution of Poisoned Samples / TPD .....	77
4.3. Thermo-Gravimetric Analysis (TGA) experiments.....	80
4.4. Semi batch experiments results.....	82
4.5 Conclusion .....	90
<b>Chapter Five .....</b>	<b>92</b>
<b>Catalyst Deactivation and Reusability .....</b>	<b>92</b>
5.1 Introduction.....	92
5.1.1 US-Y Catalyst .....	93
5.1.2. Cracking catalyst 1 (20 % US-Y catalyst) .....	96
5.1.3. Commercial Cracking Catalyst 2 (40 % US-Y) Catalyst.....	98
5.1.4. HZSM-5 Catalyst .....	101
5.2 Discussion .....	103
5.3 Conclusion .....	105
<b>Chapter Six.....</b>	<b>106</b>
<b>Temperature Effects .....</b>	<b>106</b>
6.1 Introduction.....	106

6.2 Experiment results discussion.....	107
6.3 Boiling point distribution of liquid yield .....	110
6.4 Conclusion .....	114
<b>Chapter Seven .....</b>	<b>115</b>
<b>Effect of Polymer to Catalyst Ratio.....</b>	<b>115</b>
7.1 Introduction.....	115
7.2 Basic Experiments .....	117
7.2.1 Experiment 1 .....	117
7.2.2 Experiments 2 and 3.....	120
7.3 Experiments involving mixtures of US-Y and 3-A-zeolite .....	122
7.3.1 Results of Single Experiments .....	122
7.3.2 Discussion of Results regarding US-Y-Acidity of the Catalyst.....	130
7.3.2.1 Conversions / Yields over Different Acidities.....	131
7.3.2.2 Boiling Point Distributions over Different Acidities .....	136
7.4 Conclusions.....	142
<b>Chapter Eight .....</b>	<b>143</b>
<b>Conclusion and Directions for Future Work.....</b>	<b>143</b>
8.1 Conclusions.....	143
8.1.1 Role of external sites on degradation.....	143
8.1.2 Catalytic reusability .....	144
8.1.3 Effect of Polymer and Catalyst Ratio .....	144
8.2 General Conclusions .....	145
8.3 Future Work.....	145
8.2.1 Experimental Work.....	145
<b>Bibliography .....</b>	<b>147</b>



**Nomenclature .....157**

# List of Figures

---

<i>Figure 1: Post-consumer Plastic Waste for different sectors.....</i>	<i>20</i>
<i>Figure 2: Activation Energy of Chemical Reaction with and without a Catalyst .....</i>	<i>26</i>
<i>Figure 3: The building blocks of zeolites: a) silicate and b) aluminate tetrahedron ...</i>	<i>42</i>
<i>Figure 4: 3-D tetrahedral forming a cage-like zeolite structure.....</i>	<i>42</i>
<i>Figure 5: A 3-D representation of the zeolite catalyst with a clear illustration of the active cavity structure. ....</i>	<i>43</i>
<i>Figure 6: A 3-D representation of the two types of interconnecting pores of ZSM-5 sinusoidal (running horizontally) and straight. ....</i>	<i>44</i>
<i>Figure 7: Picture depiction of channel system in a zeolite catalyst .....</i>	<i>51</i>
<i>Figure 8: Diagrammatic illustration of mechanics of TPD system.....</i>	<i>52</i>
<i>Figure 9: Data graph of TPD experiment illustrating desorption of CO.....</i>	<i>53</i>
<i>Figure 10: Schematic representation of experimental semi-batch reactor set-up. (MFC): mass flow controller, (TC &amp; TR): thermocouples for the controller and reactor respectively.....</i>	<i>59</i>
<i>Figure 11: Photograph of the top and bottom halves of Glass Reactor section with its nitrogen inlet and product outlet. The thermocouples for the controller and the reactor are also displayed. ....</i>	<i>60</i>
<i>Figure 12: A typical temperature profile of both controller and the semi-batch reactor .....</i>	<i>61</i>
<i>Figure 13: Boiling point distribution for liquid products produced during degradation of lldPE over a ZSM-5 catalyst.....</i>	<i>71</i>
<i>Figure 14: Scheme of the thermo-gravimetric analyser .....</i>	<i>72</i>
<i>Figure 15 NH<sub>3</sub>-TPD of fresh and poisoned HZSM-5 catalyst .....</i>	<i>78</i>
<i>Figure 16 DTBPy-TPD of fresh and poisoned MFI-90 (HZSM-5 catalyst) .....</i>	<i>78</i>
<i>Figure 17: TGA results of lldPE degradation over Fresh HZSM-5, 3x-poisoned HZSM-5 and in the absence of any catalyst.....</i>	<i>80</i>
<i>Figure 18: TGA results of hdPE degradation over Fresh HZSM-5, 3x-poisoned HZSM-5 and in the absence of any catalyst. ....</i>	<i>81</i>

<i>Figure 19 Temperature against time chart of both the reactor and controller for catalytic degradation of lldPE with HZSM-5 catalyst.....</i>	<i>82</i>
<i>Figure 20 Reactor and controller temperature profiles during catalytic degradation of lldPE with ZSM-5 catalyst using two different controller set points (<math>T_{max} = 725K</math> and <math>T_{max} = 673K</math>.....</i>	<i>83</i>
<i>Figure 21 Conversion against time during catalytic degradation of lldPE using set point temperature T-max 725K.....</i>	<i>86</i>
<i>Figure 22 Yield against time during catalytic degradation of lldPE using set point temperature T-max 725K.....</i>	<i>86</i>
<i>Figure 23 Conversion graph versus time at lldPE at lower T max. ....</i>	<i>89</i>
<i>Figure 24 Yield graph versus time for catalytic degradation of lldPE at lower T max with HZSM-5 catalyst .....</i>	<i>89</i>
<i>Figure 25: Conversion over US-Y catalyst samples (fresh and deactivated) against time during catalytic cracking of lldPE.....</i>	<i>94</i>
<i>Figure 26: Liquid Yield for US-Y Catalyst samples (fresh and deactivated) against time during catalytic degradation of lldPE .....</i>	<i>94</i>
<i>Figure 27: Boiling point distribution of liquid product formed during cracking of lldPE with US-Y catalyst over successive experimental runs.....</i>	<i>96</i>
<i>Figure 28: Conversion over Cracking Catalyst 1 (20% US-Y samples (fresh and deactivated)) against time during catalytic degradation of lldPE.....</i>	<i>97</i>
<i>Figure 29: Cumulative liquid yield over Cracking Catalyst 1 (20 % US-Y Catalyst) fresh and deactivated samples against time during catalytic degradation of lldPE .....</i>	<i>97</i>
<i>Figure 30: Boiling point distribution for Cracking Catalyst 1 (20 % US-Y), fresh and deactivated. ....</i>	<i>98</i>
<i>Figure 31: Conversion over cracking catalyst 2 (40 % US-Y), fresh and deactivated samples against time during catalytic degradation of lldPE.....</i>	<i>99</i>
<i>Figure 32: Cumulative liquid yield over Cracking Catalyst 2 (40 % US-Y fresh and deactivated samples) against time during catalytic degradation of lldPE.....</i>	<i>100</i>
<i>Figure 33: Boiling point distribution curves for Cracking Catalyst 2 (40 % US-Y)..</i>	<i>101</i>
<i>Figure 34: Conversion HZSM-5 Catalyst samples of fresh and deactivated against time during catalytic degradation of lldPE. ....</i>	<i>102</i>
<i>Figure 35: Cumulative liquid yield over HZSM-5 catalyst samples fresh and deactivated against time during catalytic degradation of lldPE .....</i>	<i>102</i>

<i>Figure 36: Boiling point distribution curves for HZSM-5 catalyst samples .....</i>	<i>103</i>
<i>Figure 37: Reactor temperature against time at different controller set-point temperatures. ....</i>	<i>107</i>
<i>Figure 38: Reactor Temperature against time at different heating rates (Final controller set-point temperature: 713 K).....</i>	<i>108</i>
<i>Figure 39: Time profiles of cumulative liquid yield during degradation of lldPE over US-Y at different controller temperature set points (heating rate = 20 K/min). .</i>	<i>109</i>
<i>Figure 40: Cumulative liquid yield as a function of reaction temperature during catalytic degradation of lldPE at different heating rates. (Final temperature – 713 K).....</i>	<i>110</i>
<i>Figure 41: Boiling point distribution of liquid products formed between 2.5 – 7.5 minutes (condenser 1), during catalytic degradation of lldPE over US-Y for all final set point temperatures .....</i>	<i>111</i>
<i>Figure 42: Boiling point distribution of liquid products formed between 7.5 – 12.5 minutes (condenser 2) during the catalytic degradation of lldPE over US-Y for all final set point temperatures .....</i>	<i>112</i>
<i>Figure 43: Boiling point distribution of liquid products formed between 12.5 – 17.5 minutes (condenser 3) during catalytic degradation of lldPE for all final set point temperatures .....</i>	<i>113</i>
<i>Figure 44: Average boiling point distribution of liquid products formed during catalytic degradation of lldPE over US-Y at different heating rates.....</i>	<i>113</i>
<i>Figure 45: Gas Yield, Liquid Yield and Temperature Profile of Experiment 1. Polymer: lldPE, Catalyst: US-Y, ratio: 2:1(mass ratio).....</i>	<i>118</i>
<i>Figure 46: Boiling Point Distribution: Composition of the Liquid Yield of Experiment 1. Polymer: lldPE, Catalyst: US-Y, Ratio: 2:1 .....</i>	<i>119</i>
<i>Figure 47: Gas Yield, Liquid Yield and Temperature Profile of Experiment 2. Polymer: lldPE, no Catalyst .....</i>	<i>121</i>
<i>Figure 48: Gas Yield, Liquid Yield and Temperature Profile of Experiment 3. Polymer: lldPE; zeolite: inactive 3-A- zeolite .....</i>	<i>122</i>
<i>Figure 49: Gas Yield, Liquid Yield and Temperature Profile of Experiment 4. Polymer: lldPE; zeolite: 0.5 g of US-Y, 0.5 g of 3-A-zeolite .....</i>	<i>123</i>
<i>Figure 50: Boiling Point Distribution: Composition of the Liquid Yield of Experiment 4. Polymer: lldPE; zeolite: US-Y, 3-A; Ratio: 2 : 0.5 : 0.5 .....</i>	<i>124</i>

<i>Figure 51: Gas Yield, Liquid Yield and Temperature Profile of Experiment 5.</i>	
<i>Polymer: lldPE, zeolite: 0.25 g of US-Y, 0.75 g of 3-A-zeolite.....</i>	<i>125</i>
<i>Figure 52: Boiling Point Distribution: Composition of the Liquid Yield of Experiment 5. Polymer: lldPE; zeolite: US-Y, 3-A; Ratio: 2 : 0.25 : 0.75 .....</i>	<i>126</i>
<i>Figure 53: Gas Yield, Liquid Yield and Temperature Profile of experiment 6. 2 g lldPE, 0.1g of US-Y, 0.9g of inactive 3-A-zeolite.....</i>	<i>127</i>
<i>Figure 54: Boiling Point Distribution: Composition of Liquid Yield of Experiment 6. Polymer: lldPE; zeolites: US-Y, 3-A-zeolite; Ratio: 2: 0.1: 0.9.....</i>	<i>128</i>
<i>M,Figure 55: Gas Yield, Liquid Yield and Temperature Profile of experiment 7. Polymer: lldPE; zeolites: 50 Vol.-% (=0.5 g) of US-Y, 50 Vol.-% (=1.125 g) of 3-A .....</i>	<i>129</i>
<i>Figure 56: Temperature Curves vs. Time of Experiments 1,4,5,6.....</i>	<i>131</i>
<i>Figure 57: Cumulative Gas Yields vs. US-Y-Acidity divided by different Heating Steps. ....</i>	<i>133</i>
<i>Figure 58: Cumulative Liquid Yields vs. US-Y-Acidity divided by different Heating intervals.....</i>	<i>135</i>
<i>Figure 59: Overall liquid yield vs. Acidity content of catalytic degradations of lldPE via 1<sup>st</sup> Cracking catalysts 1 (according to [Gobin K. et al (2001)]) and 2<sup>nd</sup> US-Y / 3-A zeolite mixtures.....</i>	<i>136</i>
<i>Figure 60: Overall Averaged Boiling Point Distribution: Compositions of the Liquid Yields of Experiments 1, 4, 5, 6. Polymer: lldPE; different ratios of zeolites ....</i>	<i>137</i>
<i>Figure 61: Averaged Boiling Point Distribution of 1<sup>st</sup> and 2<sup>nd</sup> Condensers: Compositions of the Liquid Yields of Experiments 1, 4, 5, 6. Polymer: lldPE; different ratios of zeolite .....</i>	<i>139</i>
<i>Figure 62: Averaged Boiling Point Distribution of 3<sup>rd</sup> and 4<sup>th</sup> Condensers: Compositions of the Liquid Yields of Experiments 1, 4, 5, 6. Polymer: lldPE; different ratios of zeolites.....</i>	<i>140</i>
<i>Figure 63: Share of different product ranges and gas yield against US-Y percentage of catalyst for experiments 1,4,5,6. ....</i>	<i>141</i>

# List of Tables

---

<b>Table 1: Operating conditions of the GC for liquid sample analysis</b> .....	63
<b>Table 2: Boiling Point Distribution Groups</b> .....	68
<b>Table 3: Boiling Point Distribution of a real sample</b> .....	70
<b>Table 4: Mass Fraction of liquid products</b> .....	84
<b>Table 5: Conversion, liquid yield, liquid selectivity, coke yield for catalytic degradation of lldPE with ZSM-5 at standard T max 725K</b> .....	84
<b>Table 6: Mass Fraction of liquid products at lower T-max of 673K</b> .....	88
<b>Table 7: Conversion, liquid yield, liquid selectivity, coke yield for catalytic degradation of lldPE with HZSM-5 at lower T max 673K</b> .....	88
<b>Table 8: US-Y Catalyst Results</b> .....	93
<b>Table 9: Cracking Catalyst 1 (20 % US-Y) Results</b> .....	96
<b>Table 10: Cracking Catalyst 2 (40 % US-Y) Results</b> .....	99
<b>Table 11: HZSM-5 Catalyst Results</b> .....	101
<b>Table 12: Overview of experimental conditions and participating substances for all experiments</b> .....	116
<b>Table 13: Summary of Results regarding Yield, Conversion, and Selectivity</b> ....	117

# Chapter One

## Introduction

---

*In this chapter, a general background to polymers and its degradation is given. Applications, advances and the effects and influence of global trends in environmental policy with regards to polymer recycle are described. The overall structure of this thesis is given along with my motivation for this work.*

### 1.1 Background

Polymers make up a high proportion of the global solid waste both in volume and range. There has been an exponential increase in the rate of polymer production resulting in a similar increase in plastic waste over recent decades. Like most other technological advancements, polymers were initially utilised empirically with limitations in the understanding of the relationships between their properties and structure. Their non-biodegradable properties and wide variety of applications worldwide make it accessible and an influential component in virtually all works of life. This also makes it subject to extreme scrutiny as an environment pollutant with rapid increase in plastic waste in the second half of the 20<sup>th</sup> century leading to serious environmental problems.

According to figures released by the Association of Plastics Manufacturers in Europe [APME Report (1999)], in 1998, the post consumer plastic waste amounted to 35 million tonnes in Europe. This was generated from agricultural, automotive,

construction, distribution and domestic applications. The vast majority of post consumer plastic waste is land filled or incinerated and on average 7 % is recycled to produce low-grade plastics [www.dti.gov.uk]. Although land filling is regarded as environmentally acceptable the sheer volumes of current and projected plastic waste make it unfeasible because landfill spaces are getting scarce and thus increasingly too expensive. The incineration of plastics is another alternative but because combustion of plastics releases toxic gases, it leads to severe environmental pollution. Mechanical reprocessing of used plastics to form new products is not suitable simply because the new products tend to be of lower quality [Liedner J et.al].

Among the various plastic recycling methods, thermal and/or thermal catalytic degradation of plastic waste to gas and liquid products, which can be utilised as fuels or chemicals are the most promising techniques for development into viable commercial recycling process [Manos G. et al., 2000a].

In ordinary thermal degradation there is an absence of a catalyst. The polymer recycling process is subject to very high temperatures and the polymer's macromolecular structure is broken to smaller molecules. The wide product distribution and the high temperatures employed in such a process makes thermal catalytic degradation a more favourable solution to the problem of plastic waste [Manos G. et al., (2000a and 2000b), Seoud S.H Ng. Et al., (1995), Shabtai J. et al., (1997), Arandes J. et al.,(1997), Arguado J. et al., (1997)].

The recycling method pertinent to this study involves thermal catalytic degradation of plastic waste to reusable gas and liquid fuel products. This is because lower temperatures are employed and the products formed are of a higher quality and narrower distribution. This should thus eliminate the need of further product upgrading. [Manos G. et al., 2000a].

.

## 1.2 Motivations and Objectives of this Work

From an academic point of view, the inherently complex nature of polymer waste and recycle due to incessant political and environmental legislation regulations make it a very interesting and challenging problem with global implications.

As a result, alternatives to the traditional procedures of incineration and land filling of waste polymers are being undertaken in this study with the application of catalytic



degradation. Polymer degradation with the application of zeolite-based catalysts is predicted to have tremendous future potential as a viable and environmentally friendly commercial recycle process. This is due to the fact that in comparison to conventional degradation methods, catalytic degradation significantly reduces degradation temperature while producing high quality hydrocarbons in the range of motor engine fuels eliminating the necessity for further processing. This work primarily aims to investigate the effect of liquid product yield, product distribution and overall fuel quality when catalytic systems are applied and the catalysts being utilised in the system are manipulated.

### 1.3 Outline of this Thesis

The first chapter gives a general introduction into the subject of plastic waste recycling, overall motivation and objectives of the research programme. The second chapter presents the literature review in which the catalysis, polymers and areas relating to thermal catalytic degradation are discussed. Previous and current work relevant to the thermal catalytic degradation and their global importance is brought to attention. The chapter also draws attention to the global importance of recycling plastic waste with emphasis being placed on the pyrolysis of plastic waste. It also considers the methods and effects of manipulating the catalyst would have on the end products. Chapter 3 goes on to describe the various experimental procedures and provides details of the materials and equipment used for each relevant experiment.

In chapter 4 an investigation was carried out to discover the extent to which the internal catalytic active sites play a role in the initial reaction of the catalytic polymer degradation process when the external sites were rendered inert or partially inactive with aid of the silylation process.

In chapter 5 a study is carried out to investigate catalytic reusability which is an important factor in the economies of scale in every catalytic process. An evaluation of the effects of catalytic deactivation and reusability on product yield and distribution is carried out, specifically with regards to the catalytic reusability for numerous reaction cycles without regeneration.

In chapter 6 temperature effects on product yield from catalytic polymer degradation was investigated. This was achieved by exploring the effect on product yields from varied temperature rates and experimental conditions.

Chapter 7 investigates the impact of the application of a non-active filling material to the reaction system as a proportion of the reaction mixture to discover the effect on overall system performance as a result of changing catalytic surface area and potential contact enhancement. Finally the overall conclusions on the study were drawn in chapter 8, and further scope for future work was outlined.

## Chapter Two

# Literature Survey

---

*This chapter reviews previous open publications of studies and research on the thermal catalytic degradation of polymer waste. The structure of zeolite catalyst and polymers used in this investigation are also discussed in detail. The effect of the application of silanisation procedures on the ZSM-5 catalyst is investigated. A description of how tetraethoxysilane (TEOS) was used as a silanisation agent in a chemical liquid deposition (CLD) procedure on catalyst is covered.*

## 2.1 Plastics

The word “plastic” covers a wide range of macromolecules, ranging from polyolefins to polystyrene, polyvinyl chloride, metacrylic resin, polyurethane foam unsaturated polyester and urea resin. The reason for this is the large variety of applications that different plastics can be applied to, e.g. boxes of apparatus, non-returnable packaging, disposables of any kind and industrial plastic waste. The plastic waste itself is composed as shown in Figure 1. Polyolefins, including all types of polyethylene and polypropylene, account for 61 wt. % of all plastic waste. For this reason, polyethylene has been chosen as a representative for all types of plastic in the following experiments. Polyethylene was first synthesised about 50 years ago. It is a semi-crystalline semi-opaque whitish commodity with thermoplastic characteristics and is soft, flexible and tough at low temperature but its temperature resistance is extremely low. A polyethylene molecule is nothing but a long chain of carbon atoms, with two hydrogen atoms attached to each carbon atom. Traditionally differentiated by their

density that acts as a good measure of the degree of crystallinity, but from a scientific point of view the better distinction is the degree of branching. The first polyethylene, later called low-density polyethylene (ldPE), was and is made by a high-pressure polymerisation of ethylene using a free radical initiator/catalyst. Its comparatively low density arises from the presence of a small amount of branching in the chain (on about 2 % of the carbon atoms). This creates a more open structure. Enhanced technology is now being used to create a family of chemically closely related polyethylenes all of which are linear, one of which is the linear low-density polyethylene (lldPE). It is inert to chemicals at normal temperature and is a poor conductor of electricity and this is one of the reasons for its application in wiring and electronic applications. Since their introduction as materials for packaging, containers and for use as films, plastics have seen an incredible expansion in both depth and breadth of application that shows little sign of slowing. Due to their common properties of formability, shatter resistance and stability as well as their relatively inert nature and the wide range of rigidity possible, plastics have become an indispensable part of daily life and an increasingly large waste problem. Plastics constitute 7 – 10 % w/w of domestic waste but comprise 20 – 30 % of the volume [Curto et.al]. The six main types of plastics that arise in municipal solid waste are high-density polyethylene (hdPE), low-density polyethylene (ldPE), polyethylene terephthalate (PET), polypropylene (PP), polystyrene (PS) and polyvinyl chloride (PVC).

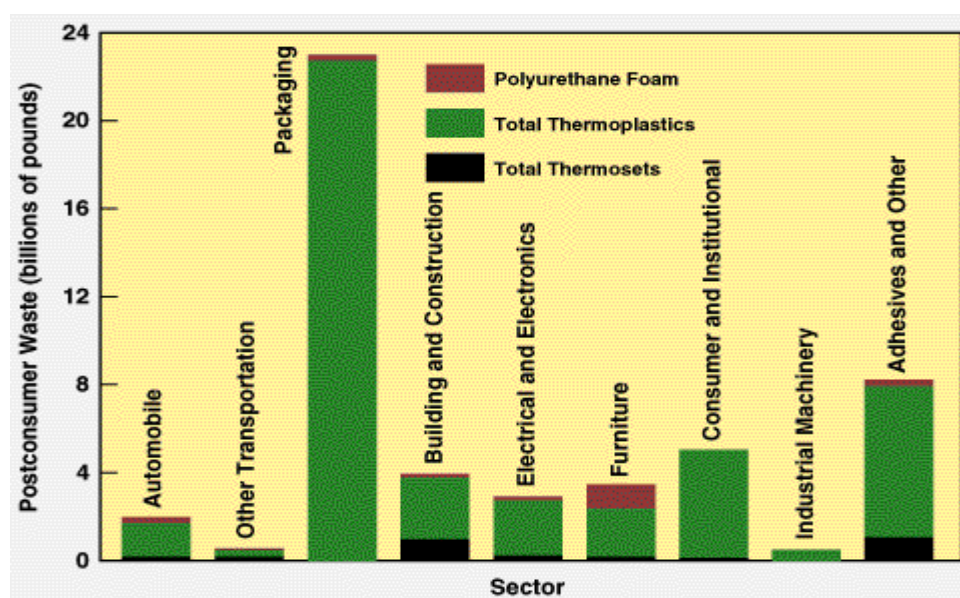


Figure 1: Post-consumer Plastic Waste for different sectors

[[www.lotfi.net/recycle/plastic.html](http://www.lotfi.net/recycle/plastic.html)]

## 2.2 Basics of Polymers

The most established types of plastic are (a) polyethylene (PE) and (b) polypropylene (PP). Both of them are introduced in the following sections.

### 2.2.1 Polyethylene (PE)

Polyethylene is a semi-crystalline thermoplastic which is whitish and has a semi-opaque commodity. Compared to other materials, PE is soft and flexible, is tough at low temperatures, and has poor temperature, environmental stress and UV resistance and poor barrier properties except to water. On the other hand, the chemical resistance of PE is very good. For this reason, PE is very often used as a basic material for laboratory equipment and in the consumer goods industry.

The structure of a PE molecule is comparable to the structure of an alkane molecule. To each carbon atom in the chain, two hydrogen atoms are attached, except of the very first and the very last carbon atoms. There are several ways of distinguishing between different types of PE molecules. The material can be characterised with respect to its density (which is effectively down to the degree of crystallinity). It is more commonly characterised with respect to the level its molecular chain branching. Low-density-polyethylene (ldPE) is a product of a high-pressure polymerisation of ethylene using a free radical initiator/catalyst. Because of the very small degree of chain branching and the open structure of the molecule, this polymer has a low density compared to others. ldPE is a widely used plastic which is virtually unbreakable and at the same time quite flexible. Some solvents cause the polymers to soften or swell, so that the product life expectancy is influenced by contamination of material due to contact to chemical solutions.

Low-pressure polymerisation products have a much more linear structure with generally higher crystallinities. This causes a much higher density, so that these polymers are called high-density polyethylene (hdPE). Other similar hdPE groups are ultra-low density polyethylene (uldPE) and linear low-density polyethylene (lldPE). All of these polymers show linear chain structures.

## 2.2.2 Polypropylene (PP)

Polypropylene is a vinyl with a higher degree of chain branching. This results in higher densities. The molecule includes a carbon backbone chain like polyethylene. To each carbon atom, one hydrogen atom and one methyl group is attached, so that the PP-molecule structure is less linear than the structure of PE-molecules. PP is a product of a polymerisation of propylene in a Ziegler-Natta process. Its industrial application is separated into plastic and fibre purposes. Polypropylene has quite a high melting point (160°C), is easy to recolour and does not adsorb water (e.g. like nylon).

## 2.2.3 The plastic-linear low-density polyethylene (LLDPE)

The “plastic waste” used in this investigation was linear low-density polyethylene (lDPE), supplied as a fine white powder. This polymer was chosen as polyethylene accounts for the majority of municipal plastic waste in Europe and the U.S. with low-density polyethylene accounting for nearly 6 million metric tonnes of waste per year in the U.S. in 1995 [Gobin K. et al., (2001), Aguado J. et al., (1997)]. It is a commodity plastic consisting of individual long chain molecules (unlike thermo sets or rubbers which have a three-dimensional network). As the name implies, the chains are repeating units of ethylene (-CH<sub>2</sub>-CH<sub>2</sub>-) with ethyl and butyl short branches. Polyethylene is classified by its density (low, medium or high) with lDPE corresponding to those with  $\rho = 920 - 930 \text{ kgm}^{-3}$ . Roughly 80 % of lDPE is used as a film, mainly for packaging. It is also used to make bags, bin liners, squeezable bottles and containers.

## 2.3 Classification of Plastic Recycling

As shown in the previous chapter, plastic waste is composed of several types of plastic. Therefore, it is important to know which kind of recycling process, integrated in a life cycle of a product that is the most effective one for each application regarding economic and environmental coherences. Life cycle assessment is an objective process to evaluate environmental and resource impacts associated with a product, process or

activity by identifying and quantifying energy and material usage and environmental releases. “The environmental impact can be assessed in terms of local, regional and global impact [Williams P. T.]”. In the following paragraphs, the different recycling processes are described.

### 2.3.1 Primary recycling

During a primary recycling process also known as mechanical reprocessing, the plastic waste is fed into the original production process of the basic material. Therefore, one receives a product with the same level of specification as the original one [Zahavich A. T. et al]. The virgin material is partly substituted by the degraded plastic waste. Thus, the quality of the product decreases with an increasing recycled plastic fraction in the feed mixture. Primary plastic recycling requires clean and not contaminated waste of the same type as the virgin resin. For this reason, the following steps form the primary recycling procedure:

1. The waste had to be sorted by specific resin types and sorted by different colours.
2. The waste has to be washed.
3. Because of better melting properties, the waste has to be re-extruded into pellets.
4. These pellets are added to the original resin.

Because of the requirements regarding the plastic properties mentioned above, this kind of recycling is very expensive compared to others. If the waste is easy to sort by resin but difficult to pelletise due to mixed colouring or contamination, it is possible to feed the waste into a moulding application, which is less demanding regarding the reactants properties.

## 2.3.2 Secondary Recycling

Some processes to recycle plastic waste reuse the plastics as a component of less importance (lower valued product) regarding the product configuration. In a production process of lumber, e.g. mixed or contaminated plastics are used to achieve better results due to different material properties. In secondary recycling, the objective is to retain some of the energy used for plastic production to achieve financial advantages. In opposition to primary recycling, the secondary recycling process is complying with contaminated or less separated waste. However, this waste has to be cleaned, [Zahavich A. T. et al], the recycling process is different compared to the original production process, and involves a different product.

## 2.3.3 Tertiary Recycling

The so-called cracking process involves breaking down the plastics at high temperatures (thermal degradation) or at lower temperatures in the presence of a catalyst (catalytic degradation) back to feedstock material. These molecules contain smaller carbon chains than the un-cracked molecules and the number of carbon atoms in a molecule varies more or less (the distribution depends on the catalyst) [Hamid S.H et al]. This feedstock can be used as basic material of lower quality for any chemical production process (e.g. polymerization or fuel fabrication), so that the original value of the raw material is lost. Due to high levels of waste contamination the tertiary recycling process gets more and more important. Therefore, this research project is concentrating on a tertiary recycling process to break down the polymer. Mechanisms like hydrolysis, methanolysis, or glycolysis are able to recover the monomers of condensation polymers, e.g. PET (polyethylene terephthalate), polyesters, polyamides, and polyurethanes. On the other hand, addition polymers like polyolefin, polystyrene, and PVC need stronger thermal treatment, gasification, or catalytic degradation to be cracked, see chapter (2.4).



### 2.3.4 Quaternary Recycling

In quaternary recycling only the energy content is recovered. Usually, the plastic waste is incinerated because of the high heat content of most plastics. The only advantage of this process is the heat energy the process generates. The residual of this incineration, which form 20 wt. % respectively 10 vol. % of the original waste, are placed in landfills. All in all, this recycling process doesn't solve the solid waste problem, but shifts the problem to an air pollution one.

## 2.4 Thermal and Catalytic Degradation

In the prior chapter, lots of different recycling processes were introduced. This research project concentrates on tertiary recycling because of its great importance in future industry. Both thermal and catalytic degradation belong to the group of tertiary recycling processes. When the process temperature reaches a certain value, the structure of the polymer molecules becomes unstable. This causes the carbon chain to break into several feedstock molecules with less carbon atoms belonging to each molecule than the original [Bond et al.]. The number of carbon atoms per molecule varies, so that the cracking product shows a wide distribution of different kinds of feedstock. For this reason, a further upgrading process is necessary to filter the large molecules out of the product. [Manos G. et al., (2000a), Manos G et al. (2000b), Garforth A.A. et al. (1998), Sharatt P.N. et al. (1997), Aguado J et al., (1997), Arandes M. J et al., (1997), Shabtai J et al., (1997)]. By using thermal degradation as a recycling mechanism, process temperatures up to 900°C are required and the product distribution is very wide. Thermal cracking process using kilns or fluidised beds are very well known in case of pilot plant experiments.

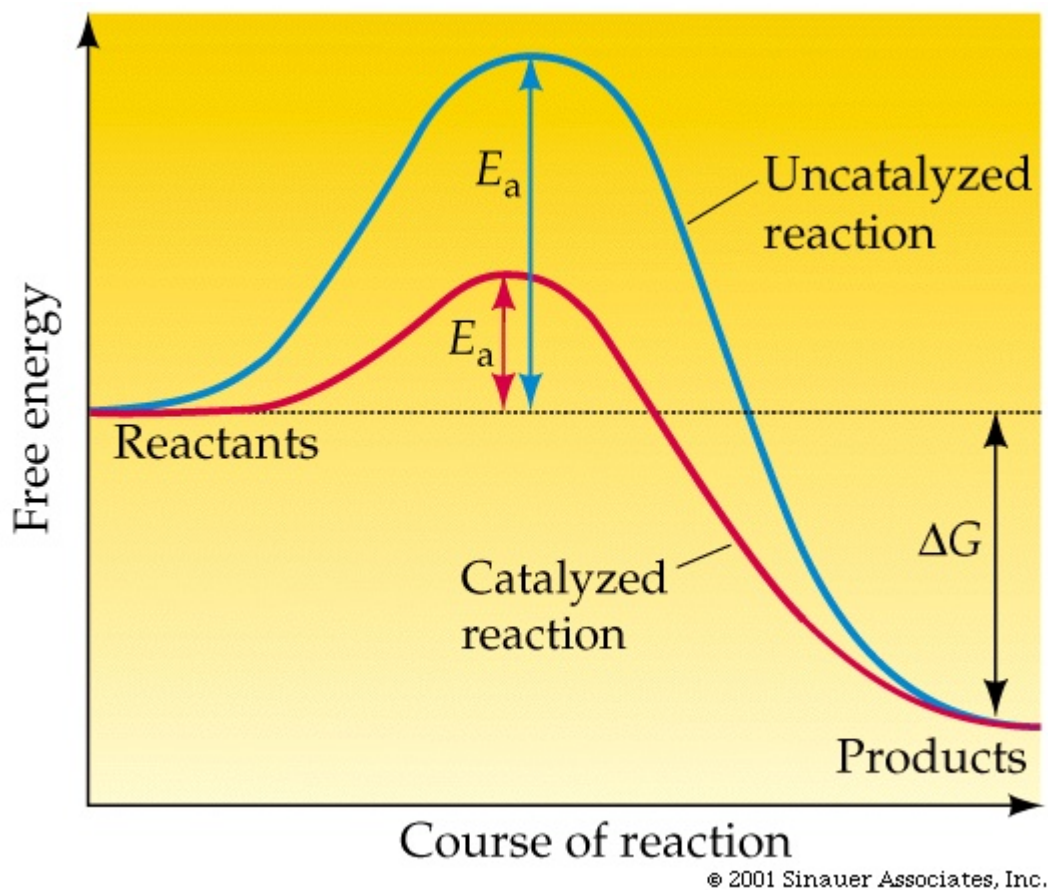


Figure 2: Activation Energy of Chemical Reaction with and without a Catalyst

The advantages of catalytic degradation compared to thermal degradation are

1. the lower cracking temperature (due to lower activation energy, see Figure 2) and a shorter cracking time is required,
2. the higher cracking ability of plastics,
3. the lower concentration of solid residue in the product,
4. and the narrow product distribution with peaks at lighter hydrocarbons in the boiling point range of motor fuel and a higher selectivity to liquid products.

Therefore, the energy costs on the one hand and the costs of subsequent upgrading procedures [Chiu S.J. et al., (1999)] on the other hand are lower, so that catalytic degradation is a cheaper alternative to thermal degradation. In contrast to the primary recycling process, e.g., catalytic degradation involves the recycling of non-PVC resins,

of contaminated plastics or plastics which contain foreign matter and of waste which is different to separate or is only available in limited quantities [Menges G et al.].

Although the heat value of plastics while burning is high, the quality of plastics-derived fuels is worse than the quality of conventional fuels regarding combustion related maintenance and costs. Thus, plastics-derived fuels are only used in energy-intensive industries and the intention of scientific studies is to increase the quality of these fuels.

In pilot plant experiments, the plastic and the catalyst are in contact in a closed environment and both are heated to reaction temperature. After a certain period of time, an amount of liquid and gas is extracted and analysed in a gas chromatograph (GC). During the experiment, the conditions are changing continuously and the measuring system is not able to detect every variation. That's why the data represent an integral value for the period of time in-between two measurements.

It's possible to feed continuously the melted polymer into a catalytic bed reactor, [Hardman et al.] which is more unusual for laboratory applications and has had very little investigation. The advantages of fluidised bed reactors are:

1. excellent heat and mass transfer characteristics,
2. a low tendency for clogging with the molten polymer,
3. and the ability to maintain a constant temperature throughout the reactor.

Although a catalyst was used, thermal degradation caused the polymer cracking in a fluidised bed reactor in some experiments [Hamid et al.], and the already cracked components passed the catalyst without any further reaction. By using fixed bed reactors, the fraction of residue in the product is increasing due to poor contact between catalyst and polymer, so that the scale-up to industrial scale is not feasible.

The aim of those studies was to co-feed the plastic waste with gas oil into the FCC (Fluid Cracking Catalyst) unit. [Aguado J et al., (1997)]. On one hand, the already existing plants are able to involve this recycling process, so that costs of development are decreasing. On the other hand, the waste has to be carried from the landfill site to the production plant, which compensates the decreasing costs. Furthermore, it is

necessary to know more about the catalyst and about the reaction conditions to implement this sub process in industrial plants.

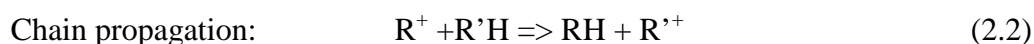
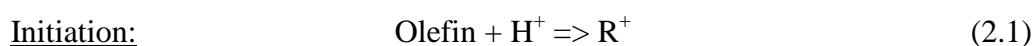
Apart from these procedures, mechanical and incineration to recover energy are also quite common procedures to recycle plastic waste.

## 2.5 Mechanism of the Degradation Process

These days, lots of different requirements have to be achieved by fuels for industrial or automotive applications. The following properties distinguish an effective fuel:

1. The volatility of the fuel should be suitable regarding the conditions while incineration.
2. Especially for internal combustion engines, the burning properties of the fuel are very important, because phenomenon like 'knocking' cause shorter life expectancy of the engine. Therefore, the octane rating for each fuel was established, which characterises the tendency to knocking. Aromatic and branched aliphatic hydrocarbons have higher-octane values than alicyclic or linear aliphatic hydrocarbons. Thus, first-mentioned fuels have a poorer accomplished tendency to knocking than others.

Due to these requirements, the catalytic mechanism has to be designed very carefully. The typical generalised reaction scheme of an autocatalytic cracking process is defined as [Hamid et al.]:



Where R'H is the reactant paraffin, RH and olefin are the products, and R<sup>+</sup> is the chain carrier. Equation (2.1) describes the protonation of olefin and the production of

carbenium ions ( $R^+$ ), equation (2.2) characterises the  $\beta$ -scission to achieve smaller carbenium ions. According to equation (2.3), olefin is rebuilt and the initiation mechanism starts again. Cracking mechanisms as shown above can produce methane and ethane as major products. In virtual reaction mechanisms, there are lots of side reactions which are more or less important regarding the conversion to volatile products. In these mechanisms, paraffin and olefins ( $C_3$  to  $C_6$ ) are major products, of which many have boiling points in the gasoline range. Coke is a high molecular weight aromatic material, which is a product of side reactions like isomeration, disproportionation, and formation process, e.g. agglomerated coke molecules damage the catalytic effect of the catalyst (catalyst poisoning) by clogging the pores and covering the active sites at the surface of the particles (see chapter (2.6)). Hence, the degree of effectiveness of the catalyst is decreasing with an increasing coke formation. Thus, the coked catalyst is cleaned in a regenerator, where the coke is burned off in the presence of air. The energy for an endothermic cracking process is provided by this combustion. In industrial applications, a fluidised bed is very often used as a reactor, because it's in this case very easy to combine the cracking procedure with a parallel running generation process. If the catalyst tends to degrade with regeneration it is replaced by fresh particles.

## 2.5.1 Mechanism of Polymer Thermal Degradation

In chapter (2.4) and (2.5) the degradation process is explained as a chi scission of the backbone obtaining free radical segments. Again from that, elimination of small molecules and double bond formations are also causing a thermal degradation of polymer. Polyethylene (PE) and polypropylene (PP) are degrading in random homolytic cleavage to a complex mixture of low molecular weight degradation polymers. Apart from this random cleavage, other reactions like intra- and intermolecular reactions and secondary reactions in the gas phase are taking place.

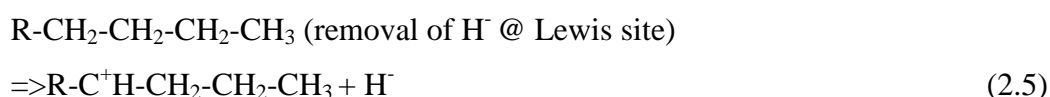
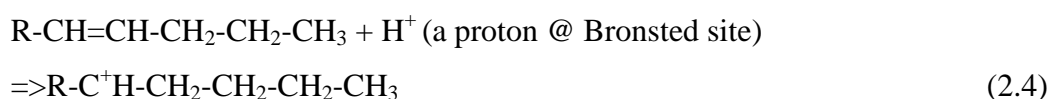
As another example, polystyrene (PS) is degraded by polymerisation via isolating the active chain end. In the presence of air, the polyolefin degradation is influenced, so that hydro peroxides are formed and the cleavage of polymer chains is accelerated. In some other processes, the molecular weight of polymer degradation products increases

or decreases depending on the level of cross linking reactions that take place during the reaction in the presence of certain accelerators or contaminants.

## 2.5.2 Mechanism of Catalytic Cracking Reactions

When the polymer feed contacts the catalyst in the reactor, the degradation is proceeding in two steps. During the first step, the polymer is vaporised by the hot surface of the catalyst. The second step contains the formation of positive charged carbon ions, so called carbocations. Both, carbenium and carbonium ions belong to the group of carbocations.

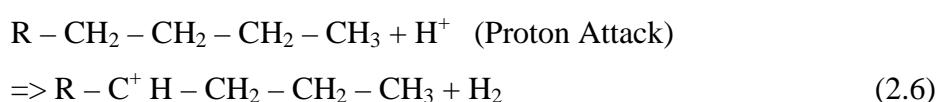
Carbenium ions ( $R-CH_2^+$ ) are formed either by adding a positive or negative charge to an olefin or effectively by removing a hydrogen ion and two electrons from a paraffin molecule. These reactions are shown in equation (2.4) and (2.5).



In a reaction illustrated by the equation (2.4), the Bronsted site of the molecule donates a proton to an olefin molecule. Due to equation (2.5), the Lewis site of the molecules removes electrons to form a paraffin molecule. Hence, the Bronsted and the Lewis sites of a molecule are responsible for generating carbenium ions.

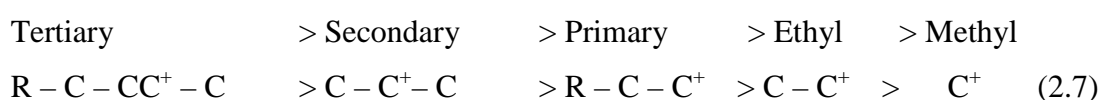
A Bronsted acid is a compound that donates a hydrogen ion ( $H^+$ ) to another compound [Abbot et al.]. A Lewis acid is any species that can accept a pair of electrons and form a coordinate covalent bond.

Carbonium ions ( $CH_5^+$ ) are formed by adding a hydrogen ion to a paraffin molecule as explained in equation (2.6).



In this reaction, the catalyst's Bronsted site attacks the proton. In comparison to the carbenium ions, the charge of the carbonium ion is not stable. Furthermore, the catalyst's sites are not strong enough to form many carbonium ions, so that the most common catalytic degradation in the industry is the formation of carbenium ions.

The stability of a carbocation is determined by the nature of the attached atoms to the positive charge. The following equation describes generally and qualitatively the stability of carbenium ions.



As an advantage of catalytic cracking compared to thermal cracking, primary and secondary ions rearrange themselves to form a tertiary ion. A tertiary ion is a carbon with three other carbon bonds attached (see equation (2.7)). While rearranging the structure of the molecule to form a tertiary ion, the stability is increasing due to a higher degree of branching.

These carbenium ions are educts in several further reactions. The most important reactions are:

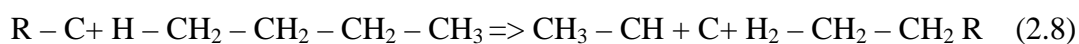
- a) cracking of a carbon-carbon bond
- b) isomerisation
- c) and hydrogen transfer.

Which of the above-mentioned reactions takes place, depends on the nature and the strength of the catalyst's acid sites? The procedure of adsorption and desorption, the chemical reaction at the surface of the catalyst, and the properties of acid sites of catalysts are described in section (2.5.3).

### 2.5.2.1 Cracking of a Carbon-Carbon Bond

$\beta$ -scission is defined as the cracking process, in which the carbon chain is split at the second chain counted from the positive-charged atom. The cracking procedure requires less energy than cracking the chain at the first bond, next to the positive-charged carbon atom.

Long-chain hydrocarbons are more reactive than short-chain hydrocarbons. Hence, the rate of cracking reactions decreases with chain length. Thus, the cracking of a carbon-carbon bond will proceed until one is no longer able to form stable carbenium ions by breaking down the molecule as shown by the reaction equation;



The initial products of the mechanism are an olefin and a new carbenium ion, which will further react in several chain reactions. Small molecules with four or five carbon atoms will react with larger molecules and transfer the positive charge, so that the large molecule can be cracked as well. Smaller molecules are more stable than larger ones, so that those won't be cracked. They will transfer their charge into a larger molecule. The positive charge will resist, until two ions with different charges become in contact.

Cracking is an endothermic reaction, because  $\beta$ -scission is a monomolecular process. Therefore, the cracking rate is increasing with temperature, so that the equilibrium state is compensating the disturbance by favouring the cracking reaction.

### 2.5.2.2 Isomerization

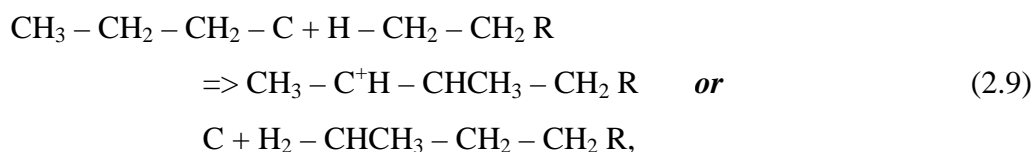
The chemical process by which a compound is transformed into any of its isomeric forms, i.e., forms with the same chemical composition but with different structure or configuration and, hence, generally with different physical and chemical properties. An example is the conversion of butane, a hydrocarbon with four carbon atoms joined in a straight chain, to its branched-chain isomer, isobutane, by heating the butane to 100° C or higher in the presence of a catalyst. Butane and isobutane have widely different properties. Butane boils at -0.5° C and freezes at -138.3° C, whereas isobutane boils at -11.7° C and freezes at -159.6° C. More important from the



commercial standpoint, branched-chain hydrocarbons are better motor fuels than their straight-chain isomers. The isomerization of straight-chain hydrocarbons to their corresponding branched-chain isomers is an important step (called reforming) in gasoline manufacture. There are numerous other examples of isomerization reactions of great industrial importance.

In a catalytic process, it is more common for carbocations to form tertiary ions as these are more stable than secondary or primary ones.

According to the reaction equation [1]:

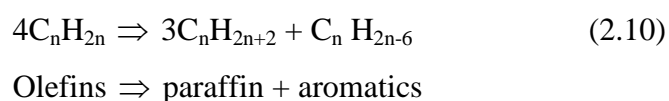


The product of this reaction is a small branched molecule. This kind of reaction is untypical for free radicals as such radicals would usually form normal or straight compounds. The advantages of isomerism reactions are:

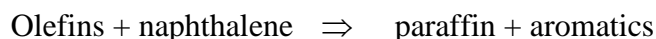
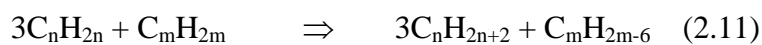
- Higher octane numbers
- Chemical and oxygenate feedstock of a higher value
- And a lower cloud point for diesel fuel

### 2.5.2.3 Hydrogen Transfer

Hydrogen transfer is a bimolecular reaction in which one of the reactants is olefin and the products are paraffin and cyclo-olefins. Further hydrogen transfer reaction with cyclo-olefins yield to cyclo-diolefins and these as a reactant then yield further to aromatics. The structure of some aromatics is based on a benzene ring and is extremely stable. The generalised hydrogen transfer reaction is shown in equation (2.10).



Another hydrogen transfer reaction is a reaction of three olefin molecules with naphthalene as a hydrogen donor, see equation (2.11).



Hydrogen transfer reactions are favoured by the catalyst's acid sites. Hence, bridging these sites with rare earth promotes these reactions. Secondary reactions are taking place in the presence of olefins. As explained in the prior paragraphs, hydrogen transfer reactions are degrading olefin molecules. Therefore, hydrogen transfer reduces over cracking.

Apart from the above-mentioned reactions, also dehydrogenation and coking are two important reactions regarding catalytic cracking processes. For contaminated catalysts, e.g. catalysts containing metals such as nickel and vanadium, dehydrogenation will proceed. If the contamination of the catalyst is negligible, dehydrogenation reactions won't take place.

Catalyst coke formation is a bimolecular reaction with carbenium ions or other free radicals. Yet the formation process is very little investigated. In general, coke formation is increasing with an increasing hydrogen transfer, because the products of this reaction (e.g. olefins, diolefins, and multiring polycyclic olefins) are very reactive and can polymerise to form coke.

## 2.6 Past Work Involving Methods of Recycling Plastic Waste

In the mid- to late-nineties, Europe was producing 13.6 billion kilograms (30 billion pounds) of post-consumer plastic waste each year and the U.S. was producing over 20 billion kilograms (44 billion pounds) annually [Manos G. et al., (2000a and 2000b),]. Most of this waste is land filled or incinerated; only 7 % is recycled (to low-grade plastic products) so clearly a more advanced and cost effective method of recycling is needed. As public concern rises and government regulation becomes stricter, new approaches, like the use of zeolite catalysts, are increasingly looked into as a means for returning plastic waste to a valuable form.

Conventional recycling of plastics involves washing and compounding mixed post-consumer plastics to produce a low quality product with broad properties, unattractive colours and containing impurities. Advanced methods (tertiary recycling methods) look to depolymerise plastic waste, i.e. degrade the polymer back to monomers or further to the raw materials from which commercial plastics are made [Manos G. et al., (2000a and 2000b),]. If this is achieved, a much better product can be manufactured from the recycled material. Current advanced techniques have increased the overall quantity of plastic, which can be recycled and has decreased the need for costly separation of different plastic types. The products obtained using advanced recycling techniques are “virtually indistinguishable” from those made from virgin materials [Gobin K. et al., (2001), Aguado J. et al., (1997), Vansant E.F., (1996)]. Comparing recycling to virgin production, 15.4 GJ of energy can be saved per tonne of plastic while producing lower air emissions.

The waste problem has spawned a wide range of research including the use of super-critical water to degrade polyethylene to oils [Garforth A et al., Arandes M et al.] and more imaginative approaches such as the use of fungi capable of excreting depolymerise to degrade plastics [Buchanan J. S et al.].

At present the recycling of plastic materials is mostly done using homogeneous polymers. Therefore a separation from a municipal collection of plastic objects is necessary before recycling operations. The easiest way of separation is by flotation in water, i.e. the separation of the different plastics based on the different densities with respect to water. This means that all the plastic materials are separated in a “light fraction” mostly of polypropylene and polyethylene and in a “heavy fraction” mainly of poly(vinyl chloride) (PVC) and poly(ethylene terephthalate). The recycling of the light fraction should, in principle, be easy because of the relative similarity of the chemical structure of the components. The presence of small amounts of polystyrene foam (lighter than water) or of some polymer, such as PVC, or non-polymeric impurities can, however, make the properties of the secondary material quite poor. In this work, the recycling of a light fraction sample has been studied, considering also the effect of the addition of wood fibers, an “environment friendly” filler. Although the similar chemical nature of the two main components, the mechanical properties of the recycled mixture are quite scarce, mainly because of the incompatibility and the possible presence of some heterogeneous particles. The addition of wood fibres (20-40 wt %) leads to a remarkable increase in the elastic modulus while elongation at

break or impact strength decrease and the tensile strength remains almost unchanged. Thermomechanical properties are also improved. In order to improve these properties, two functionalized polypropylene samples were used as adhesion promoters. Both polypropylene-grafted maleic anhydride and polypropylene-grafted acrylic acid improve the mechanical properties in particular at very low concentrations.

To return plastic waste back into valuable product, it may be simply heated, usually in an inert atmosphere of hydrocarbon gas, and allowed to thermally degrade. This is a mechanical reprocessing method and is usually applied to pure or high quality waste in a plastic-processing factory and even then the quality of the resulting products tends to be of a lower grade. Plastic reprocessing is carried out in modern large-scale plants, which are usually located near centres of high population density where reasonable quantities of feedstock exist. In recent years most mechanical recycling requires streams of specific resins, which may be reprocessed into products such as pellets that bare closer resemblance to their virgin counterparts. This effectively means that waste plastics destined for recycling must be sorted into specific resin types, sorted by colour in some cases, washed and re-modified into pellets. This makes it a fairly expensive time consuming process [Aquado J et al.].

Hardman et al., used a fluidised bed containing quartz sand, silica, or other refractory materials. The temperatures suggested were relatively high in the range of 450°C to 550°C. The products of thermal degradation show a wide product distribution requiring further processing for their quality to be upgraded [Manos G et al.,(2000a) Manos G et al.,(2000b), Songip A et al., Aquado J et al., Park D.et al.]. On the other hand, catalytic degradations yields a much narrower product distribution of carbon atom number with peaks at lighter hydrocarbons [Manos G et al., Garforth A et al., Sharratt P.N et al., Aquado J et al., Arandes M. J et al., Shabtai J et al.]. In these studies acidic catalysts were used: amorphous silica-alumina [Audisio G et al., Ohkita H et al., Seoud Ng et al.]; zeolites [Akovali G et al., Garforth A et al., Arandes M et al., Audisio G et al.]; zeolite based commercial FCC catalyst [Arandes M. J et al.] and superacidic zirconia [Shabtai J et al.].

Over the years, the combination of public pressure for recycling and a general desire to divert waste from landfill or incineration has led to a major increase in street side

collection programmes for recyclables. A variety of materials ranging from paper to metal plastics are collected. In addition, some jurisdictions handle household organics (kitchen wastes) as well as compostable yard waste (grass and brush). By far the most plastics collected are PET soft drink bottles and polyethylene milk jugs [Aquado J et al.].

If a catalyst is added, however, less costly operating conditions could potentially be used and the degradation may be considerably quicker.

## 2.7 Catalysis

### 2.7.1 Basics of Catalysis

A catalyst is defined as “... a substance that changes the rate of reaction but that is not itself consumed in the process”. The catalyst and the solvent, in which the reactants are released, are active participants of the reaction. In industrial applications, all reaction are favoured by substances with catalytic properties or inhibited by contaminations in the reactor or the solvent. Temperature is also very important to the degree of effectiveness of a reaction mechanism. In this connection, there are some mechanisms in which, an optimum of conversion is reached at a certain temperature. In this case, both an increasing and decreasing temperature will cause a decreasing degree of effectiveness.

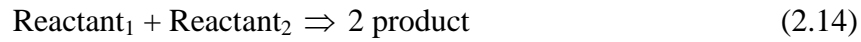
The generalised catalytic cycle is shown in equations (2.12) and (2.13) below.



In a first step of this reaction scheme, the reactants and the catalyst form a complex, as shown in equation (2.12). The main reaction is taking place on the surface of the catalyst. Thus, the complex includes the products and the catalyst after the first sub reaction. The dissociation of this modified complex to the main products and the catalyst is shown in equation (2.13).

There are two different mechanisms to describe the adsorption procedure of reactions at the surface of catalysts. The Eley-Rideal mechanism is based on the supposition that

the reaction velocity is increasing by adsorbing only one reactant, so that the main reaction due to equation (2.14) is taking place.



Regarding the above-mentioned mechanism, the volumetric reaction flux density  $\dot{r}_v$  is defined as;

$$\dot{r}_v = k \frac{b_1 c_1}{1 + b_1 c_1} c_2 \quad (2.15)$$

The formula shows the reaction velocity constant  $k$  [1/s], the adsorption coefficient of reactant<sub>1</sub>  $b_1$  [m<sup>3</sup>/mol], and the concentration of reactant<sub>1</sub> respectively reactant<sub>2</sub>  $c_1$  respectively  $c_2$ .  $k$  can be calculated using the Arrhenius Equation.

$$k = C e^{-\frac{E_A}{RT}} \quad (2.16)$$

$k$  is a function of the activation energy  $E_A$ , the universal gas constant  $R$ , the total temperature  $T$  and a constant  $C$ , which summarises other dependencies. The value of  $b_1$  is dependent on the adsorption properties of reactant<sub>1</sub> due to certain catalyst.

The second mechanism, the Langmuir-Hinshelwood mechanism, is based on the theory that both reactants are adsorbed at the same time at two different acid sites of the same particle. Only if both of them were attached, the activation energy would decrease enough to achieve a main reaction due to equation (2.14). An acid site is a non-filled electron orbital of a molecule near the surface of a catalyst which is able to form bonds with ions, which means to adsorb ions.

In this case, the volumetric reaction flux density  $\dot{r}_v$  is defined as;

$$\dot{r}_v = k \frac{b_1 b_2 c_1 c_2}{(1 + b_1 c_1 + b_2 c_2)^2} \quad (2.17)$$

As shown in equation (2.17), reactions according to the Langmuir-Hinshelwood mechanism are described by two further parameters, the concentration of reactant<sub>2</sub>  $c_2$  and another adsorption coefficient  $b_2$  [ $\text{m}^3/\text{mol}$ ].

## 2.7.2 Different Types of Catalysts

Catalysts are improved to maximise the product flow rate or to block side reactions. Therefore, lots of different types of catalyst are used in industrial applications. These catalysts are divided into two broad groups.

1. Homogeneous catalyst is added to the reacting phase and improves the reaction velocity. After the reaction, the catalyst is lost or has to be separated from the products in a continuative process. Examples of homogeneous catalysts are acids or bases, metal salts, enzymes, radical initiators and solvents.
2. Heterogeneous catalysts promote reactions by allocating a surface at the boundary of the phase, at which the catalysed chemical reaction is taking place. The shape of the catalysts varies between pellets, powders, or other solids. Hence, it is very easy to separate the catalyst from the products. For this reason, heterogeneous catalysts are very often preferred compared to homogeneous ones. Heterogeneous catalysed reactions are slower than homogeneous, because the reactants have to move to the catalyst's surface by diffusion. Commonly used heterogeneous catalysts are supported metals, transition metal oxides and sulphides, solid acids and bases, immobilised enzymes and other polymer-bound species.

Catalysts are able to change the local environment around the reactants. Therefore, catalysts are used to:

- Initiate reactions
- Stabilise the intermediates of a reaction
- Hold the reactants in close proximity
- Hold the reactants in the right configuration to react
- Block side reactions

- Sequentially stretched bonds and otherwise make bonds easier to break
- Donate and accept electrons
- And act as efficient means for energy transfer

## 2.8 Zeolite based catalysts

Zeolites are microporous crystalline solids with well-defined structures. Generally they contain silicon, aluminium and oxygen in their framework and cations, water and/or other molecules within their pores [Gates B.C., (1992)]. Many occur naturally as minerals, and are extensively mined in many parts of the world. Others are synthetic, and are made commercially for specific uses, or produced by research scientists trying to understand more about their chemistry. Because of their unique porous properties, zeolites are used in a variety of applications with a global market of several million tonnes per annum. In the western world, major uses are in petrochemical cracking, ion exchange (water softening and purification), and in the separation and removal of gases and solvents. Other applications are in agriculture, animal husbandry and construction. They are often also referred to as molecular sieves [Magee J.S et al., (1994), Maselli J.M. et al., (1984), Wojciechowski W.B. et al., (1986)]. Zeolites contribute to a cleaner, safer environment in a great number of ways. In fact nearly every application of zeolites has been driven by environmental concerns, or plays a significant role in reducing toxic waste and energy consumption.

In powder detergents, zeolites replaced harmful phosphate builders, now banned in many parts of the world because of water pollution risks. Catalysts, by definition, make a chemical process more efficient, thus saving energy and indirectly reducing pollution [Bond G.C., (1987), Bhatia B.S., (1990)].

Moreover, processes can be carried out in fewer steps, minimizing unnecessary waste and by-products. As solid acids, zeolites reduce the need for corrosive liquid acids, and as redox catalysts and sorbents, [Gates B.C., (1992)] they can remove atmospheric pollutants, such as engine exhaust gases and ozone-depleting CFCs. Zeolites can also be used to separate harmful organics from water, and in removing heavy metal ions, including those produced by nuclear fission, from water.



There are 34 known natural zeolites, but of those with potential use in catalysis, only a few are abundantly found and even fewer have found industrial use. In all, over 130 different framework structures are now known. In addition to having silicon or aluminium as the tetrahedral atom, other compositions have also been synthesised, including the growing category of microporous aluminophosphates, known as ALPOs.

Using the blueprint provided by natural zeolites, roughly 100 synthetic zeolites have been produced [Magee J.S et al., (1994), Maselli J.M. et al., (1984), Wojciechowski W.B. et al., (1986)]. These man-made structures, along with synthesis of naturally occurring constructions, are vital to industrial use of zeolites and have allowed new applications of zeolite catalysis to be discovered.

There are four properties that make zeolites especially interesting for heterogeneous catalysis:

- They have exchangeable cations allowing the introduction of molecules with various properties.
- If  $H^+$  is exchanged, it yields a high number of very strong acid sites.
- Zeolites can have pore diameters of less than  $10\text{\AA}$ .
- These pores have one or more discrete sizes.

Zeolites have received a great deal of attention from researchers in recent years due to their catalytic properties and shape selectivity. In general, zeolites contain pore diameters that can account for 50 % of the crystal volume. The intersections of these pores are called cavities or cages a diagrammatic representation is shown in Figure 4. Prior to that, in Figure 3, the primary building blocks of zeolites are silicate or aluminate tetrahedral. These tetrahedral are not always perfect and where the structure is not fully linked is known as a defect site. Hydroxyl groups terminate uncoordinated linkages. The electron withdrawing effects of the four oxygen atoms in the tetrahedral (the hydroxyl oxygen and the three others in linkage) render the hydroxyl hydrogen strongly acidic and hence these uncoordinated linkages are Brønsted acid sites.

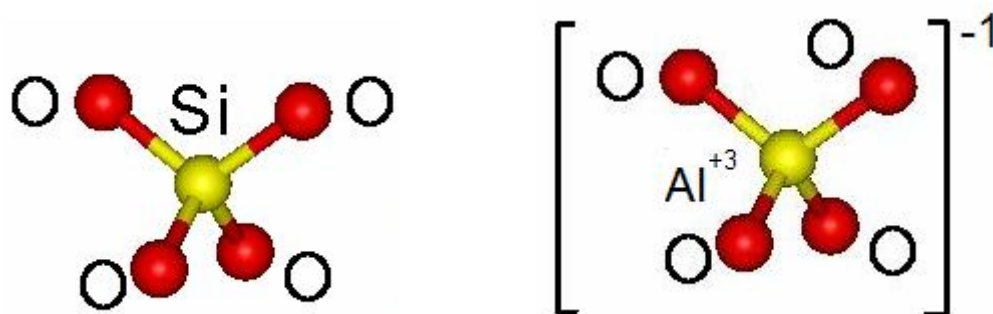


Figure 3: The building blocks of zeolites: a) silicate and b) aluminate tetrahedron

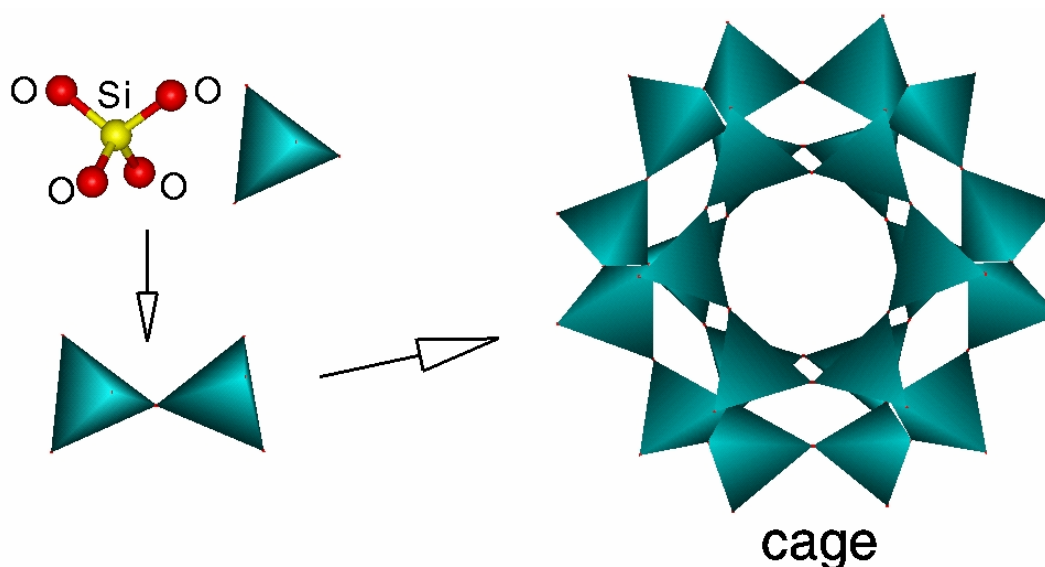
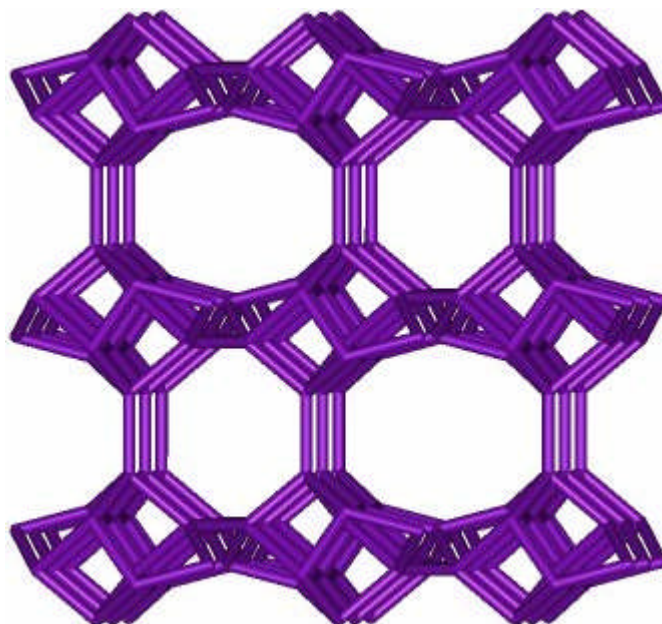


Figure 4: 3-D tetrahedral forming a cage-like zeolite structure

When these sites catalyse a reaction occurs in the confined spaces, smaller, straighter products are favoured. This is ideal for cracking reactions and specifically for degrading plastic waste back into a valuable form. In fact, solid strong acids are necessary in the petroleum industry for catalytic cracking of hydrocarbons and the most effective solid acids known are silica-aluminas; of which, crystalline zeolites have the most pronounced properties primarily as a result of their cavity structure as shown Figure 5. In 1979, 250,000 tonnes per year of zeolites were already being used in catalytic applications, a number that has increased significantly since [Kung H.H et al., (1999), Bhatia B.S., (1990), Scherzer J., (1993), Al-Khattaf S., (2002)]. In the United States, 90% w/w of zeolites in use in the chemical and fuel industries are involved in cracking reactions [Gates B.C., (1992)]

The use of a zeolite may be preferred over organic materials if high temperatures, oxidizing conditions, or radiation fields are required as these all increase the possibility of degrading organics [Gobin K. et al., (2001), Aguado J. et al., (1997), Vansant E.F., et al. (1996)].



*Figure 5: A 3-D representation of the zeolite catalyst with a clear illustration of the active cavity structure.*

### 2.8.1 Silicalite and ZSM-5

The catalyst used in these experiments is an HZSM-5 zeolite (ZSM stands for Zeolite Scony Mobil after the founders and the H signifies that this is the hydrogen form). This class of zeolites has medium pore sizes (critical diameter of  $6.3\text{\AA}$ , cavities with a spherical diameter of 0.9 nm) and consists of linked ten-member rings of alternating silicon and oxygen atoms with the general formula  $\text{Na}_n\text{Al}_n\text{Si}_{96-n}\text{O}_{192}\sim 16\text{H}_2\text{O}$  (where  $n < 27$  and usually around 3) [Gates B.C., (1992)]. They offer a great deal of molecular transportation and chemical reaction discrimination through their channel system that consists of interconnecting sinusoidal and straight pores (Figure 4). ZSM-5 zeolites can be produced with a silica/aluminium ratio of 5 – 8000 and changes in this ratio do not significantly affect the structure. However, as the Si/Al ratio increases, thermal, hydrothermal and acid stability increase [Wojciechowski W.B. et al., (1986), Scherzer J., (1993)]. The number of acid sites and hence acid strength is related to the number of aluminium atoms present. Therefore, the strength of a zeolite's acidity increases

with decreasing Si/Al ratio and can be comparable to strong mineral acids such as concentrated sulphuric acid [Herbst H., et al.]. In this investigation, a zeolite with a ratio of 90 (known as HMFI-90 by IUPAC code) is primarily used.

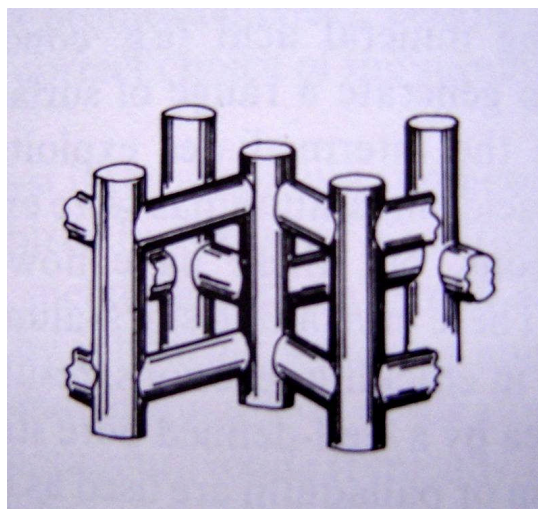


*Figure 6: A 3-D representation of the two types of interconnecting pores of ZSM-5 sinusoidal (running horizontally) and straight.*

A secondary building block, which means a two-dimensional, chain-type building block, in which  $\text{SiO}_4^-$  and  $\text{SiO}_2^-$  blocks respectively are assembled, is called Silicalite. [Bond G.C., (1987), Bhatia B.S., (1990)]. ZSM-5 is also a secondary building block, but contains Al- instead of Si-atoms. ZSM-5 contains pores of approximately 5.2 to 5.8 Å, and shows a low coking tendency. It is usually added to increase the formation of olefin and octane in FCC gasoline yields. The chain-type building blocks can be length wisely connected by charring O-atoms to form a layer. These layers contain openings of the size of quite large molecules. The three-dimensional structure of silicalite and ZSM-5 is schematically shown in Figure 6. This structure contains intracrystalline pores. Many small molecules are able to diffuse into these cavities, where there are catalytically converted. Generally, the size of these apertures is dependent on the size of the embedded cations, which may partially block the openings. The dimensions for the cavity size, the average channel size and the critical molecular dimensions of any reactant are inherent to the various zeolite applications. As a result of these dimensions, a common application of zeolites is molecular sieving. This is applied to filter molecules which are larger than the critical molecular dimension (the

maximum size of a molecule which is able to form a complex due to equation (2.12)). The cavity size varies between 0.66 and 1.3 nm, the average channel size is between 0.4 and 0.74 nm. Due to its small channel size (0.53 to 0.55 nm) and thereby less over cracking, the main products of polymer degradation over ZSM-5-catalysts are olefins. [Gates B.C., (1992)].

The aluminosilicate structure obtains  $\text{Si}^{4+}$ -,  $\text{Al}^{3+}$ -, and  $\text{O}^{2-}$  ions. To achieve ZSM-5,  $\text{Si}^{4+}$  is replaced by  $\text{Al}^{3+}$ . Positive non-framework ions (cations) have to be added to maintain electric neutrality of the molecule, these ions charges are different. The properties of the zeolite-based catalyst are heavily dependent on these embedded cations. Therefore, one is able to modify the catalyst's properties very easily by ion exchange. The composition of the catalyst is very important regarding the ion exchange capacity, e.g. Catalysts containing more  $\text{Al}^{3+}$ -ions compared to  $\text{Si}^{4+}$ -ions have higher concentrations of catalytic sites than others, because the molecules contain more embedded cations. Therefore, the ion exchange capacity and the acidity of the molecule are increasing with a decreasing Si/Al ratio due to a higher concentration of embedded cations. All these molecules show a great affinity to water. The magnitude of hydrophobicity respectively hydrophilicity of a material is a function of the Si/Al ratio. With an increasing Si/Al ratio,

- The stability of the crystal framework is increasing in presence of concentrated acids
- The stability of the crystal framework is decreasing in presence of solutions
- The decomposition temperatures are increasing
- Finally the proton donor strength is increasing

A high number of catalytic sites and the stability at high temperatures are two reasons why zeolites are widely-used catalysts in industry.

### 2.8.2 Ultrastable Y Zeolite (US-Y)

Ultrastable Y zeolites (US-Y) are modified Y zeolite molecules. This modification is taking place under controlled conditions and at high temperatures by steam treatment and is necessary due to structural collapse of unmodified Y zeolite during the regeneration process. Y zeolites belong to so-called faujasites which are composed of several secondary building blocks. The secondary building block is called a sodalite cage. In zeolite Y frameworks, these sodalite units are joined through their hexagonal

faces to a tertiary building block. Each sodalite cage is connected to four other cages. These zeolites contain apertures of 0.74 nm. The super cage (the opening into the cavity) is even 1.2 nm large. The pore structure of Y zeolite molecules is large enough to admit reactant molecules, but the pore apertures are still smaller than these molecules. Thus, molecular transport of the reactants through these openings is prevented this is thus the catalyst selectivity.

The advantage of modified Y zeolites, US-Y, is a higher thermal stability of the molecular structure. The very high cracking activity is attributed to the Bronsted acidity of the zeolite. During hydrothermal treatment, the structure of Y zeolites changes:

- The framework of Y zeolite molecules is partially destructing in the first step of the modification process
- Some  $Al_F$ -ions, which belong to the framework (index F), are removed out of the zeolite structure. These ions exist as an extra-framework species  $Al_{EF}$  (index EF) in a kind of mesoporous system.
- In the last step of this procedure, new Lewis acid sites and hydroxyl groups appear.

The chemical composition of zeolite and US-Y regarding the whole molecule is nearly the same. Compared to Y zeolite, the US-Y molecule is 1 to 1.5 % smaller because of contraction due to removed  $Al_F$ -ions out of the framework. Furthermore, the ion-exchange capacity is decreasing during this modification, which is also a reason of  $Al_F$  extraction. Regarding catalytic properties, US-Y zeolites are more active in cracking purposes. This enhancement is dependent on the method and the intensity of the steaming process and on the  $Al_F$  concentration in the Y zeolite. US-Y exhibit very strong acidic sites because of the formation of a mesoporous system out of  $Al_{EF}$ .

### 2.8.3 Commercial Cracking Catalysts

Commercial cracking catalysts consist of particles with 60  $\mu\text{m}$  in diameter composed of dispersed zeolites of 1-2  $\mu\text{m}$ . the properties of these commercial FCCs (Fluid Cracking Catalysts) are influenced by the following parameters;

1. The silica/alumina ratio is directly related to the unit cell size
2. Additives like ZSM-5 are used to modify the catalyst's structure.

3. The cracking reaction is influenced by the matrix the particle structure is based on.

A typical commercial cracking catalyst is composed of 5 to 40 wt % of a Y-type, a faujistic zeolite, a silica-alumina binder or matrix and clay filler. These components are mixed in a certain concentration and the mixture is pH-neutral and spray dried. The resulting matrix is highly porous and contains catalytically active silica/alumina components. Usually the zeolite component in a commercial cracking catalyst is a rare earth exchange or a US-Y. For the purpose of this research project, pure US-Y zeolite is used as a reference catalyst on the one hand and as the main component (20 wt %) of commercial cracking catalysts on the other. In practice, most of the matrix is inert due to small zeolite fractions. Only the active part of the matrix is able to initiate the cracking reactions because only this part bears enough acid sites associated with aluminium atoms. With an increasing zeolite fraction in the FCC catalyst;

1. the yield of gasoline and light cycle oil is increasing,
2. the formation of coke and dry gas is decreasing,
3. and the aromatic content and the octane number (which means the knocking resistance) of the gasoline are increasing.

Not only in thermal degradation but also in catalytic degradation processes, parallel reactions to the main reaction are taking place and are not completely avoidable. The products of these side reactions are light gases and coke which is formed on the surface of the catalyst and decreases the catalyst's activity. Therefore, an ideal degradation procedure achieves

1. a high selectivity to the C<sub>5</sub>-C<sub>10</sub>-fraction,
2. a low gas and coke yield,
3. and a high yield of aromatics and isomeric alkanes in the gasoline range.

As a summary, zeolite cracking catalysts have the following advantages:

- high activity,
- good activity retention,
- good thermal and hydrothermal stability,
- high gasoline yields,
- low coke and gas yields,
- good attrition resistance (regarding the regeneration process).

#### 2.8.4 Secondary Reactions and Over-Cracking

According to the selectivity of the catalyst, the micropores of zeolites are smaller than large polymer molecules. Hence, the molecules are not able to reach the interior cavities of the porous catalyst, where the majority of the active sites are located. The products of the cracking procedure are lighter hydrocarbons with smaller molecule structures in comparison to the reactants. Therefore, these molecules are able to enter the porous particle and are adsorbed inside the catalyst where secondary reactions are taking place. The products of this reaction are smaller than the products of the initial reaction and are collected in the gaseous phase. As a result of this so-called over-cracking process, the gaseous yield is increasing with a decreasing liquid yield. All in all secondary reactions lead to smaller degrees of effectiveness of the recycling process due to a smaller amount of saleable products. For this reason, commercial cracking catalysts contain only 5 to 40 % of Y zeolites to achieve less acidity of the catalyst and by that less over-cracking.

Industrially ZSM-5 zeolites are used to increase the octane number in gasoline produced, high-yield ethyl benzene and convert methanol to high-grade gasoline, amongst many other uses [Zahavich A. T. et al.]. Owing to its wide commercial availability and intrinsic properties, ZSM-5 is often looked into for novel applications. Sinha et al., studied the possibility of using the zeolite in the removal of caesium from radioactive waste. Though they found it was not suitable for this application, it provides an example of the far-reaching potential of zeolites and ZSM-5 in particular. Extensive research has been performed with various catalysts to determine their performance in degradation reactions. [Aguado et al.], compared MCM-41, a mesoporous aluminosilicate, to ZSM-5, and amorphous  $\text{SiO}_2\text{Al}_2\text{O}_3$ . MCM-41 was found to be more active than amorphous  $\text{SiO}_2\text{Al}_2\text{O}_3$  but not as active as the zeolite though it showed greater selectivity toward petroleum range fuels than ZSM-5 that could potentially make up for some lower activity. Other researchers have compared acidic to non-acidic solids in the degradation of PE and polypropylene (PP) with various advantages and disadvantages for each. Manos G et al., 2000a investigated a range of zeolites (ZSM-5, mordenite,  $\beta$ , Y and US-Y) for PE degradation. They found typical production distribution in the  $\text{C}_3\text{-C}_{15}$  range with ZSM-5 and mordenite (medium-pore zeolites) giving smaller hydrocarbons.



The thermal and catalytic degradation of structurally different types of polyethylene including (hdPE) high density polyethylene, (ldPE) low density polyethylene, (lldPE) linear low density polyethylene, and cross-linked low density polyethylene (xldPE) into fuel oil both in the absence on (thermal) and presence of the silica-alumina catalyst in liquid phase contact has also been studied [Uddin A. et al., (1997)]. In the thermal degradation, hdPE and xIPE produced significant amounts of wax-like compounds and the yields of liquid product were lower than that for ldPE and lldPE. The latter polymers also produced less quantity of wax-like compounds. Their findings suggested polyethylenes with a branching structure on its backbone like ldPE and lldPE degrade more easily to liquid hydrocarbon products than the long straight chain PE (hdPE and xIPE).

Commercial cracking catalysts have been used in catalytic degradation of polymers and have shown promising results. Gobin, K et.al., reports that these catalysts give a high liquid yield and low coke content; this makes them suitable for large-scale recycling processes. Potentially a refinery's cracking unit could have a co-fed plastic waste stream. This approach could potentially save some of the cost of constructing new facilities purpose-built for polymer recycling. Other microporous materials being considered for degradation of polyethylene include the clays saponite and montmorillonite and their pillared analogues. These have been shown to be less active than zeolites but still able to degrade the polymer [Mokaya R. et al., (1995)]. The HZSM-5 catalyst has shown promise for use in feedstock recycling. Serrano et al. report that of several acid catalysts studied in the cracking of real plastic film waste from a Spanish greenhouse, HZSM-5 "was the only catalyst capable of degrading completely the refuse at 420°C", and this was despite using a high plastic-to-catalyst ratio of 50. Other mesoporous catalysts showed conversion similar to thermal cracking. The "remarkable performance" of HZSM-5 led to high selectivity to shorter chain hydrocarbons and olefins both of which make the method attractive as a profitable recycling process. Manos and Gobin reported recently that the catalytic degradation of polyethylene over HZSM-5 formed liquid products with "boiling point distribution in the range of motor engine fuels." Such valuable products make the method financially attractive for potential scale up as a recycling method for post-consumer plastic waste.

## 2.9 Silylation (Poisoning)

Poisoning or Silylation with the application of chemical liquid deposition (CLD) is conducted on the zeolite ZSM-5 catalyst in order to create acidity variations in the external active sites of the catalyst and thus investigate the effects on catalytic degradation.

The objective of this study was to determine the effect on product yield and composition by making inert the surface acid sites of an HZSM-5 zeolite used in catalysing the degradation of linear low-density polyethylene (lLDPE). The yield to both liquid and gaseous products will be calculated and their compositions determined by gas chromatography. This will allow conclusions to be made about the effect of poisoning on the strength of acid sites and the possibility of using chemical liquid deposition as a preparatory step for catalytic degradation.

Bhatia defines poisoning of a catalyst as “chemisorption of an impurity”. Usually it is the bane of a catalyst’s performance but selective poisoning of the external sites of a zeolite would allow only the internal sites to be involved with the reaction that can lead to a more refined product. The external sites are non-shape selective, unlike the internal sites; thus, poisoning the external sites renders these sites inactive. It has also been proposed that poisoning may lead to a decrease in the deactivation of the catalyst as a result of the formation of polyaromatic molecules on the external acid sites and this is believed to hinder access to the pores.

The study is conducted with a view to characterise the extent to which the external sites were made inert and the catalysts pore openings narrowed. The structural characteristic of most interest for catalysis in zeolites is the channel system as a result of its shape selective properties. Although the channel system has a large surface area as shown in the Figure 7, it has been demonstrated that the external surface, particularly in ZSM-5 is relatively much greater than initially expected.

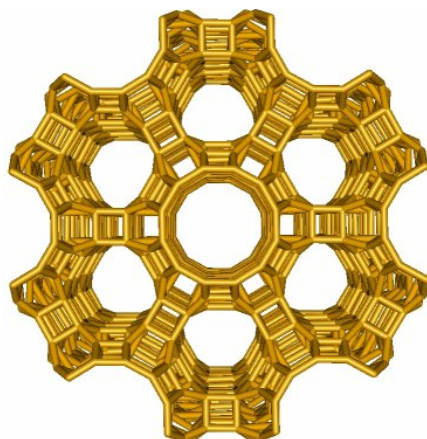


*Figure 7: Picture depiction of channel system in a zeolite catalyst*

Crucially, although the internal sites may be shape selective the external sites remain fully accessible to all molecules and thus it behaves catalytically in a non-shape selective manner. As a result there is tremendous interest surrounding the investigation of the effects of poisoning the external acid sites of the zeolites. The shape-selective properties of zeolites are also the basis for their use in molecular adsorption. The ability to preferentially adsorb certain molecules, while excluding others, has opened up a wide range of molecular sieving applications. Sometimes it is simply a matter of the size and shape of pores controlling access into the zeolite. In other cases different types of molecule enter the zeolite, but some diffuse through the channels more quickly, leaving others stuck behind as in the purification of *para*-xylene by silicalite. Cation-containing zeolites are extensively used as desiccants due to their high affinity for water, and also find application in gas separation, where molecules are differentiated on the basis of their electrostatic interactions with the metal ions. Conversely, hydrophobic silica zeolites preferentially absorb organic solvents. Zeolites can thus separate molecules based on differences of size, shape and polarity.

In previous work by Lercher et al., it was demonstrated that the deposition of an inert silica layer onto the external surface of the zeolite crystals, can be achieved by chemical liquid deposition (CLD). Thus, the shape selectivity of the HZSM-5 zeolites can be controlled.

In this contribution, tetraethoxysilane (TEOS) was used to modify the external surface of HZSM-5 zeolite MFI-90. As the molecular diameter of TEOS (1.03 nm) is larger

than the micropore openings of HZSM-5 zeolites (0.55 x 0.52 nm), it is expected that the reaction will only take place on the external surface and the pore mouth region of the zeolite crystals. When the deactivation of the external acid sites of the catalyst by chemical liquid deposition (CLD) is undertaken using TEOS, the products the general performance derived from degradation experiments over the poisoned catalyst is compared to those obtained using the fresh zeolite samples.

## 2.10 Temperature Programme Desorption (TPD)

There are a range of techniques for studying surface reactions and molecular adsorption on surfaces that utilise temperature programming to discriminate between processes with different activation parameters [Uguina, M.A et al.].

The basic experiment is very simple involving:

1. Adsorption of one or more molecular species onto the sample surface at low temperature (frequently 300 K, but sometimes sub-ambient).
2. Heating of the sample in a controlled manner (preferably through a linear temperature ramp) whilst monitoring the evolution of species from the surface back into the gas phase.

In modern implementations of the technique the detector of choice is a small, quadruple mass spectrometer (QMS) and the whole process is carried out under computer control with quasi-simultaneous monitoring of a large number of possible products.

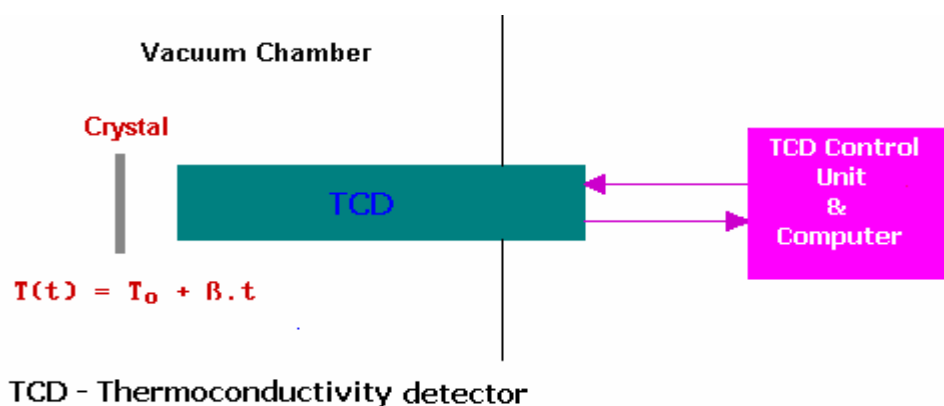


Figure 8: Diagrammatic illustration of mechanics of TPD system

The data obtained from such an experiment consists of the intensity variation of each recorded mass fragment as a function of time and temperature. In the case of a simple reversible adsorption process it may only be necessary to record one signal - that is attributable to the molecular ion of the adsorbate concerned.

The graph below shows data from a TPD experiment following adsorption of CO on to a Pd (111) crystal at 300 K.

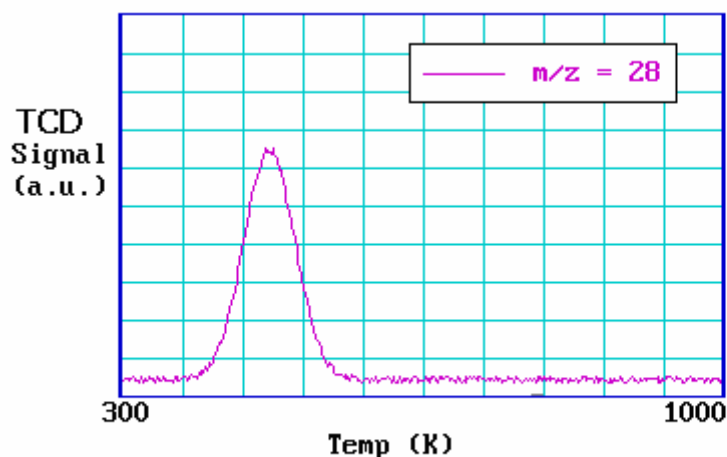


Figure 9: Data graph of TPD experiment illustrating desorption of CO

Since thermal conductivity detection is used, the sensitivity of the technique is good with attainable detection limits below 0.1 % of a monolayer of adsorbate.

The following points are worth noting:

1. The area under a peak is proportional to the amount originally adsorbed, i.e. proportional to the surface coverage.
2. The kinetics of desorption (obtained from the peak profile and the coverage dependence of the desorption characteristics) give information on the state of aggregation of the adsorbed species e.g. molecular versus dissociative.
3. The position of the peak (the *peak temperature*) is related to the enthalpy of adsorption, i.e. to the strength of binding to the surface.

One implication of the last point is that if there is more than one binding state for a molecule on a surface (and these have significantly different adsorption enthalpies) then this will give rise to multiple peaks in the TPD spectrum.

To test the extent to which silylation occurred on the external sites of the HZSM-5 catalyst, an assessment of the level of adsorption of 2,6-di-tert-butylpyridine (DTBPy), was carried out using Temperature Programmed Desorption (TPD). This is due to the fact that the minimum kinetic diameter of DTBPy is larger than pore openings of the HZSM-5 catalyst and thus DTBPy would only be expected to react with any active hydroxyl groups on the external surface of the catalyst. As a result the extent to which DTBPy desorption occurs in direct relation to the level of silylation that is recorded and analyzed.

## 2.11 Thermo-Gravimetric Analysis (TGA)

A thermo-gravimetric analysis (TGA) was also carried out to determine the rate of polymer catalytic and thermal degradation. TGA studies the relationship between a sample's mass with temperature. It is a useful application where quantitative compositional analysis of polymers is concerned, since they have different thermal stabilities.

This technique is very useful where quantitative compositional analysis of polymers is concerned, since they have different thermal stabilities. The qualitative “fingerprint” afforded by TG in terms of the temperature range, extent and kinetics of decomposition provides a rapid means to distinguish one polymer from another using only milligram quantities [Price D.M. et al., (2000)].

In most experiments, the temperature is increased in a linear system with time or the sample is held isothermally at an elevated temperature, although more sophisticated temperature profiles are occasionally used for compositional and kinetic analysis. TG does not detect processes, which do not result in a change in sample mass. It can be used in investigating and comparing the activity of different catalyst towards polymer degradation using data obtained from TG experiments. The interpretation of the TG curves can provide useful information on the kinetic parameters of the reaction.

## 2.12 Deactivation of Catalysts by Coking

Many side reactions can occur during the process of catalytic degradation including isomerization, disproportionation, and formation of coke (via countless possible mechanisms). Coke is an aromatic product with high molecular weight [Gates, B et al., Butt, J et al.]. It has the effect of blocking further reaction at catalytic sites and resulting in decreased activity. The typical strategy to deal with the problem of coking in industrial processes is to include a regeneration step where the coke is burned off thermally [Bhatia et al.]. Although coking and catalyst deactivation are commonly observed simultaneously and coking is often cited as the major cause of deactivation, [Ivanov et.al., Paweewan et.al.] the relationship between the two is probably much more complex than simple cause and effect. This is true to two main reasons: coke itself is not a well defined substance, so it is difficult to determine the precise nature and extent of its effect in blocking catalytic sites; also, hydrocarbon feeds, which are usually used in coking studies, are complex mixtures of components that affect the amount and nature of coke formed. [Butt,J et.al.]. A simple relationship would depend on whether the coke is actually formed on active sites and whether it prevents catalytic activity. There are many studies on the process and effects of coking and there exists examples of substantial catalytic activity despite the presence of coke. [Butt, J et al., Paweenan et al. (1999)]. For this reason, it will be interesting to examine the effect of coking on above mentioned catalysts in the process of polymer catalytic degradation.

### **Previous Work on Catalytic Deactivation and Coking**

There has been extensive research performed on the topic of catalytic degradation and the process of coking. Gobin et al., (2001) in particular tested catalyst performance (including US-Y, ZSM-5) in degrading lldPE as a plastic recycling technique; this research found US-Y to be the most active and also produced the most coke. The two commercial cracking catalysts (made up of 20% and 40% US-Y) resulted in less coke build up and also higher liquid yield. ZSM-5 produced almost no coke at all and had mostly gaseous products. All liquid products were found to be within the motor fuel boiling point range, which are considered to be the most valuable [Gobin K et al.]. These findings support other research that discovered high weight products such as alkanes, with the application of US-Y and low weight products such as alkenes, with the application of HZSM-5. [Garforth A et al., Watson J et al.]. This selective

formation of products creates a good incentive for plastics recycling to be considered as a source of energy.

The research done specifically on the process of coking has varied results; this is because coke formation largely depends on the nature of the overall process that is, the structural and acidic properties of the particular catalyst, the reaction conditions and reactants used. [Ivanov D.P et al., Guisnet M.P et. al., Ugina M et al.]. However, the general consensus is that catalytic deactivation is caused by a decrease in one or more of the following:

- The amount of active catalytic sites,
- The quality of these sites, and
- Accessibility to these active sites.

Paweenan et al found that the cracking of *n*-hexane with US-Y catalyst resulted in the selective deactivation of a few acid sites, which led to the overall deactivation of the catalyst. Infrared spectroscopy and diffusion measurements with pulsed field gradient (PFG) NMR revealed that most acid sites remained active on the catalyst and that the movement of *n*-butane and *n*-hexane was not inhibited by the formation of coke [Paweenan et al.]. Despite this compelling evidence, the same authors found that the deactivation of US-Y under ethane conversion was a result of both acid site deactivation and site blockage by coke. [Paweenan et al.]. These examples illustrate the significance of experimental variation in catalytic degradation by coking. What remains to be studied is how the deliberate deactivation of catalysts by coking will affect overall conversion and product yield using these parameters.

The objective of this set of experiments is to observe the effects of deactivation of different zeolite catalysts by continued use (coking), on product yield and composition in the catalytic degradation of linear low density polyethylene (lldPE). The yield of liquid and gaseous products will be calculated and analysed using gas chromatography. Conclusions can then be made about the relative deactivation of catalysts by the process of coking, and recommendations can be made about the usefulness of deactivated catalysts in achieving desired products.



## Chapter Three

# Experimental

---

*This chapter reviews experimental procedures, equipment and materials used in this work to study thermal and catalytic degradation of polymers.*

### 3.1 Introduction

The main piece of equipment used to carry out polymer degradation reactions was a bench scale semi-batch reactor. The polymer degradation was also investigated using thermo-gravimetric analysis (TGA) equipment.

For the analysis of liquid and gas products, gas chromatography was used, while for catalyst acid characterisation, a temperature programmed desorption (TPD) of ammonia was applied.

In order to study the role of external acid sites on the degradation reaction process, chemical liquid deposition (CLD) was used to selectively poison the external sites of zeolite ZSM-5 by silylation. Poisoning or silylation with experiments using chemical liquid deposition were conducted on the zeolite HZSM-5 catalyst in order to create acidity variations in the external active sites of the catalyst and thus investigate the effects on catalytic degradation. Furthermore, for the characterisation of the external acidic sites a TPD of 1, 2-di-tert-butyl-pyridine (DTBPy) was applied. DTBPy has a molecular size larger than the pores than the ZSM-5 pores that prohibits it from entering the internal pore structure and hence probes only the external acid sites.

## 3.2 Materials

The main polymer feed was linear low-density polyethylene (lIdPE) with additional experiments undertaken with polypropylene (PP), low-density polyethylene (ldPE) and high-density polyethylene (hdPE). All polymers were kindly provided by BASF AG in un-stabilised powder form. Density of the lIdPE used was  $0.928 \text{ g/cm}^3$ . The catalysts used in this study were three zeolite samples and two commercial cracking catalyst samples. Two ZSM-5 zeolite samples were used, [ZSM-5 90 (Si/Al = 45) and ZSM – 5 400 (Si/Al = 200 average particle  $14 \mu\text{m}$ )] in their acidic form. These catalysts were kindly provided by SUD-CHEMIE A.G. The reference catalyst used was Ultrastable Y zeolite (US-Y) with an original Si/Al ratio of 2.5, a framework Si/Al ratio of 5.7, and an average particle size of  $1 \mu\text{m}$ .

In addition, two commercial cracking catalysts kindly provided by AKZO-NOBEL were used; cracking catalyst 1 containing 20 % US-Y in an amorphous support (average particle size  $100 \mu\text{m}$ ) and Cracking catalyst 2 containing 40% US-Y in an amorphous support (average particle size  $100 \mu\text{m}$ ).

Tetraethoxysilane (TEOS) was used, as a silanisation agent in the chemical liquid deposition on HZSM-5 zeolite catalyst samples.

## 3.3 Semi Batch Reactor

### 3.3.1 Equipment

Figure 10 provides a schematic diagram of the experimental apparatus being described. The experimental apparatus for catalytic degradation of lldPE consisted of a semi-batch Pyrex reactor in which the reaction took place, heated by two semi-circle infrared heating elements for fast heating and thus preferred to electric heating furnaces.

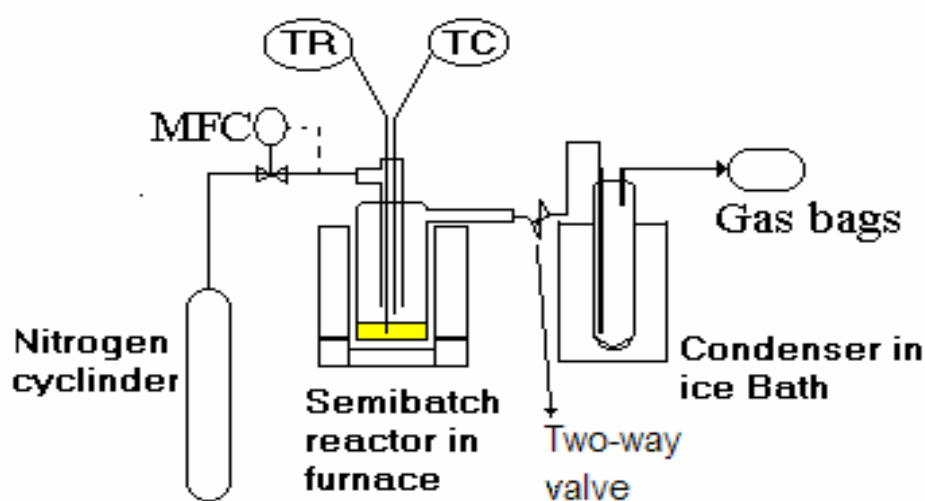


*Figure 10: Schematic representation of experimental semi-batch reactor set-up. (MFC): mass flow controller, (TC & TR): thermocouples for the controller and reactor respectively.*

The reactor is connected to a programmable temperature controller (CRL, M4). For each experimental run, the reactor temperature profile against time was recorded. The reactor was purged prior to each run, with nitrogen 50 mL/min, determined by a mass flow controller was in order to remove any oxygen from the reactor that could cause sample combustion. The amounts of polymer and dry catalyst added into the reactor were about 2 g and 1 g respectively. During the experimental run nitrogen was flowing through the reactor (50 mL/min) in order to purge volatile reaction products out of the reactor. Liquid product samples were collected in condensers placed in an ice bath and

analysed by a gas chromatograph (GC) equipped with a flame ionisation detector (FID) using a J&W scientific DB-Petro capillary column (100 m × 0.25 mm × 0.5 μm). Gas product samples were collected in gas sampling bags and analysed by a packed column GC. Using a two-way valve aided the collection of multiple liquid and gaseous product samples at different time intervals and temperatures.

### 3.3.2 Experimental procedure

At the beginning of every experiment the empty Pyrex reactor and all empty condensers were weighed. The sample was then dried in a furnace. After drying the catalyst for 30 minutes at 200°C and letting it cool to room temperature, approximately 2 g of the polymer (lIdPE) and 1 g of the catalyst were weighed and placed into the Pyrex reactor. The reaction tube was then closed with the top half of the glass apparatus, which sealed the bottom half reactor tube. The glass apparatus had an inlet for nitrogen that was flowing at 50 mL/min during the experiment and it also housed two thermocouples. One of the thermocouples was the sensor for the controller and the other monitored the temperature within the reacting solids. The photograph of the glass batch reactor is displayed in Figure 11.

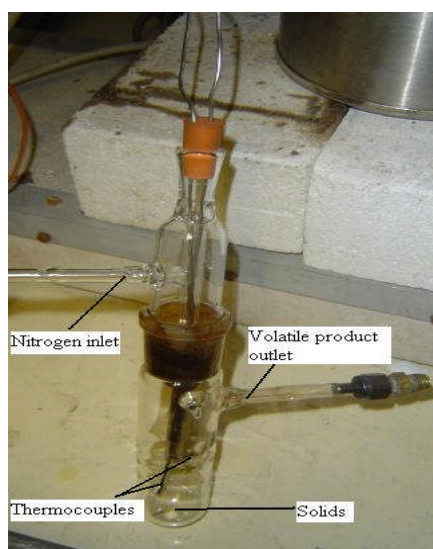


*Figure 11: Photograph of the top and bottom halves of Glass Reactor section with its nitrogen inlet and product outlet. The thermocouples for the controller and the reactor are also displayed.*

The nitrogen helped purge the products along via the product outlet as illustrated in Figure 11. This outlet is connected to a condenser as shown in Figure 10. In the experiment the three condensers were set up in parallel to collect the liquid products in different sequential time intervals. The switch between the condensers was enabled by a two way valve placed at the reactor exit. The arrangement was that of a cooling trap. The condensers, as seen in Figure 10, were sealed with silicon stoppers that had an inlet for the product stream and an outlet connected to a valve Tedlar gasbag that collected any gaseous products. The condensers were packed in ice so that the products were collected at atmospheric pressure and 0°C.

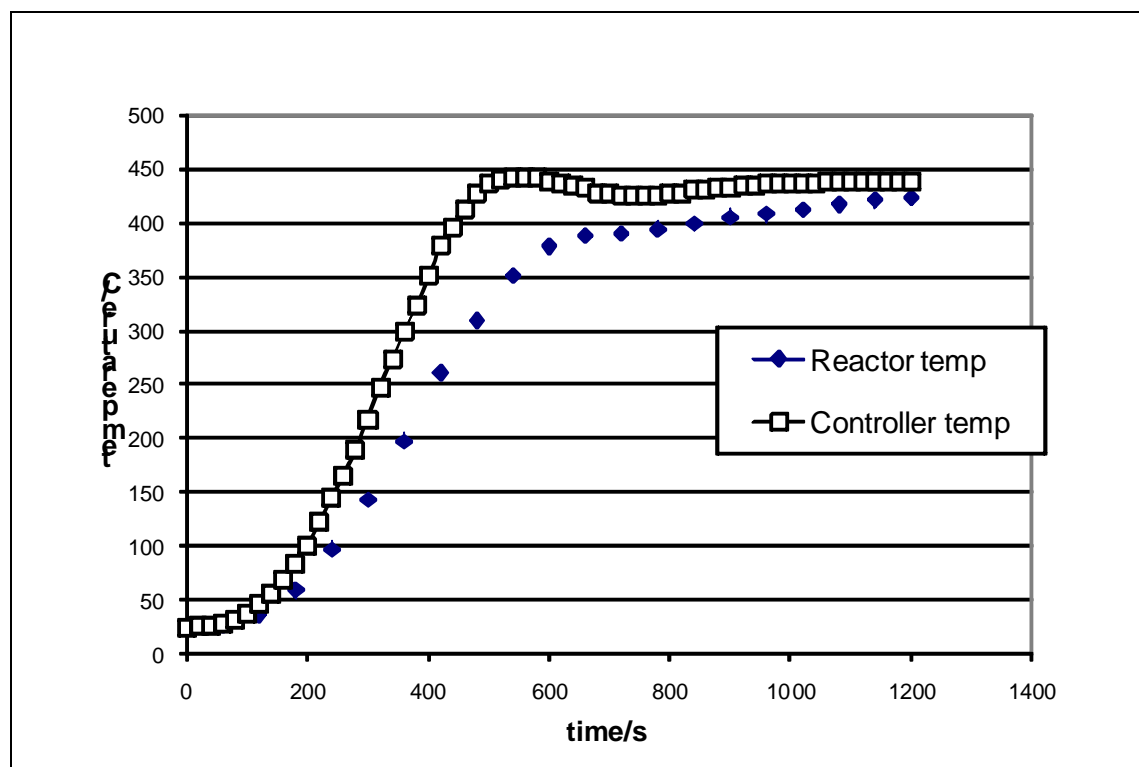


Figure 12: A typical temperature profile of both controller and the semi-batch reactor

The reactor top (above furnace) was insulated to minimize heat losses. Prior to the start of the each experiment, nitrogen was flowing for about 30 minutes through the reactor in order to remove oxygen. The reactor program was then commenced. In a typical experiment the program produces the temperature profile (Figure 12) with a maximum temperature referred to as  $T_{max}$  of roughly 440°C typically for the controller that corresponds to a maximum temperature in the reactor about 15 K lower (typically

roughly 425°C). The temperature controller is designed to not significantly overshoot the desired  $T_{\max}$ . As shown in Figure 12, during each experiment the temperature of the controller and the reactor were both recorded.

At the end of each experiment, the condensers containing the liquid products were sealed and weighed to estimate the mass of liquid collected. Following this, the reactor was cooled and weighed in order to determine the mass of un-reacted polymer. This was evident in most of the experiments by the coke formed on the catalyst in the reactor after the experiment was completed.

The product samples are subsequently analysed with aid of a Gas Chromatograph (GC). Due to the complexity of the liquid samples (with more than 400 detected peaks), the liquid analysis is always presented in the form of a boiling point distribution as explained in the following chapter. This was possible as the employed non-polar capillary column separates the components of a mixture according to their volatility i.e. boiling point. To begin with, a calibration mixture containing normal alkanes ( $C_5 - C_{20}$ ) was used to assign boiling points to retention times.

Operating conditions for the liquid chromatograph are given in the tabulated in Table 1 below.

**Table 1: Operating conditions of the GC for liquid sample analysis**

<b>Parameters</b>	<b>Liquid Analysis Operating Settings</b>
Injection	0.2 µl
Attenuation	8
Oven Temperature 1	40°C
Isothermal Time 1	10 minutes
Ramp 1	5°C/min
Oven Temperature 2	270°C
Isothermal Time 2	19 minutes
Ramp 2	0°C/min
FID Sensitivity	LOW
Detector	ON
Injector Temperature	270°C
Detector Temperature	300°C
GC column flow rate	0.6 mL/min
Split control valve	30 mL/min
Relay 0	ON (Split mode) 50:1
Data Run	75 minutes

### 3.3.3 Experimental Calculations

During the degradation reaction, the polymer may be broken down into gaseous and liquid products or undergo a complex series of condensation, polymerisation and cracking reactions to produce coke, or may remain unconverted. Therefore, the overall polymer mass balance is:

$$m_{p0} = m_g + m_l + m_c (+ m_{up})$$

Where  $m_{p0}$  = initial mass polymer

$m_g$  = total mass of gas collected

$m_l$  = total mass of liquid collected

$m_c$  = mass of coke on catalyst in reactor

$m_{up}$  = mass of unconverted polymer

Generally the conditions in the reactor were such that it may be assumed that the entire polymer amount was volatilised to form either liquid or gaseous products or coke (i.e. no un-reacted polymer), as it was visually obvious at the end of the experimental run. The exceptions to this are the experiment with poisoned catalyst at a low temperature profile as well as the experiment in the absence of catalyst. In both of these cases there was a low conversion of the polymer to volatile products; therefore, it could be observed and thus recorded that some of the substance left in the reactor was un-reacted polymer (in addition to the coke that was normally formed). In these experiments the ' $m_{up}$ ' term would appear on the right hand side of the above equation to account for polymer that has not been converted, but this term can be ignored for all other experimental runs.



As it was not possible to weigh the amount of product collected in each gas bag, these were estimated using the fractions of total gas collected in each bag which was estimated chromatographically as the total peak fraction of each bag divided by the sum of all total area.

$$a_i = \frac{A_{gi}}{\sum_{n=1}^3 A_{gn}} \quad [3.1.1]$$

where  $a_i$  = Area fraction of gas collected in interval  $i$  = mass fraction of gas collected in interval  $i$

where  $A_{gi}$  = total area of the peaks corresponding to the gas collected during interval  $i$ .

Then total mass of gas collected during interval  $i$  is  $m_{gi}$

where  $m_g$  is the total mass of gas calculated as:

$$m_g = m_{p0} - m_l - m_c (-m_{up}) \quad [3.1.2]$$

where  $m_{gi}$  = mass of gas collected at each time interval  $i$

$$m_{gi} = a_{gi} * m_g \quad [3.1.3]$$

The conversion to volatile product was calculated as the fraction of converted polymer

$$X = \text{mass reacted polymer/mass initial polymer} = \frac{(m_p - m_c)}{m_{p0}} \quad [3.1.4]$$

The yield to liquid product was calculated as the fraction of initial polymer converted to liquid:

$$Y_l = \frac{m_l}{m_{p0}} \quad [3.1.5]$$

Correspondingly the yield to gaseous product was calculated as the fraction of initial polymer converted to gas

$$Y_g = \frac{m_g}{m_p} \quad [3.1.6]$$

And coke yield is calculated as the fraction of initial polymer converted to coke

$$Y_c = \frac{m_c}{m_p} \quad [3.1.7]$$

Coke concentration was calculated as the mass of coke formed divided by the catalyst mass

$$C_c = \frac{m_c}{m_{cat}} \quad [3.1.8]$$

### 3.3.4 Boiling Point Distribution

The product distributions of the liquid hydrocarbon fractions over various catalysts are presented as boiling point distribution curves. Table 2 shows the boiling point distribution intervals. Table 3 illustrates the product distribution obtained from the degradation of lldPE over a HZSM-5 catalyst. The use of non-polar capillary column aids in the separation of the components of the liquid product mixture according to their volatility/boiling point [Cheng S., (1999), Kikuch E. et al., (1985), Matsuda T. et al., (1998), Shabtai J. et al., (1997), Lourvanij K. et al., (1994) Lourvanij K. et al., (1993)].

A calibration mixture containing equal quantities of normal alkanes, pentane to eicosane, C<sub>5</sub>-C<sub>20</sub> was utilised. This is used to assign each retention time observed for each component from chromatogram to its boiling point. The whole sample for analysis was then divided in intervals taken as being between the boiling points of the normal alkanes of the calibration mixture.

The mass fraction corresponding to each interval was calculated from the sum of the area fractions of all components in this interval assuming that the area of each peak is proportional to the mass fraction of the corresponding component as shown in [Brillis et al.]. To each interval the probability density function value was then calculated as being equal to the mass fraction of this interval divided by the interval width. The probability density function is expressed as % / K. In the graphs of the boiling point distribution each interval is represented by its middle value. It is very important to mention that because of the complexity and reduced clarity in processing 19 different boiling point distribution curves for each component, it was decided that the BPD results be produced in three component groups. These were as follows the Light fractions, which included components from C<sub>4</sub>-C<sub>9</sub> with temperature ranges between 272.7 K to 424.0 K. Next are the Middle fractions, which include components from C<sub>9</sub>-C<sub>14</sub> with temperature ranging between 424.0 K to 526.7 K. Finally, the Heavy fractions, which included components from C<sub>14</sub>-C<sub>20</sub> with temperature ranges between 526.7 K to 617.0 K. The reason is to provide a better overview when the detailed BPD presentation becomes complex and makes comparisons difficult.

**Table 2: Boiling Point Distribution Groups**

<b>Group of carbon atoms</b>	<b>Average Boiling point [K]</b>	<b>Boiling Point Range (Interval Width) <math>\Delta T</math> (K)</b>
<b>C4-C5</b>	290.95	36.5
<b>C5-C6</b>	325.55	32.7
<b>C6-C7</b>	356.75	29.7
<b>C7-C8</b>	385.2	27.2
<b>C8-C9</b>	411.4	25.2
<b>C9-C10</b>	435.65	23.3
<b>C10-C11</b>	458.2	21.8
<b>C11-C12</b>	479.3	20.4
<b>C12-C13</b>	499.05	19.1

<b>C13-C14</b>	517.65	18.1
<b>C14-C15</b>	535.25	17.1
<b>C15-C16</b>	551.9	16.2
<b>C16-C17</b>	567.6	15.2
<b>C17-C18</b>	582.35	14.3
<b>C18-C19</b>	596.3	13.6
<b>C19-C20</b>	610.05	13.9

**Table 3: Boiling Point Distribution of a real sample**

<b>Group of carbon atoms</b>	<b>Area%(A)</b>	<b><math>\square A/\square T(K)</math></b>
<b>C4-C5</b>	13.3801	0.366578
<b>C5-C6</b>	26.7469	0.817948
<b>C6-C7</b>	22.2179	0.748077
<b>C7-C8</b>	10.1912	0.374676
<b>C8-C9</b>	6.1558	0.244278
<b>C9-C10</b>	5.7642	0.247391
<b>C10-C11</b>	3.2561	0.149362
<b>C11-C12</b>	2.9727	0.145721
<b>C12-C13</b>	1.6543	0.086613
<b>C13-C14</b>	1.1471	0.063376
<b>C14-C15</b>	1.6823	0.09838
<b>C15-C16</b>	1.944	0.12
<b>C16-C17</b>	0.9639	0.063414
<b>C17-C18</b>	1.1785	0.082413
<b>C18-C19</b>	0.5109	0.037566

<b>C19-C20</b>	0.2773	0.01995
<b>&gt;C20</b>	0.1938	-

A graphical example of the boiling point distribution of the liquid products produced from the degradation of lldpe over a zsm-5 catalyst is shown in Figure 13.

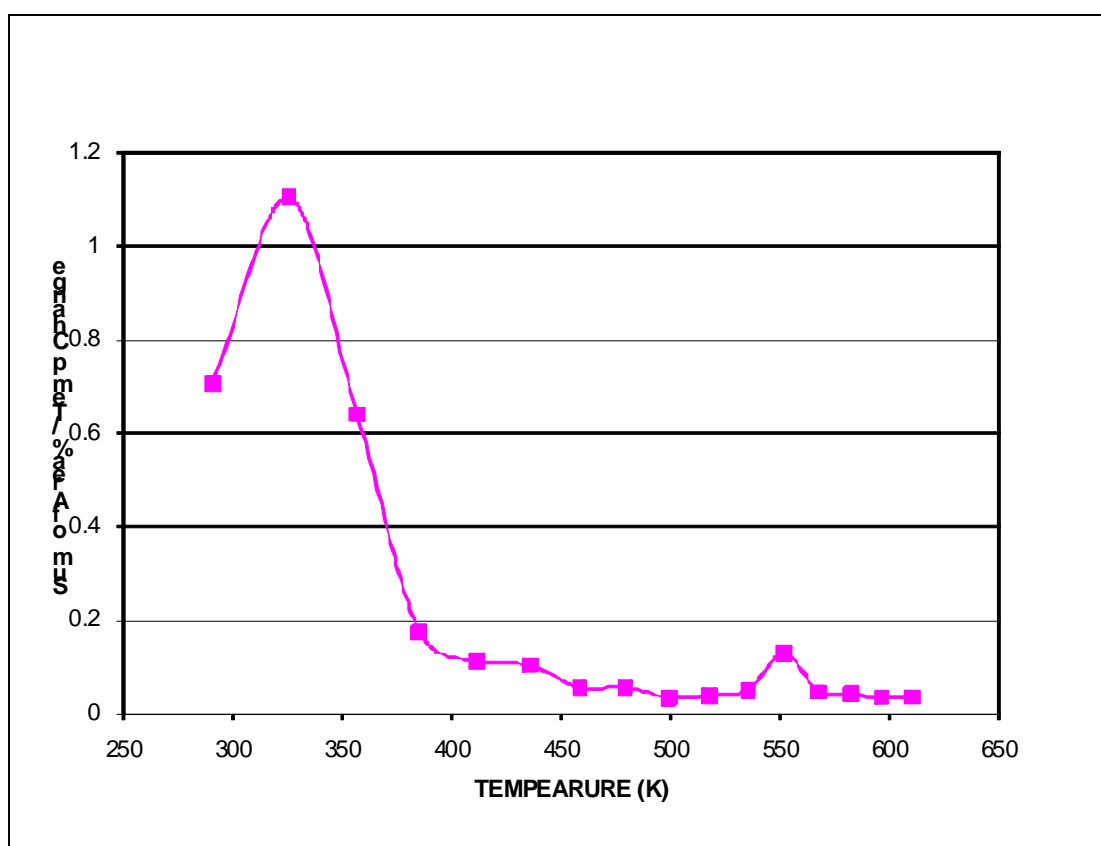


Figure 13: Boiling point distribution for liquid products produced during degradation of lldPE over a ZSM-5 catalyst

Occasionally the total average boiling point distribution was calculated for all samples collected during a run as their weighted average using the following equation:

$$\text{Total Boiling Point Distribution: } X_i^{\text{tot}} = \sum X_{ij} (\text{LF})_j \quad [3.2.9]$$

Where  $X_i^{\text{tot}}$  is the total average probability density function ( $\%/\Delta T$ ) value of group  $i$

$X_{ij}$  the probability density function ( $\%/ \Delta T$ ) value of group  $i$  in liquid sample  $j$  and (LF) is the mass fraction of liquid sample  $j$  (as fraction of total liquid amount).

### 3.4 Thermo-gravimetric Analysis Equipment (TGA)

Thermogravimetry is the study of the relationship between a sample's mass and its temperature [Price D.M. et al., (2000)]. Any process physical or chemical that causes mass change of a sample can be analysed by TGA. A diagrammatic illustration of the process is shown in Figure 14. In this work, the polymer degradation over various modifications of the microporous zeolite catalysts was carried out with TGA. TGA equipment was used to study the mass change of polymer samples with temperature in the presence of a catalyst.

The thermal analysis equipment (ATI Cahn TG instruments, model TG 131) consisted of three main components:

1. A sensitive recording balance
2. A furnace and associated controller / atmospheric management system
3. A computer controlled data collection station that recorded the results of the analysis.

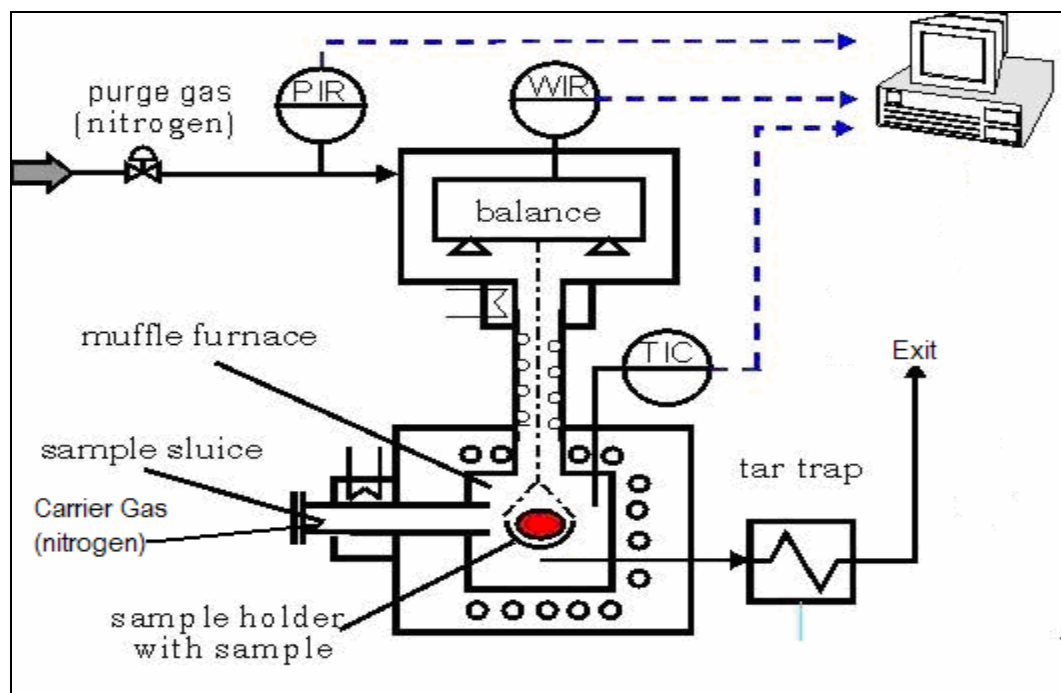


Figure 14: Scheme of the thermo-gravimetric analyser



In the TGA experiments polymer powder was mixed with the catalyst at a specific polymer to catalyst mass ratio, usually 2:1. The amount of catalyst was around 10-20 mg. Each mixture was placed into the sample basket of the TGA equipment. The basket was then lowered into the furnace, which followed a precise temperature profile of ramps and constant temperature intervals, established by the user, under computer control. In this study, the samples were subject to a constant heating rate of 5 K/min in nitrogen with a flow rate of 50 mL/min. The gases used included carrier gas (nitrogen), air and a purge gas (also nitrogen). Air was only used at the end of the experiment in order to burn the coke. These were controlled by an on-off switching sequence defined in the same user-specified method. Time, weight and temperature data were acquired at defined intervals with ATI Cahn's software and presented as sample mass fraction against temperature.

### 3.5 Temperature Programmed Desorption (TPD)

Temperature Programmed Desorption (TPD) was conducted to estimate the acidity of individual catalyst samples in a Micromeritics ASAP 2910 Chemisorption equipment (ca. 50 – 100 mg of sample at 10 K/min from a temperature range of 373 to 1073 K), which uses a temperature conductivity detector (TCD) for detecting the desorbed probe molecules. TPD is one of the most widely used and flexible techniques for characterising the acid sites on oxide surfaces. It is used in determining the quantity and strength of the acid sites solid acidic catalysts and it is crucial to understanding and predicting their performance. TPD of ammonia is a widely used method for characterisation of site densities in solid acids due to the simplicity of the technique. Ammonia often overestimates the quantity of acid sites particularly in specific reactions. Its small molecular size allows ammonia to penetrate into all pores of the solid where larger molecules commonly found in cracking and hydrocracking reactions only have access to large micropores and mesopores. In addition, ammonia is a very basic molecule, which is capable of titrating weak acid sites which may not contribute to the activity of catalyst.

TPD analyses determine the number, type, and strength of active sites available on the surface of a catalyst from measurements of the amounts of gas desorbed at various temperatures. The higher the desorption temperature, the stronger is the active site.

The results of TPD are presented as TCD signal and this signal is proportional to the amount of the probe agent released with change in the desorption temperature. Such a graph represents an acid strength distribution. In this research the level of external surface acidity of the poisoned catalysts was assessed using temperature programmed desorption (TPD) of 1, 2-di-tert-butylpyridine (DTBPy). (DTBPy) has a molecular size of 10.5 Å and hence cannot enter the internal structure of HZSM-5 whose pores have a size of 5.5 to 5.6 Å. In addition, ammonia was used as a probe agent to discover whether silylation of the catalytic active sites only affected the external sites and to what extent it affects the acidity of the internal active sites of the HZSM-5 samples, as both internal and external active sites of HZSM-5 catalyst are accessible to gaseous ammonia.

### 3.6 Chemical Liquid Deposition (CLD)

The starting HZSM-5 sample (Si/Al = 45) with average particle size of 10 µm is used as the parent material. 2 g of HZSM-5 was suspended in 50 mL of hexane and heated under reflux with consistent stirring. TEOS (0.3 mL), which is equivalent to 4 wt % SiO<sub>2</sub>, was added into the mixture and the silylation was carried out for 1 h under reflux. Hexane was removed by evaporation and the sample was calcined at 773 K in dry air for 4 h. The process was repeated another two times on the same catalyst sample. The resulting poisoned sample is called 3 x poisoned catalyst. When this procedure was carried out on the same sample nine times in total it was referred to as a 9 x poisoned catalyst. This was done to achieve a higher, if not complete, level of poisoning.

The catalyst being analyzed was soaked into DTBPy for a period of 12 h and then allowed to evaporate. This was applied to all the catalyst samples being used in DTBPy TPD. Following DTBPy pretreatment, the sample was heated to 150°C, inside the TPD equipment in order for physisorbed DTBPy to be removed from the catalytic surface, leaving only the stronger chemisorbed species. Following the physisorbed DTBPy desorption the reactor was heated at a rate of 5 K/min under helium gas flow from 40 to 500°C. During the temperature-programmed cycle, transient changes to each sample were recorded via a TCD.

## Chapter Four

# Role of external sites on catalytic polymer degradation performance

---

*This chapter is concerned with the results in terms of product yield and distribution obtained from the experiments involving the semi-batch reactor catalytic degradation. The effects and extent of catalytic manipulation is investigated using the TPD and TGA with methods described in the previous chapters.*

### 4.1 Introduction

The original hypotheses was to block/poison all external sites and then evaluate how much it influences the catalytic performance with regards to rate and yields. The completely poisoned sample should show no degradation (according to hypothesis only the external sites contribute to start of de-polymerisation reaction). [Lercher J et al.]. The overall summary of this exercise establishes that it is reasonable to conclude that the ammonia desorption for both the poisoned and fresh samples were similar whereas the DTBPy desorption process was function of the catalytic external active sites and DTBPy was never absorbed by the internal active sites leading to a much more significant difference in the catalytic desorption to be better demonstrated, as shown.

The main findings arising from the catalytic degradation with a zeolite based catalyst using the semi-batch experimental method served to demonstrate that the liquid fraction produced was a hydrocarbon mixture in the gasoline range and confirm the

conversion of polymer to fuels. As previously mentioned, the structural uniqueness of the zeolite being used makes it catalytically intriguing. It was noted that as the macromolecules of the plastic have to first react with the external active sites, only smaller molecules that are produced from the initial cracking reaction can enter the micro pores of the porous zeolite catalyst that contain the majority of the active sites. The strong acidity of the zeolite catalyst causes severe over cracking, resulting in the formation of high gas – to – liquid yield ratio. The yield in the liquid fuel is considered as being more saleable. [Kung H.H et al., (1999), Bhatia B.S., (1990), Scherzer J., (1993), Al-Khattaf S., (2002)]. The primary focus of this section of the investigation was to discover the extent to which the initial reaction of the internal active sites play a role in the catalytic degradation process when the external sites were rendered inert or partially inactive with aid of the silylation process.

The main findings arising from the results presented in this section are categorised below as follow:

1. The results of the level of poisoning that occurred on the zeolite catalyst as a result of silylation and thus a test of the efficiency of the catalyst with desorption in the Temperature Programmed desorption experiments.
2. The results obtained from TGA experiments and study of the changes in rates of degradation.
3. The results obtained from catalytically degrading the polymer lldPE with zeolite catalysts with the semi batch experiments. An assessment of the difference in conversion, selectivity, yields to liquid, gas and coke products when the catalyst is modified by silylation.

## 4.2 Acid Site Distribution of Poisoned Samples / TPD

The TPD results are illustrated in Figures 15 (NH<sub>3</sub>) and 16 (DTBPy). In both charts the area under each peak is proportional to the amount originally adsorbed and thus proportional to the surface coverage. The position of the peak (the *peak TPD temperature*) is related to the enthalpy of adsorption, i.e. to the strength of binding to the specific catalytic active sites. Apart from the TPD of DTBPy for the study of characteristics of acid sites of the external catalyst surface, NH<sub>3</sub>-TPD study was carried out on fresh and silylated catalyst samples in order to discover if the internal acid sites were also affected. Figure 15, is a chart of a TPD signal against temperature for ammonia TPD displaying results obtained using both the fresh and silylated samples of HZSM-5 catalysts. As a result of the size of ammonia molecules being smaller than the pores of the catalyst it is unrestricted by the pore openings of the catalytic active sites. It is thus expected that ammonia is adsorbed on both the external and internal active sites of the catalyst. Although the two curves in Figure 15, which display the results of fresh sample as well as 3 x-poisoned samples, are not identical, their difference is much lower than those desorption profiles of DTBPy (Figure 16). These small differences in NH<sub>3</sub>-TPD could be attributed to poisoned external sites. As the poisoned external sites are a relatively small fraction of the total number of sites present, the difference in NH<sub>3</sub>-TPD is relatively small.

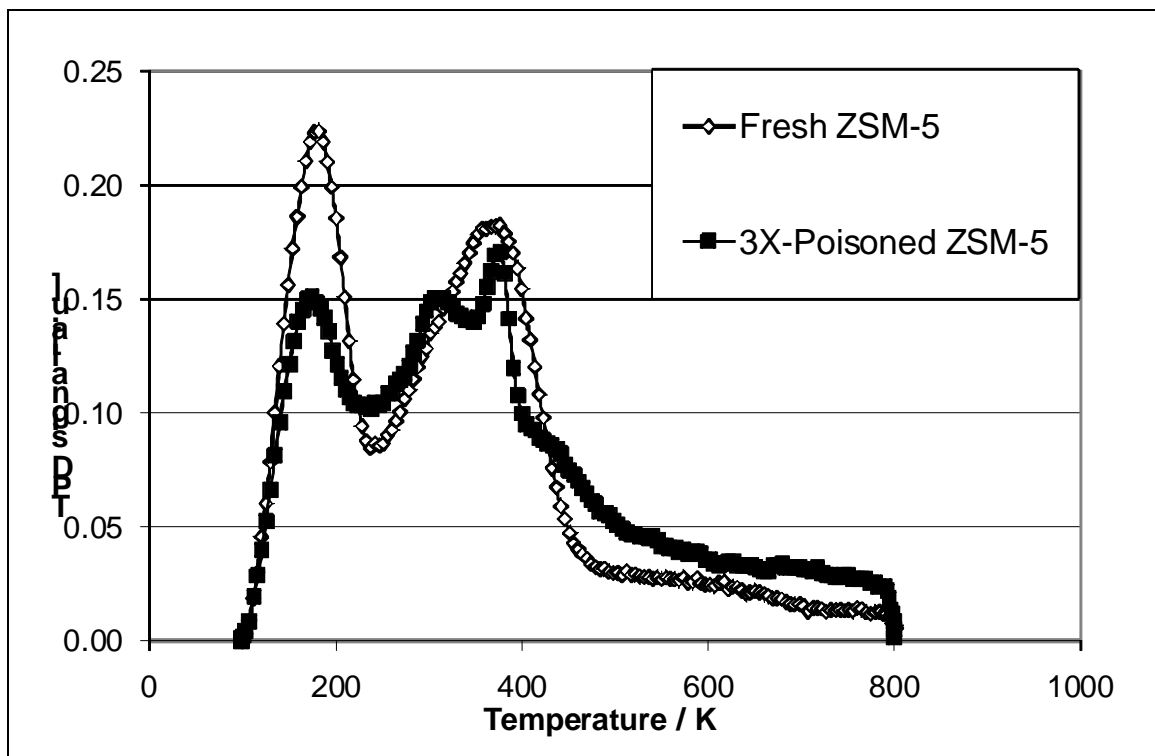


Figure 15  $\text{NH}_3$ -TPD of fresh and poisoned HZSM-5 catalyst

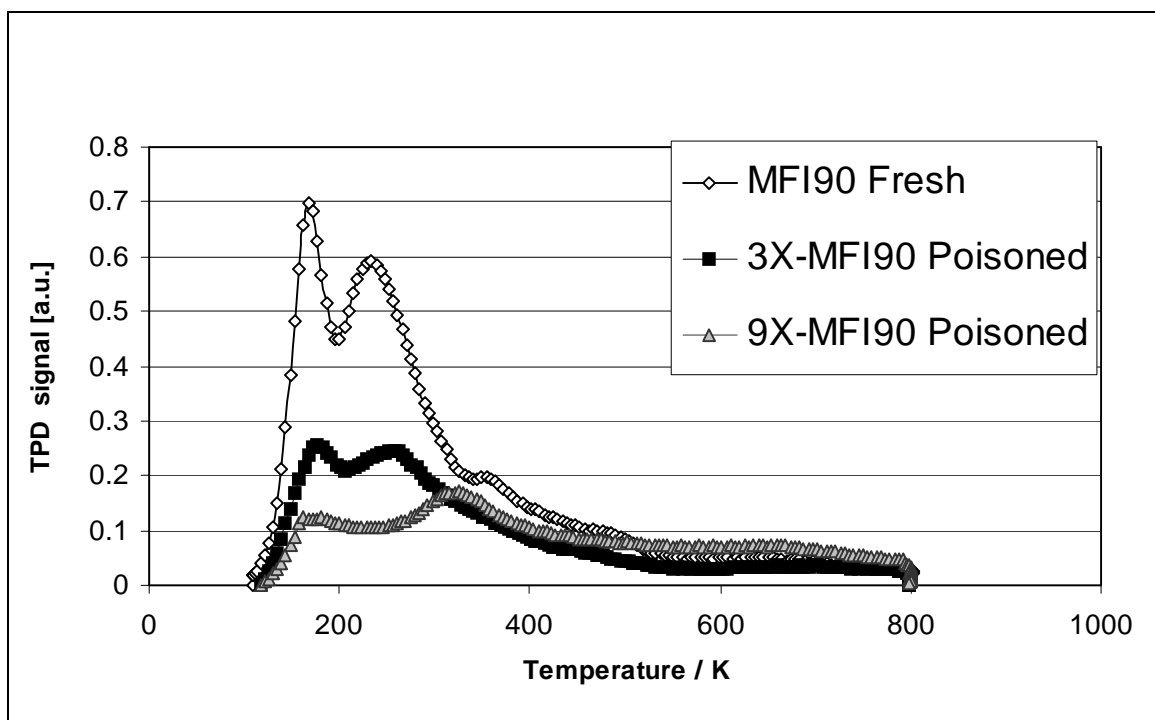


Figure 16 DTBPy-TPD of fresh and poisoned MFI-90 (HZSM-5 catalyst)

This confirms that the silylation method (CLD) has indeed poisoned a significant proportion of the external acid sites but it did not poison the entire external surface completely.

In Figure 16 the largest TPD signal was derived from the fresh HZSM-5 catalyst in DTBPy. This was reduced to about 64 % when the catalyst is poisoned (silylated) three times. In an attempt to further reduce the active sites of the catalyst the 9 x-poisoned catalyst was introduced and it could be observed that about a further 48 % less desorption took place when compared to the desorption observed using a 3 x-poisoned catalyst, thus indicating that an infinite number of silylation cycles could cause the catalyst to display no desorption at all.

Although the application of CLD was for an additional six-time cycle (triple the original producing sample for 3 x-poisoned), the further decrease of external acid sites was not proportional to the number of CLD cycles applied. Hence, it was decided, not to continue with the application of CLD, as a very large number of cycles would be needed to completely poison the catalytic external surface. The study was carried out by testing and comparing the degradation performance of three catalyst samples. These were fresh, 3 x-poisoned and 9 x-poisoned catalysts.

### 4.3. Thermo-Gravimetric Analysis (TGA) experiments

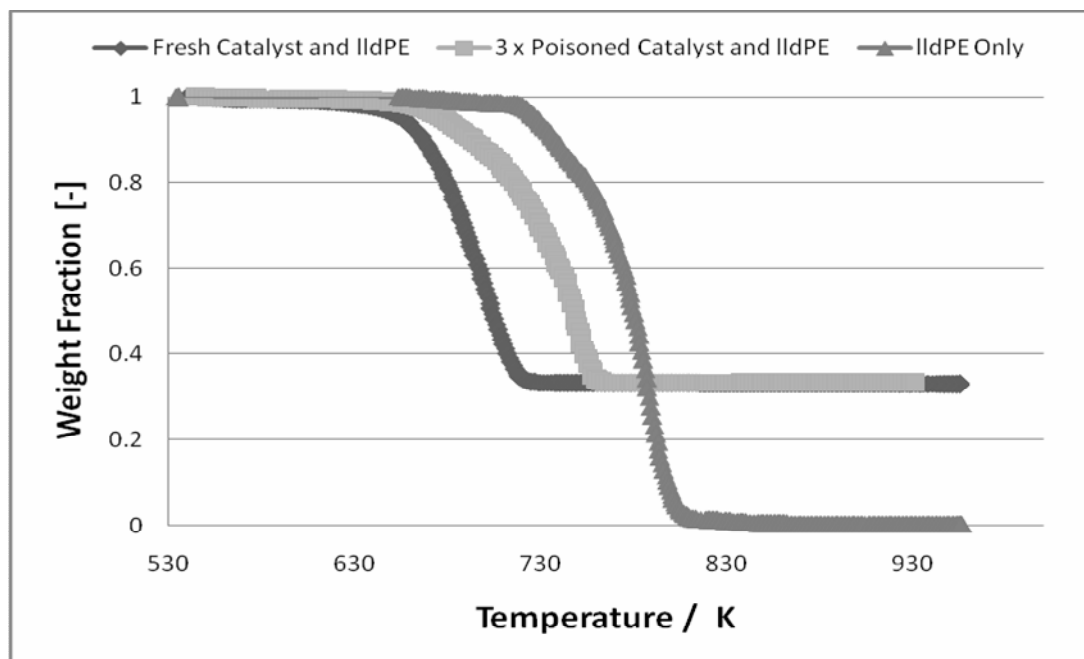


Figure 17: TGA results of lldPE degradation over Fresh HZSM-5, 3x-poisoned HZSM-5 and in the absence of any catalyst.

Figure 17 illustrates the weight fraction of TGA experiments over fresh and 3 x-poisoned HZSM-5 as well as in the absence of any catalyst. The final weight level corresponds to the amount of catalyst and coke formed on it. Therefore, there is a difference in the final weight level between the catalytic versus non-catalytic degradation. It is obvious from the results of Figure 17 that the 3 x poisoned samples degrade lldPE much slower than the fresh sample. It takes an additional 50 degrees for the 3 x poisoned sample to completely convert lldPE compared to the fresh catalyst sample. Despite the fact that 3 x-poisoned ZSM-5 had more than half of the external surface acid sites intact (64 %), the overall degradation reaction slowed down considerably, indicating that the initial macromolecule decomposition on the external surface is the overall reaction limiting step. There is a possibility of secondary reactions occurring in the internal zeolitic surface with the polymer fragments formed on the external surface after the initial decomposition. Nevertheless, even the 3 x poisoned catalyst degraded lldPE at almost 50 degrees lower than in the absence of any catalyst.



The thermo gravimetric analysis of lldPE degradation with HZSM-5 catalyst, MFI-90, demonstrates that the acidity of the catalyst is a crucial parameter in the initial degradation of lldPE.

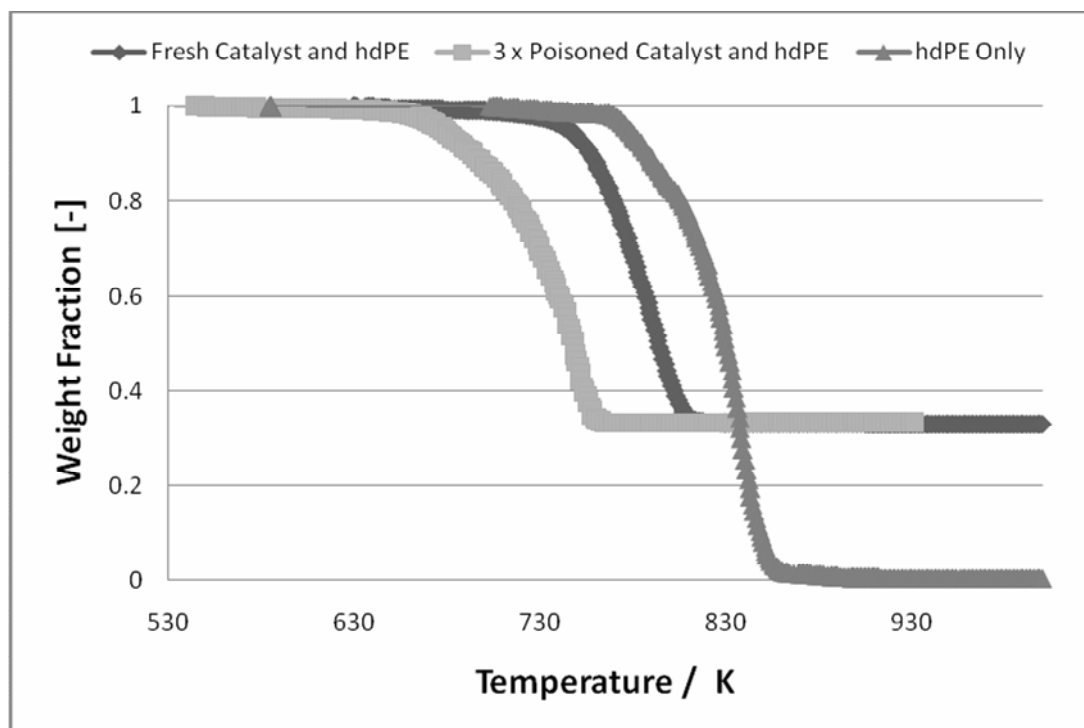


Figure 18: TGA results of hdPE degradation over Fresh HZSM-5, 3x-poisoned HZSM-5 and in the absence of any catalyst.

Similar results were observed when high density polyethylene was applied, as shown in Figure 18. This was done to clarify whether a similar effect could be obtained from utilising other polymers. In conclusion, there is a significant difference in overall catalytic degradation performance in regards to rate between the poisoned and fresh catalyst samples, which strongly suggests that the initial reaction step occurs on the external active sites of the catalyst. This gives an indication that the initial step seems to also be the overall reaction-limiting step as the rate of the degradation is clearly limited with increasing silylation. In reference to the temperature programmed desorption experiments, it is important to observe that the small difference between the  $\text{NH}_3$ -TPD desorption curves between the fresh and poisoned catalyst (Figure 15), is by far outweighed by the difference in the rate of degradation of the TGA and thus cannot be enough to justify the difference in the TGA performance. It is also worth reaffirming that even a reduced number of external active sites are enough at high temperatures to initiate faster degradation of the polymer to completion than would

have been observed with the polymer only (without any catalyst) as seen in TGA degradation curves.

#### 4.4. Semi batch experiments results

The semi batch experimental studies indicate that for the premixed polymer/catalyst particles at temperatures around 320°C, the molten polymer begins to get drawn into the spaces between particles and hence to active sites at the external surface of zeolite catalysts or in larger pores of amorphous materials. Surface reaction then produces lower molecular weight materials, which, if sufficiently volatile at reaction temperature, can either diffuse through the polymer film, as products or react further in the pores, including micropores of the zeolite catalyst. As a result, the product distributions reflect features of the zeolite catalysts in relation to their pore systems and chemical composition. In Figure 19 a standard experimental run depicting temperature increase against time of the reactor and controller is illustrated.

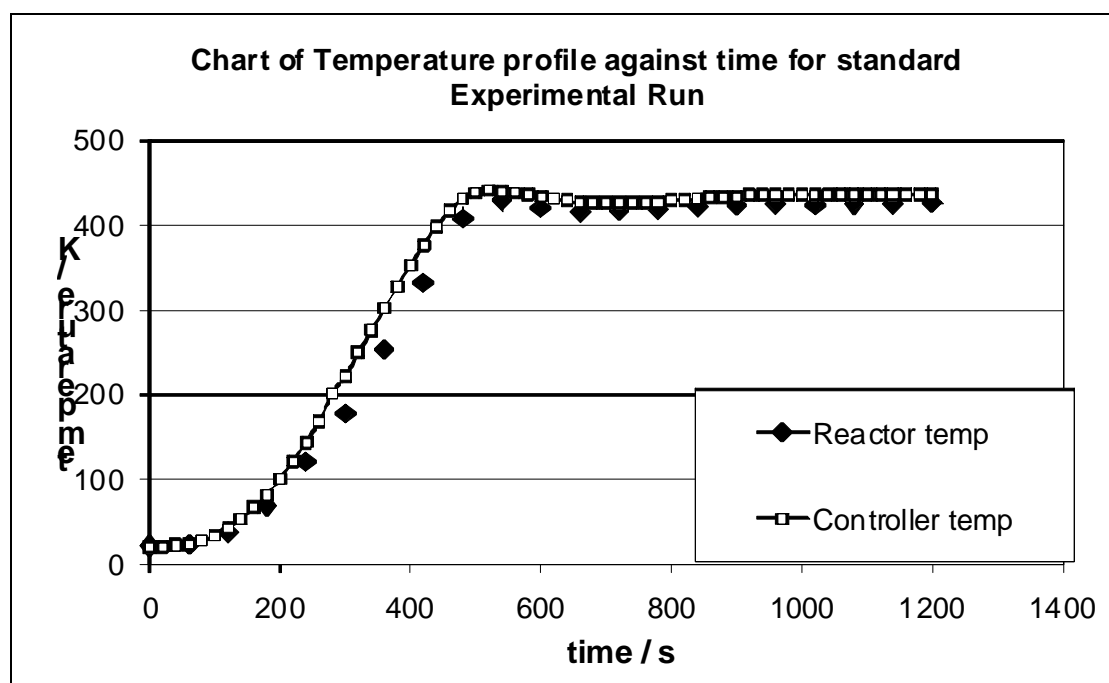


Figure 19 Temperature against time chart of both the reactor and controller for catalytic degradation of lldPE with HZSM-5 catalyst

A fast heating temperature programme that bore a close similarity to real process conditions was applied. The catalytic degradation results suggest that the largest

product yield occurs at a temperature range of 250°C to 350°C. Comparisons with the level of silylation (poisoning) of the HZSM-5 catalyst used and rate of conversion and product yield. The proficiency to which the silylated or poisoned catalyst affects the yields in comparison to fresh catalyst is greatly enhanced by the reduction of the maximum temperature for the controller temperature. The temperature profile at the lower maximum temperature can be observed in Figure 20. It means that a larger period of the experiment is focused within the region of optimum catalytic degradation. This is the temperature range in which the largest product yield is obtained. It also means that the experiment is more influenced by the strength of catalyst rather than the thermal influence during degradation.

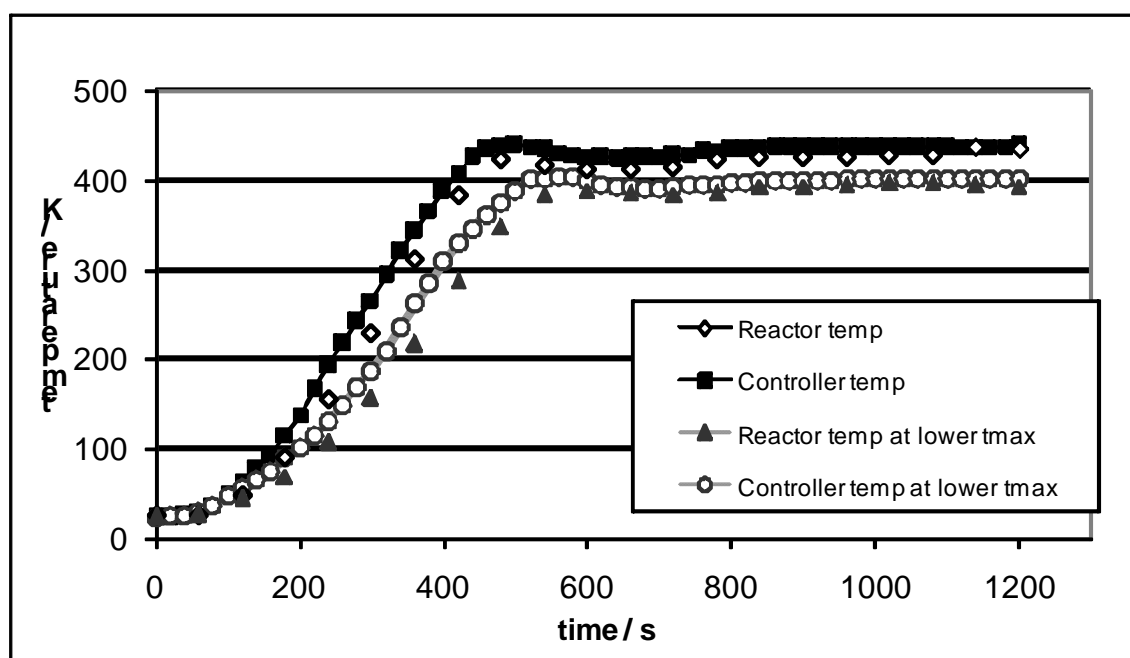


Figure 20 Reactor and controller temperature profiles during catalytic degradation of lldPE with ZSM-5 catalyst using two different controller set points ( $T_{max} = 725K$  and  $T_{max} = 673K$ ).

The difference in product yields, selectivity and conversion between the poisoned and fresh catalyst is not clear enough to make a definitive conclusion about influence of the silylation on the catalytic acid strength of each catalyst sample. Therefore the reaction was carried out at a lower maximum temperature of 400°C with the objective of creating greater disparity in the results derived.

Table 4 below illustrates the results obtained with respect to overall conversion selectivity to liquid fraction and the yield to liquid products for the ZSM-5 (HMFI 90) catalyst used in the catalytic degradation reaction that was conducted in the semi-batch reactor experiments. The experiments consider the effect of modifying the catalyst by silylation in relation to the results achieved

<b>Table 4: Mass fraction of liquid products</b>				
<b><u>Catalyst</u></b>	<b>Cumulative liquid Yield (g)</b>			
	<b><u>1</u></b>	<b><u>2</u></b>	<b><u>3</u></b>	<b><u>Total</u></b>
Fresh ZSM-5	0.06	0.27	0.34	0.34
3x-Poisoned ZSM-5	0.04	0.18	0.29	0.29
9x-Poisoned ZSM-5	0.03	0.09	0.19	0.18

The catalyst scenarios applied in this experimental study and illustrated in the table 4 below, involved experiments with pure catalyst, no catalyst, silylated and several times silylated catalyst.

<b>Table 5: Conversion, liquid yield, liquid selectivity, coke yield for catalytic degradation of lldPE with ZSM-5 at standard T max 725K</b>				
<b><u>Catalyst</u></b>	<b><u>Conversion</u></b>	<b><u>Selectivity to liquid</u></b>	<b><u>Yield to liquid</u></b>	<b><u>Coke Yield</u></b>
Fresh ZSM-5	0.99	0.35	0.34	0.01
3x-Poisoned ZSM-5	0.92	0.31	0.29	0.08
9x-poisoned ZSM-5	0.64	0.28	0.19	0.36

In Table 5, the conversion to volatile products was calculated as a fraction of the initial mass of polymer reacted to form volatile products. The selectivity was calculated as

the mass of the liquid collected divided by the mass of reacted polymer to volatile products and represents the liquid fraction of the volatile products. The yield to liquid product was derived from the mass of the liquid collected divided by the initial amount of polymer. The coke yield was obtained by dividing the mass of coke formed on the catalyst with the original mass of polymer. The coke yield represents the fraction of the original polymer converted to coke.

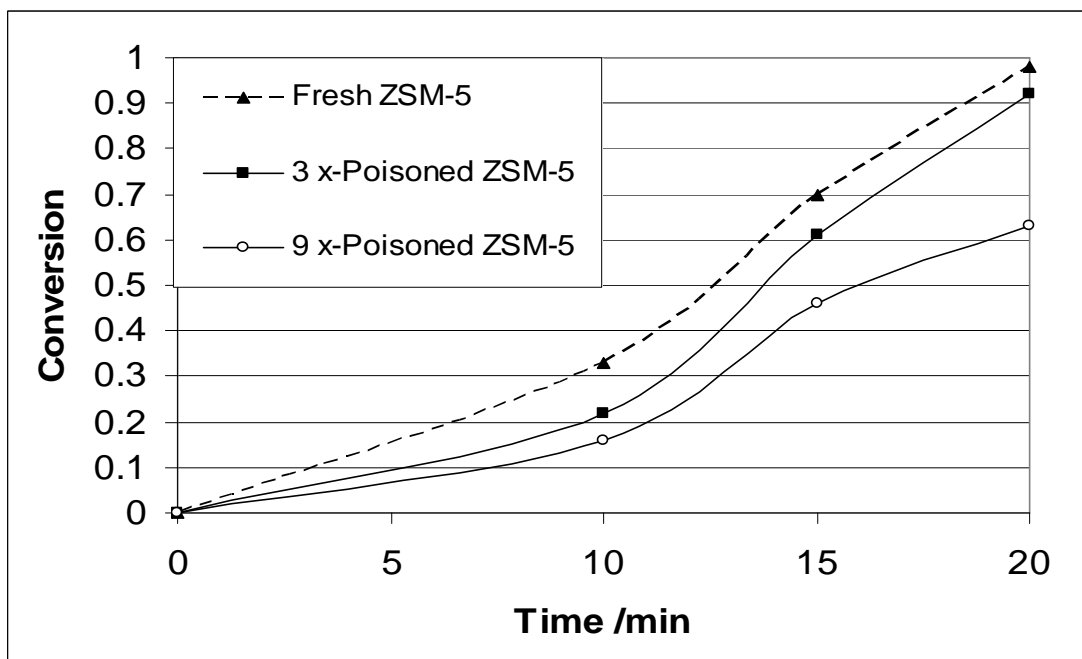


Figure 21 Conversion against time during catalytic degradation of lldPE using set point temperature  $T_{max}$  725K.

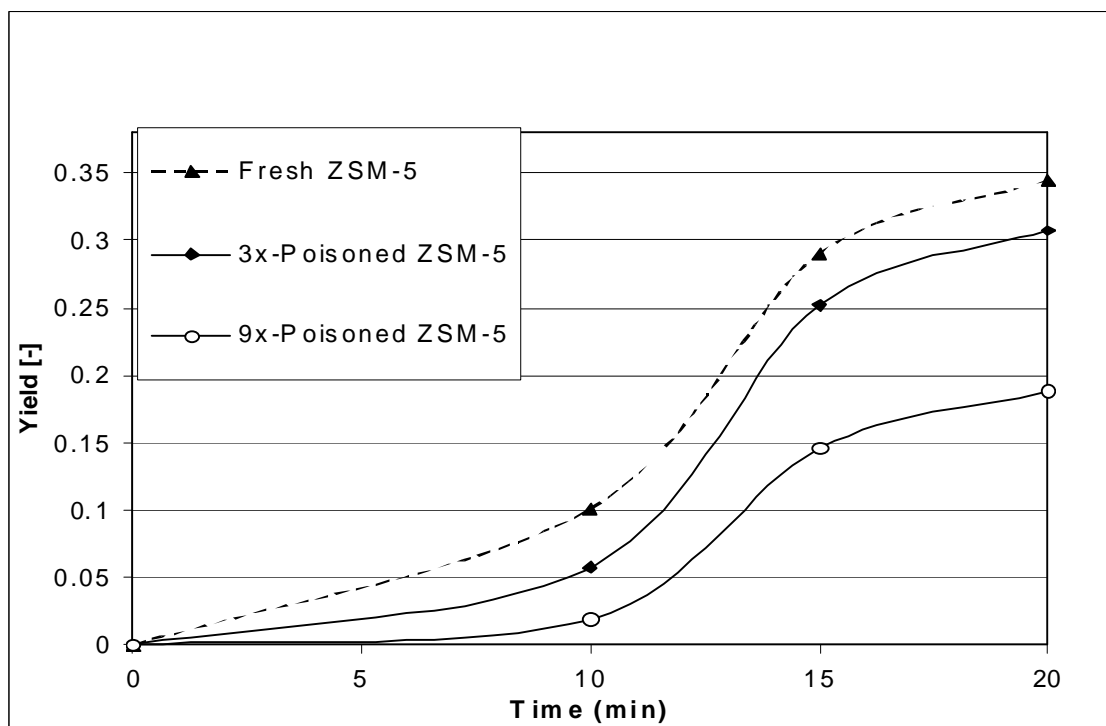


Figure 22 Yield against time during catalytic degradation of lldPE using set point temperature  $T_{max}$  725K

The results obtain from thermal catalytic degradation of lldPE with the HZSM-5 catalyst MFI-90 predictably demonstrate the highest liquid yield and overall conversion. It was observed that the bulk of liquid product obtained was produced during the second time interval, indicating the optimum activity of the zeolite occurred within a temperature range of 523 K to 623 K. The HZSM-5 catalyst MFI-90 has been silylated in this scenario and it can be observed in Figure 21 and 22, that when this manipulated catalyst is applied in the semi batch degradation of the polymer lldPE, there is a significant reduction in both the conversion and liquid yield derived.

It was concluded in previous studies that cyclic TEOS deposition involving repeated silylation of the HZSM-5 catalyst could be utilised in obtaining a more complete coverage of the external active sites by periodic removal of competitively adsorbed species [Weber et al.]. In the both Figure 21 and 22 it is clearly demonstrated that the level of silylation of the catalyst is appears to be inversely proportional to conversion and product yield. The lower conversion with the twice-poisoned catalyst indicates that a further degree of surface modification and thus reduction to the external active sites was achieved. This appears to have produced a lower selectivity and yield to liquid products. Also, the coke yield is fairly high and conversion decreases. It indicates that the poisoning of the catalyst lead to fewer acid sites, thus creating fewer opportunities for catalytic cracking but then also accounts for an increase in less refined liquid products. An experiment was performed without a catalyst to determine the extent of thermal degradation. After the reaction, a filmy clear yellow liquid, which cooled to a white solid, and some small particles, remained in the reactor. This is obviously not coke, in this case but un-reacted polymer. As expected, little volatile product was collected. This small conversion to volatile product (<2 %) in the absence of a catalyst shows that thermal degradation is a factor at the operating conditions of the semi batch reactor and must be considered in the analysis of reactions that involved catalyst. However, for the purpose of this investigation, the conversion is found to be minimal enough for most of the degradation. Therefore, it is fair to assume that polymer degradation in the other experiments is attributed mainly to the influence of the zeolite catalyst. It should be noted that the polymer used in these experiments was from a batch that is over ten years old and therefore may behave differently from fresh lldPE.

<b>Table 6: Mass Fraction of liquid products at lower T-max of 673K</b>				
<b><u>Catalyst</u></b>	<b>Cumulative liquid Yield (g)</b>			
	<b><u>1</u></b>	<b><u>2</u></b>	<b><u>3</u></b>	<b><u>Total</u></b>
Fresh ZSM-5	0.081	0.24	0.36	0.36
3x-Poisoned ZSM-5	0.022	0.05	0.09	0.09
9x-Poisoned ZSM-5	0.02	0.03	0.043	0.04

<b>Table 7: Conversion, liquid yield, liquid selectivity, coke yield for catalytic degradation of lldPE with HZSM-5 at lower T max 673K</b>				
<b><u>Catalyst</u></b>	<b><u>Conversion</u></b>	<b><u>Selectivity to liquid</u></b>	<b><u>Yield to liquid</u></b>	<b><u>Coke Yield</u></b>
Fresh ZSM-5	0.94	0.38	0.36	0.06
3x-Poisoned ZSM-5	0.44	0.2	0.09	0.56
9x-poisoned ZSM-5	0.09	0.45	0.04	0.91

The results from these semi-batch experiments clearly confirm that the zeolite loses acid strength when poisoned. This confirms that the changes in conversion and lowered product yields demonstrate that CLD of TEOS of the zeolite is an ideal option for catalytic surface modification. Figures 21, and 22, reveal that for the zeolites HZSM-5 (MFI-90) used, the temperature, overall percentage liquid yield and conversion all increased with time.



Figure 23 Conversion graph versus time at lldPE at lower T max.

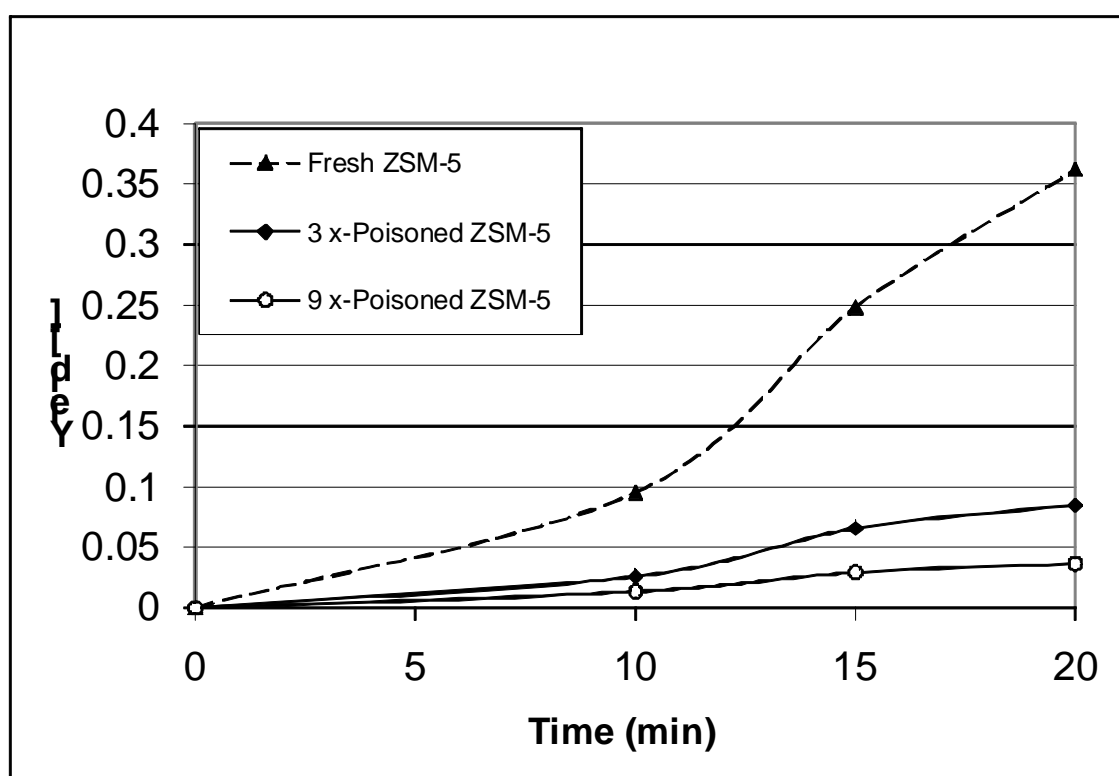
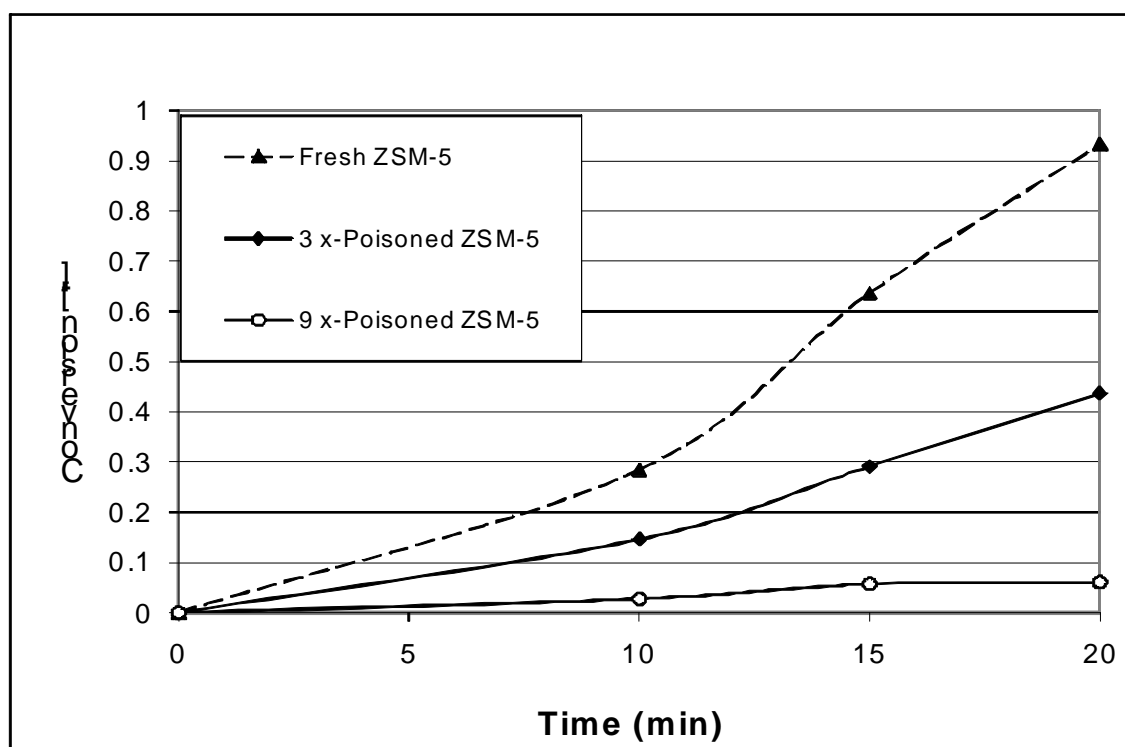


Figure 24 Yield graph versus time for catalytic degradation of lldPE at lower T max with HZSM-5 catalyst

In the results obtained from using lower maximum controller temperature and thus reaction temperature, thermal catalytic degradation of lldPE with the HZSM-5 catalyst MFI-90; predictably demonstrate the highest liquid yield and overall conversion. It was also observed that the bulk of liquid product obtained was produced during the second time interval as in the standard run. However, the conversion was less but liquid yield was slightly enhanced indicating the optimum activity of the zeolite occurs within temperature ranges of between 523 K and 623 K. The reaction also produced less gaseous products. Invariably the overall result here is similar to the previous test. When the HZSM-5 catalyst (MFI-90) has been silylated in this scenario and it can be observed in Figure 23 and 24, that when this manipulated catalyst is applied in the semi batch degradation of the polymer lldPE at the lower maximum temperature of 673 K, there is a significant reduction in the both the conversion and liquid yield derived. As previously stated [Weber et al.] concluded that cyclic TEOS deposition involving repeated silylation of the HZSM-5 catalyst could be utilised in obtaining a more complete coverage of the external active sites by periodic removal of competitively adsorbed species. This theory is better clarified in Figures 23 and 24. In both these Figures it is clearly demonstrated that the level silylation of the catalyst appears to be inversely proportional to conversion and product yield. The lower conversion with the twice-poisoned catalyst indicates that a further degree of surface modification to the external active sites was achieved. This appears to have produced a lower selectivity and yield to liquid products. Also, the coke yield is fairly high and conversion decreases. It indicates that a poisoning leads to fewer acid sites that provide fewer opportunities for catalytic cracking and this account for an increase in less refined liquid products

## 4.5 Conclusion

In summary, although the experimental temperature at the standard run of 725 K produces higher overall conversion, it also compensates for the reduction of the catalytic acid sites of the silylated catalysts. Therefore the differences in the yields and conversion were not significantly clear enough. In conjunction with this liquid yield appeared to be relatively higher than anticipated when the poisoned samples were used, thus indicating that the reduction of external active sites have reduced secondary

over-cracking reactions leading to a lower gas to liquid product ratio typical of a HZSM-5 catalyst. As a result of this, the lower maximum temperature ( $T_{\max}$ ) of 673 K is utilised to enable the experimental run to be carried out at a temperature range that is closer to what appears to be an optimum temperature boundary for the catalytic degradation of the lldPE. This was previously mentioned above as ranging from 523 K to 623 K. The results of this show that overall degradation was not as strong even without any poisoning or silylation of the catalyst ZSM-5. The conversion for the fresh catalyst dropped from 99 % to 92 % with the yields dropping slightly from 34 % to 32 %. It is quite understandable for the yield to be comparable has less secondary reactions occurred due to the lower maximum experimental temperature. As result of the maximum temperature of is lower much of the catalytic degradation is occurring within the optimum temperature range and thus leading to a more catalytic than thermal influence on the results. The conversion and yield charts in Figures 23 and 24 strongly indicate that for the three and nine times silylated catalyst there is a significant reduction in both conversion and yield. It is also clearly demonstrated that as a result of blocking the external active sites through silylation, the degradation of the polymer is significantly reduced and this reduction observed, from comparing the yield reduction witnessed with 3x and 9x silylation, could be said to be proportional to the number silylation cycles carried out on the catalyst and thus the number of external active sites available. Although some catalytic degradation still occurs it is fair to expect that an infinite number of silylation cycles would lead to no degradation as a result of the complete removal of the external active sites. Though it was not possible to completely poison the active sites on the external catalyst surface, it was shown that the external acid sites are responsible for the initial decomposition of the polymer macromolecules. Prepared catalyst samples with different levels of external blocking showed correspondingly lower activities in polymer degradation, especially its initial stages, in both experimental rigs used, TGA and semibatch reactor. In TGA the polymer degradation over fresh ZSM-5 started at considerably lower temperatures than over silylated samples. In semibatch reactor experiments the time profiles of the yield of liquid products formed over fresh catalyst showed an earlier rise than over poisoned samples. These results have been confirmed with experiments at lower reactor temperature where activity differences between the samples have been accentuated.

## Chapter Five

### Catalyst Deactivation and Reusability

---

*This chapter presents results in terms of product yield and distribution obtained from the experiments investigating catalyst deactivation and reusability.*

#### 5.1 Introduction

The investigation of catalytic reusability is important for the assessment of the economics of any potential catalytic processes. It would influence the effects of the number of cycles used, the length of time of each cycle and generally how long a catalyst is used. In light of this, the investigation in this chapter aims to evaluate the effects of catalytic deactivation and reusability on product yield and distribution. Specifically this section investigates the catalytic reusability for numerous reaction cycles without regeneration, i.e. removal after each cycle of the formed coke by oxidation. Previous studies of reusing the catalyst after burning off the formed coke have been carried out before for various catalytic groups [Gobin K et al (2001), De la Puente G., et al], these were done in order to test the regenerability of the catalysts.

The analysis of experimental results found in this set of experiments bear three levels of comparison: the results with respect to conversion and liquid yield against time of each experimental run, the comparison of three or four successive runs with each selected catalyst and a final comparison amongst the catalysts of the boiling point distribution after a set number of consecutive runs. The results section will therefore be divided into categories that discuss each individual catalyst tested (including any variations with respect to time) and a final comparison will be made in the discussion section.

### 5.1.1 US-Y Catalyst

The overall results of catalytic degradation of lldPE over USY catalysts, with fresh (1<sup>st</sup> run) as well as deactivated once (2<sup>nd</sup> run) and twice (3<sup>rd</sup> run) are presented in Table 8; the experiments had a polymer to catalyst ratio 2:1 and a final reactor temperature set at 725 K. Conversion of lldPE over US-Y catalyst proceeded much as expected. The fresh catalyst yielded a relatively high conversion, about 95 %, and the subsequent reactions resulted in progressively lower conversion values, as the catalyst became increasingly deactivated due to coke formation. Coke yield was low during the first reaction run (about 5 %), but as expected, this increased with each run as less of the polymer was successfully converted. In fact, the third reaction run resulted in leftover un-reacted polymer, which was evidenced by shiny black clumps in the semi-batch reactor. Despite these dismal results however, the additional reactions with deactivated catalyst samples actually resulted in higher liquid yield and selectivity values at 1-6 %.

**Table 8: US-Y Catalyst Results**

	<b>1st Run</b>	<b>2nd Run</b>	<b>3rd Run</b>
<b>Conversion (%)</b>	<b>95</b>	<b>88</b>	<b>85</b>
<b>Selectivity to Liquid (%)</b>	<b>28</b>	<b>35</b>	<b>36</b>
<b>Yield to Liquid (%)</b>	<b>26</b>	<b>30</b>	<b>31</b>
<b>Coke Yield (%)</b>	<b>5.4</b>	<b>6.8</b>	<b>3.2</b>
<b>Cumulative Coke Yield (%)</b>	<b>5.4</b>	<b>12.2</b>	<b>15.4</b>

Furthermore, Figure 25 shows the time profile of the polymer conversion of the three samples. Although there wasn't much overall difference in the values which were achieved, the activity of the fresh sample was much higher at low temperatures corresponding to the reaction time (5 – 10 minutes) compared to those of the deactivated ones. Higher reaction temperatures compensated, causing the gap to decrease. The time profiles of the cumulative liquid yield (Figure 26) confirm this trend. In the first interval (5 – 10 minutes) at low temperatures the fresh sample produced by far the most liquid. In fact, hardly any liquid product was collected during this interval in the third reaction run. Higher temperatures at later intervals have reversed this trend in combination with the lower acidity of the deactivated samples.

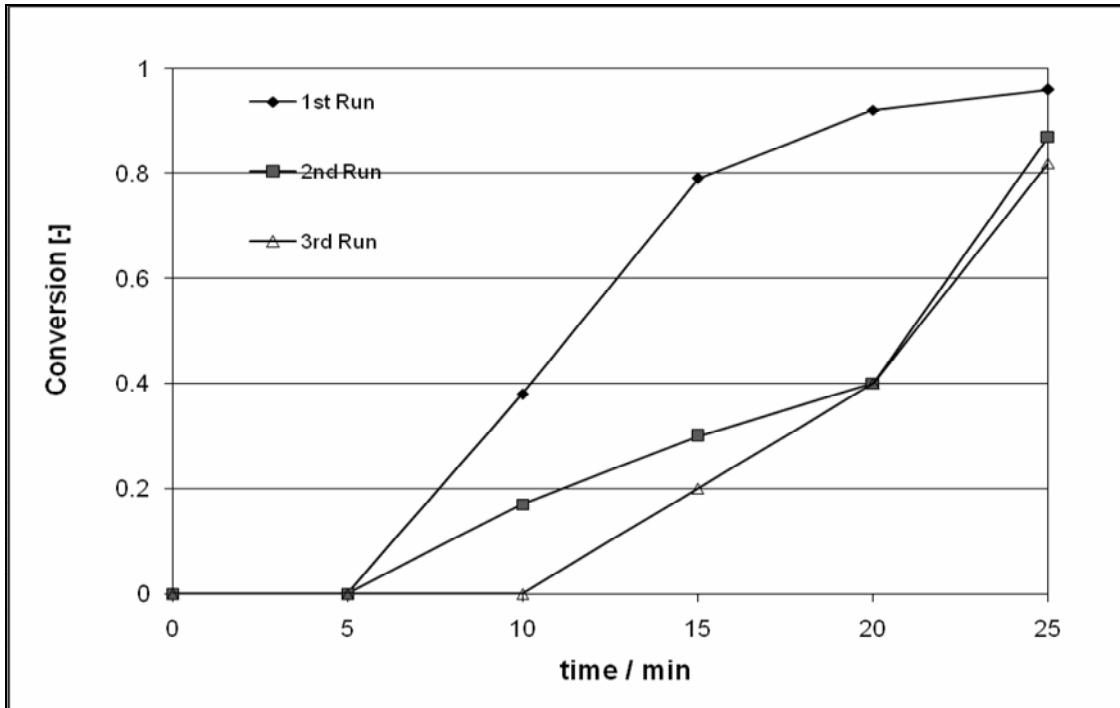


Figure 25: Conversion over US-Y catalyst samples (fresh and deactivated) against time during catalytic cracking of lldPE

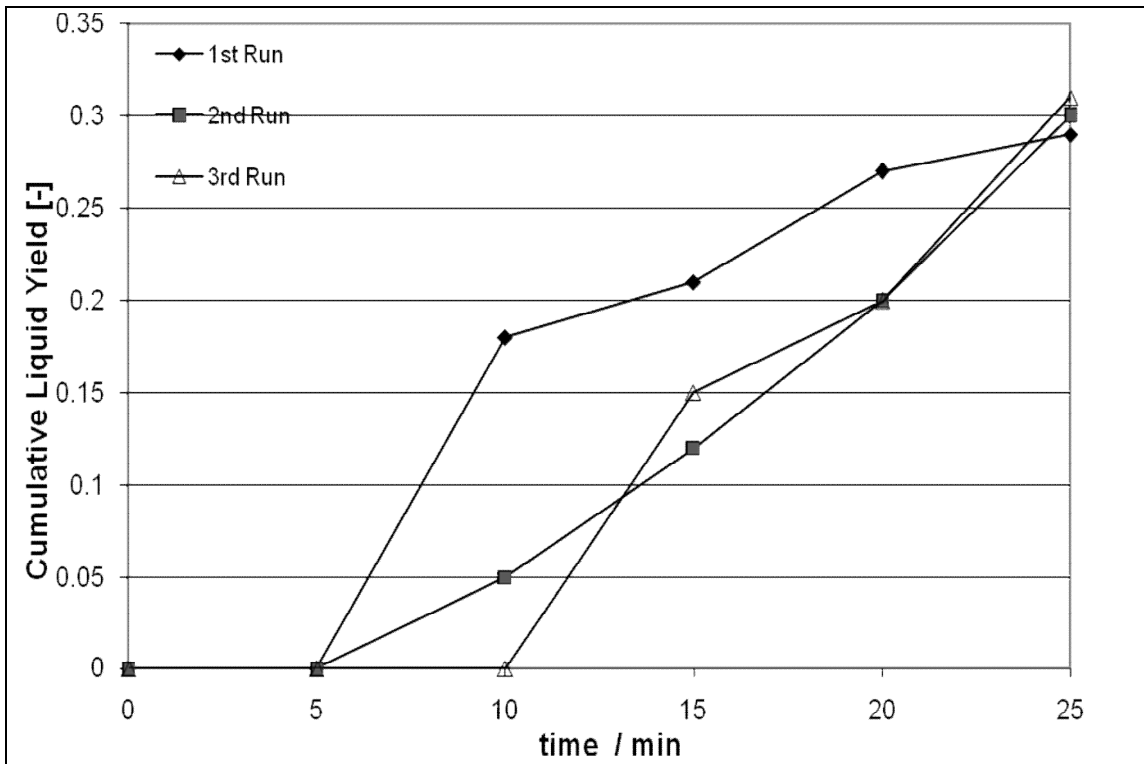


Figure 26: Liquid Yield for US-Y Catalyst samples (fresh and deactivated) against time during catalytic degradation of lldPE

The consistency of the experimental conditions is demonstrated in connection with temperature profiles (Appendix 2, Figure A3.1). The temperature profiles were similar for each reaction. This indicates that products were collected at times when the reactor reached the temperatures necessary to degrade the polymer as the catalyst was deactivated in consecutive experimental runs. All the catalysts used in the deactivation study displayed similar trends.

Progressive deactivation of the US-Y catalyst can also be seen in boiling point distributions of the liquid samples shown in Figure 27. The boiling point distributions in this chapter are presented using only three fractions light, mid-point and heavy, rather than the usual 16 fractions as previously explained in the experimental chapter. This simpler results presentation is preferred in order to have a better overview of the changing trends. In Figure 27 condensers 1, 2 and 3 represent the liquid products derived from each successive experimental runs. The boiling point distributions of liquid products formed during cracking of lldPE over fresh US-Y catalyst mostly contained light components of lower molecular weight (corresponding to C<sub>4</sub>-C<sub>9</sub> region), each following sample resulting in less of the light and more of the heavy hydrocarbons. The second reaction run produced a similar progressive trend in the same direction (Figure 27); perhaps this is as a result of the unconverted polymer. This increase in heavy hydrocarbon weight with respect to time makes sense as more volatile products are converted earlier in the reaction. The average boiling point distributions for each reaction show that fresh catalyst produced the most low molecular weight hydrocarbons, while the third and last reaction produces the most high-molecular weight hydrocarbons (Figure 27). This illustrates that the deactivated catalyst becomes less and less successful at cracking the polymer into smaller weight hydrocarbons. The lower activity of deactivated catalyst samples resulted in lower cracking activity that lead to heavier products. This is manifested in higher liquid selectivity but also the formation of heavier hydrocarbons.

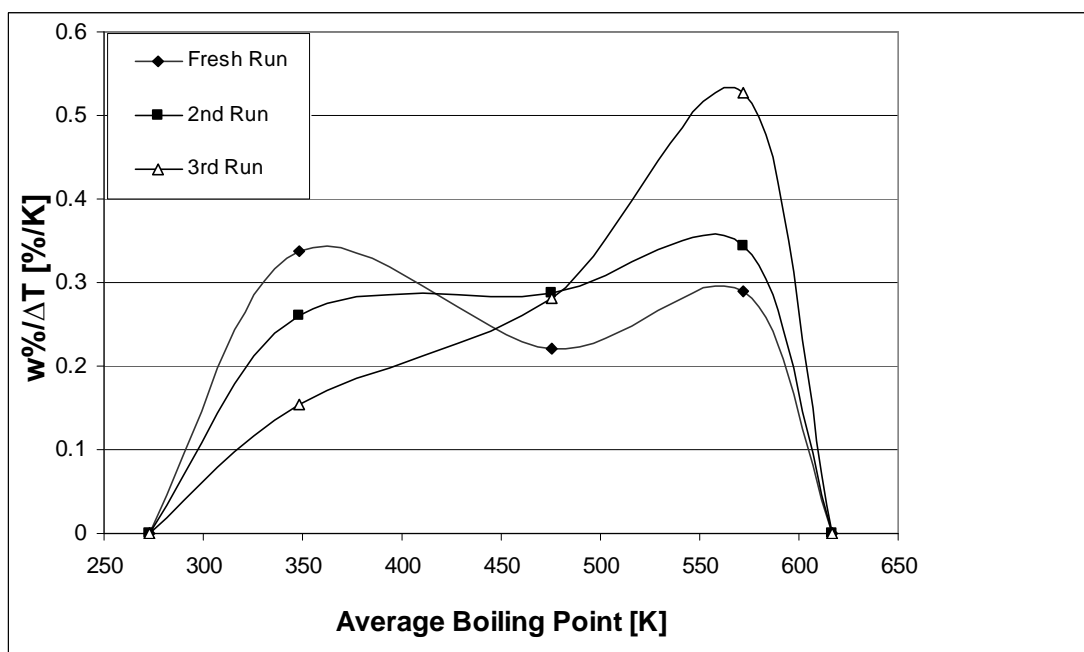


Figure 27: Boiling point distribution of liquid product formed during cracking of lldPE with US-Y catalyst over successive experimental runs

### 5.1.2. Cracking catalyst 1 (20 % US-Y catalyst)

The deactivation of cracking catalyst 1 was much slower than that of US-Y due to its lower acidity [Manos G et al (2001)]. Conversion with the commercial cracking catalyst 1 was very high, at 98 % (Table 9), and actually remained consistently high with further reaction runs. This of course also corresponded to very low coke yield 1 % for fresh catalyst (1<sup>st</sup> Run) and less than 1 % thereafter (Table 9). Like reactions with fresh US-Y, the commercial catalyst produced higher liquid yield and selectively with each successive reaction for all three reactions. Due to its lower acidity fresh cracking catalyst 1 produced significantly more liquid than US-Y [Manos G et al (2001)].

**Table 9: Cracking Catalyst 1 (20 % US-Y) Results**

	<b>1st Run</b>	<b>2nd Run</b>	<b>3rd Run</b>
<b>Conversion (%)</b>	<b>98</b>	<b>99</b>	<b>99</b>
<b>Selectivity to Liquid (%)</b>	<b>59</b>	<b>60</b>	<b>67</b>
<b>Yield to Liquid (%)</b>	<b>58</b>	<b>61</b>	<b>67</b>
<b>Coke Yield (%)</b>	<b>1</b>	<b>0.3</b>	<b>0.4</b>
<b>Cumulative Coke Yield (%)</b>	<b>1</b>	<b>1.3</b>	<b>1.7</b>



Figure 28 shows the time profile of the polymer conversion for each reaction run. The initial activity of the fresh catalyst at low temperature, up to 10 minutes, is considerably higher than that of those of the deactivated samples, obviously due to the deterioration of the acidity with each reaction run even with a relatively low amount of coke formed. Higher temperatures appear to compensate for the loss of activity, bringing the overall conversion to similar levels.

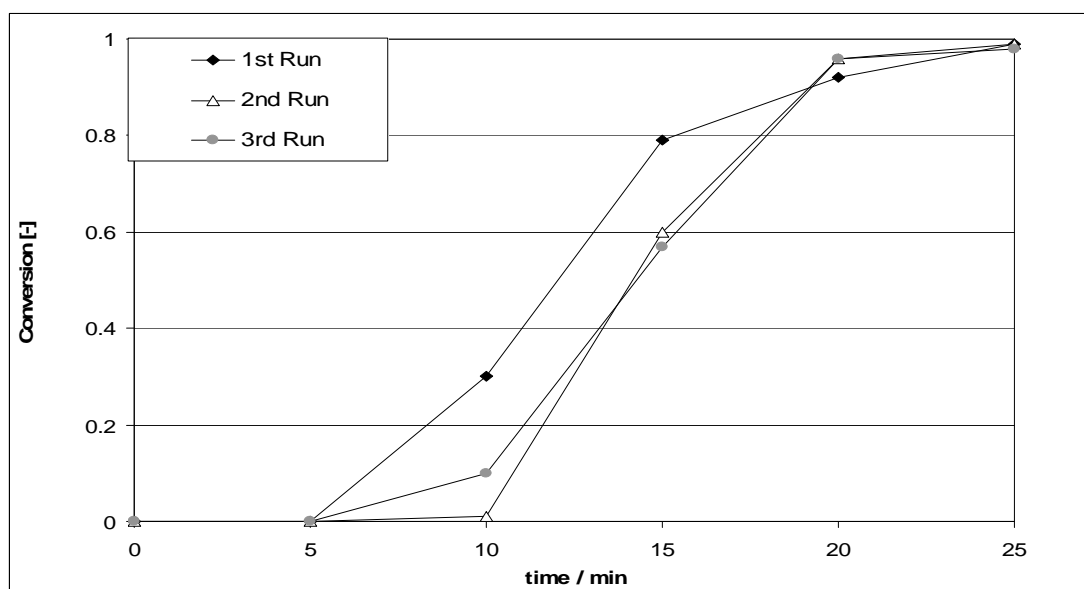


Figure 28: Conversion over Cracking Catalyst 1 (20% US-Y samples (fresh and deactivated)) against time during catalytic degradation of lldPE

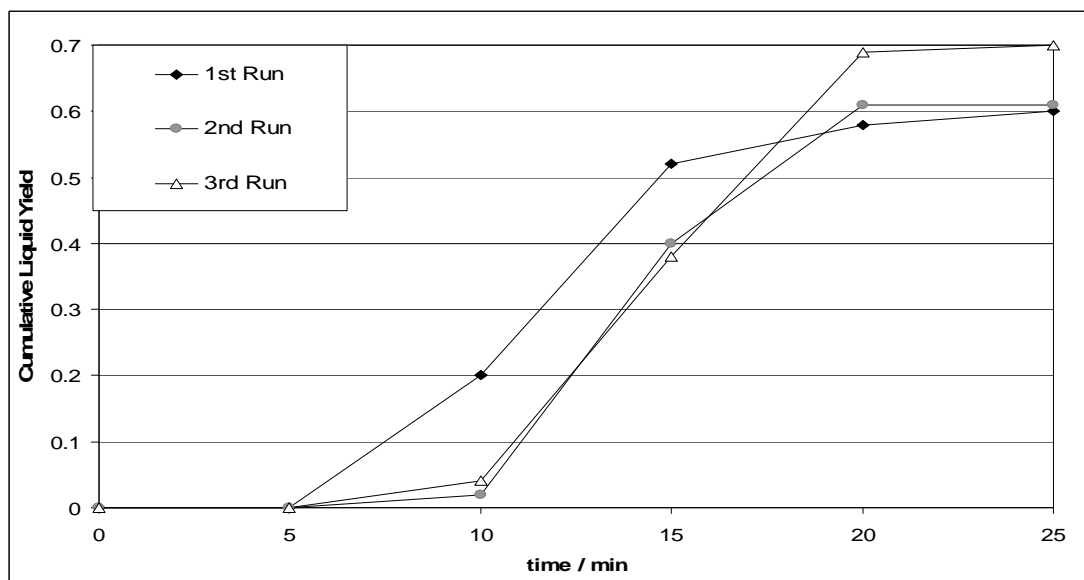


Figure 29: Cumulative liquid yield over Cracking Catalyst 1 (20 % US-Y Catalyst) fresh and deactivated samples against time during catalytic degradation of lldPE

The temperature profiles for these were also very similar as previously mentioned in (Appendix 1, Figure A3.1), so that further supports the view that commercial cracking catalyst 1 (20 % US-Y) remains mostly active with successive reactions; roughly the same amounts of products are formed during the same time periods and therefore at the same temperatures.

The relative lack of deactivation of cracking catalyst 1 (20 % US-Y) is also seen by the changes (or lack thereof) in boiling point distributions of each reaction compared to pure US-Y. The boiling point distribution over the fresh catalyst differs very little from that of the 2<sup>nd</sup> run. The liquid formed during the second run contains slightly less light components and correspondingly slightly more heavy components. This trend becomes obvious in the third run indicating a shift of product distribution towards heavier components with each deactivation cycle due to lowering of the catalyst acidity. Overall the cracking catalyst 1 has shown itself to be relatively resistant to deactivation by coking, especially much more resistant than the pure zeolite US-Y.

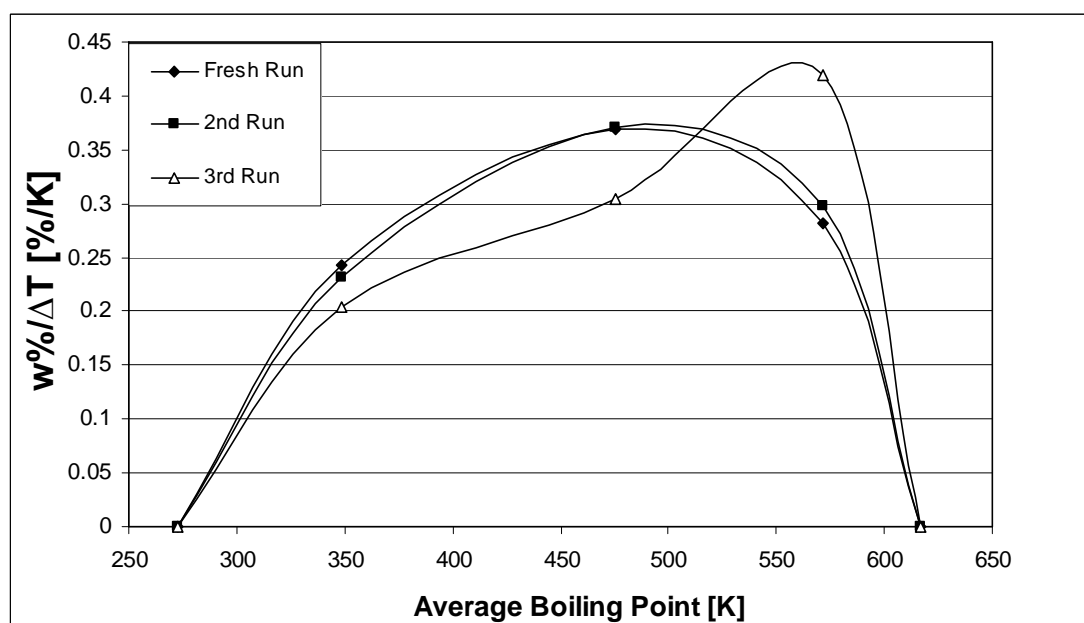


Figure 30: Boiling point distribution for Cracking Catalyst 1 (20 % US-Y), fresh and deactivated.

### 5.1.3. Commercial Cracking Catalyst 2 (40 % US-Y) Catalyst

Conversion with cracking catalyst 2 was also quite high, over fresh sample as well as deactivated catalysts (Table 10). The high conversion values and corresponding low

newly formed coke values; indicate that cracking catalyst 2 remains relatively active with continued use. Liquid product yield and selectivity values actually increase with each reaction run obviously due to lowering of the catalytic acidity with each cycle that leads to less degree of cracking of the original polymer resulting in slightly larger liquid molecules.

**Table 10: Cracking catalyst 2 (40 % US-Y) Results**

	1st Run	2nd Run	3rd Run	4th Run
<b>Conversion (%)</b>	<b>98</b>	<b>99</b>	<b>99</b>	<b>98</b>
<b>Selectivity to Liquid (%)</b>	<b>57</b>	<b>62</b>	<b>68</b>	<b>64</b>
<b>Yield to Liquid (%)</b>	<b>55</b>	<b>61</b>	<b>67</b>	<b>63</b>
<b>Coke Yield (%)</b>	<b>2.5</b>	<b>0.8</b>	<b>0.2</b>	<b>1</b>
<b>Cumulative Coke Yield (%)</b>	<b>2.5</b>	<b>3.3</b>	<b>3.5</b>	<b>4.5</b>

Figure 31 shows the time profile of polymer conversion over fresh and deactivated samples. The first reaction with fresh catalyst produced mostly liquid product, collected in sample number 1 and number 2. The other reaction runs remain relatively constant with most products collected in sample number 2.

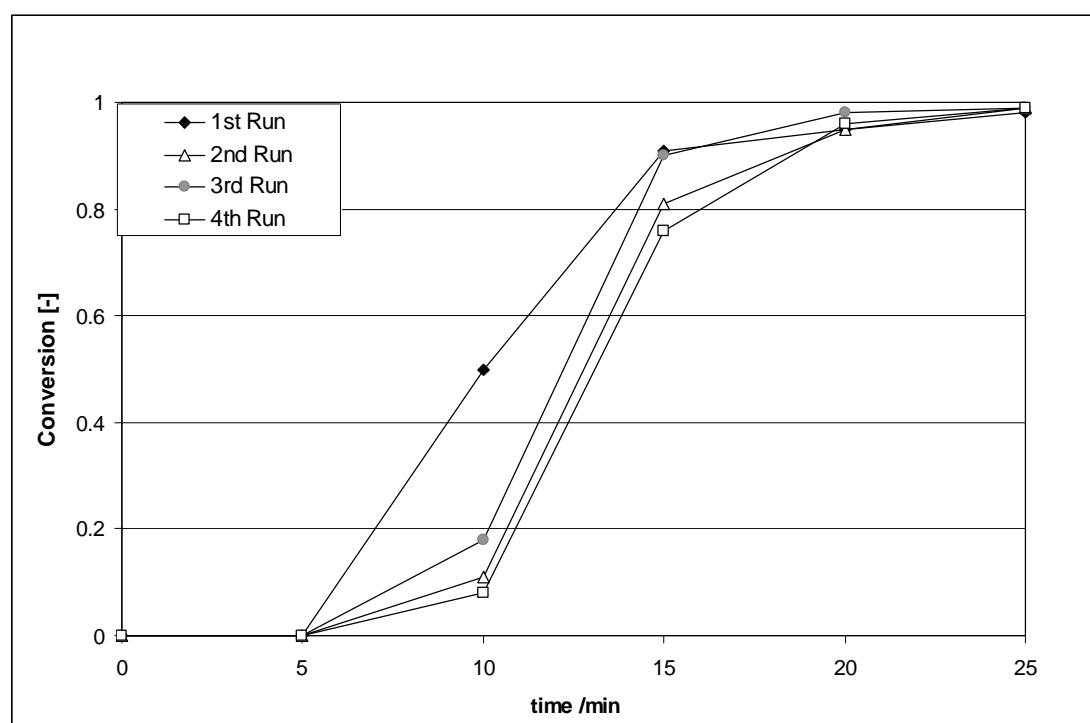


*Figure 31: Conversion over cracking catalyst 2 (40 % US-Y), fresh and deactivated samples against time during catalytic degradation of lldPE*

This trend is supported by the cumulative yield data collected for each reaction run. During the initial reaction stage up to 10 minutes (at low reaction temperature) the liquid yield over the fresh catalyst is considerably higher than over the reused catalysts due to its higher activity. At higher temperatures however, the reused catalyst samples reach higher liquid yield values. This indicates that with each reaction run the catalyst acidity weakens resulting in lower polymer cracking activity and lower amount of low molar mass components that are collected as gas.

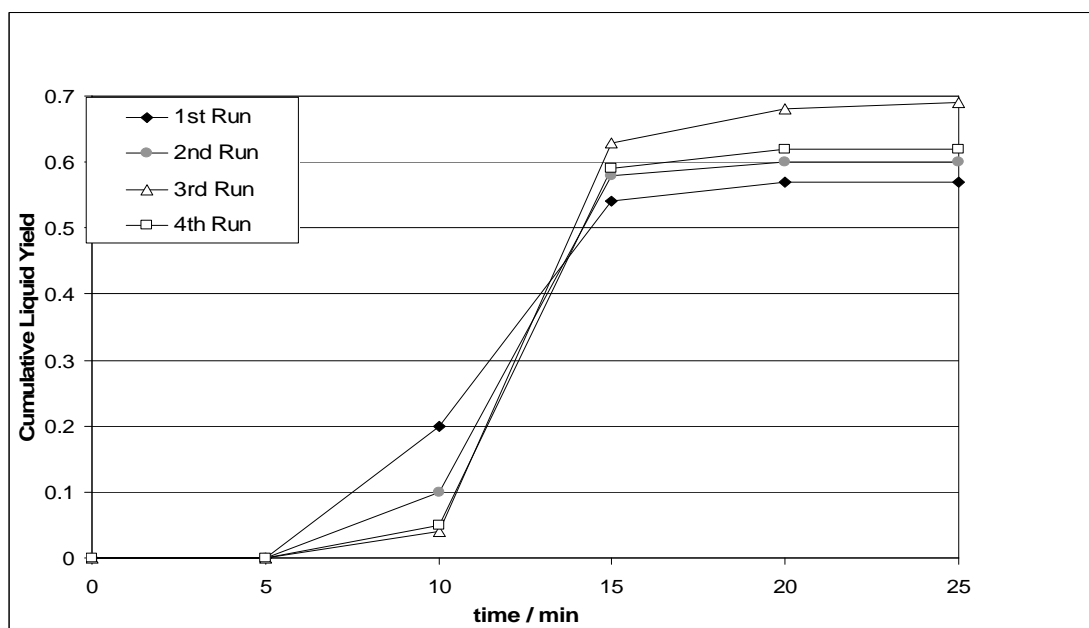


Figure 32: Cumulative liquid yield over Cracking Catalyst 2 (40 % US-Y fresh and deactivated samples) against time during catalytic degradation of lldPE

The above data does imply that the Cracking Catalyst 2 (40 % US-Y) has suffered relative deactivation; the boiling point distributions also suggest that coking has affected the composition of liquid products. The samples for the first reaction fresh catalyst have approximately the same composition, but the samples taken in the second follow a similar pattern as those in the (20 % US-Y) Cracking Catalyst 1 with products shifting from higher to lower molecular weights from lighter to heavier components with each consecutive sample (Figure 33).

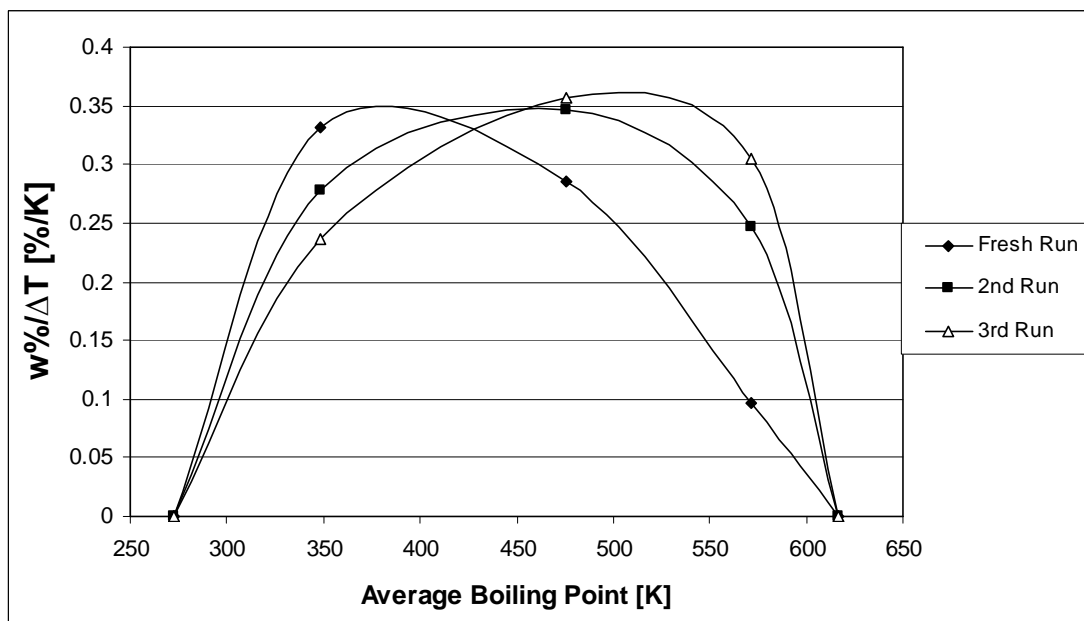


Figure 33: Boiling point distribution curves for Cracking Catalyst 2 (40 % US-Y)

#### 5.1.4. HZSM-5 Catalyst

Conversion with HZSM-5 catalyst proceeded very well across all reaction runs with final conversion values reaching 98-100 % (Table 11). This corresponded to low coke yield and reflect the high resistance of HZSM-5 catalyst to coke formation due to its small diameter pores that prohibit the formation of large coke molecules.

**Table 11: HZSM-5 Catalyst Results**

	1st Run	2nd Run	3rd Run	4th Run
<b>Conversion (%)</b>	<b>99</b>	<b>99</b>	<b>98</b>	<b>99</b>
<b>Selectivity to Liquid (%)</b>	<b>33</b>	<b>33</b>	<b>36</b>	<b>36</b>
<b>Cumulative Yield to Liquid (%)</b>	<b>34</b>	<b>35</b>	<b>36</b>	<b>36</b>
<b>Coke Yield (%)</b>	<b>0.1</b>	<b>0.2</b>	<b>1.81</b>	<b>0.01</b>
<b>Cumulative Coke Yield (%)</b>	<b>0.1</b>	<b>0.3</b>	<b>2.11</b>	<b>2.12</b>

Figure 34 illustrates the relative conversion of polymer to different products. Very small amounts of coke are produced. Most products produced are gaseous and the small amounts of liquid products shift from most being collected in sample number 1 to more in the second and third samples.

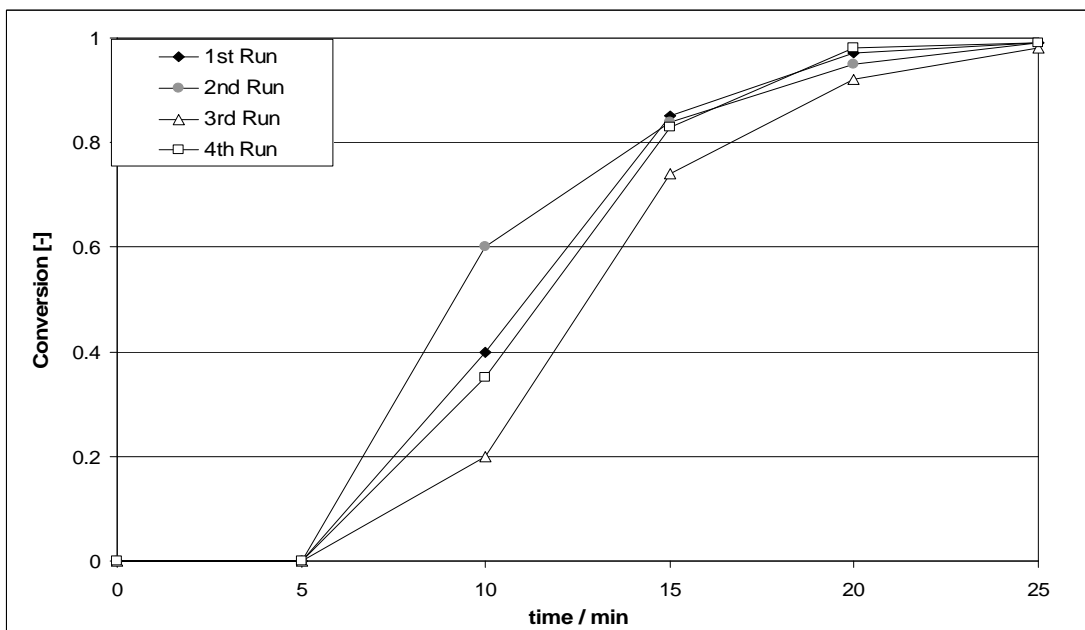


Figure 34: Conversion HZSM-5 Catalyst samples of fresh and deactivated against time during catalytic degradation of lldPE.

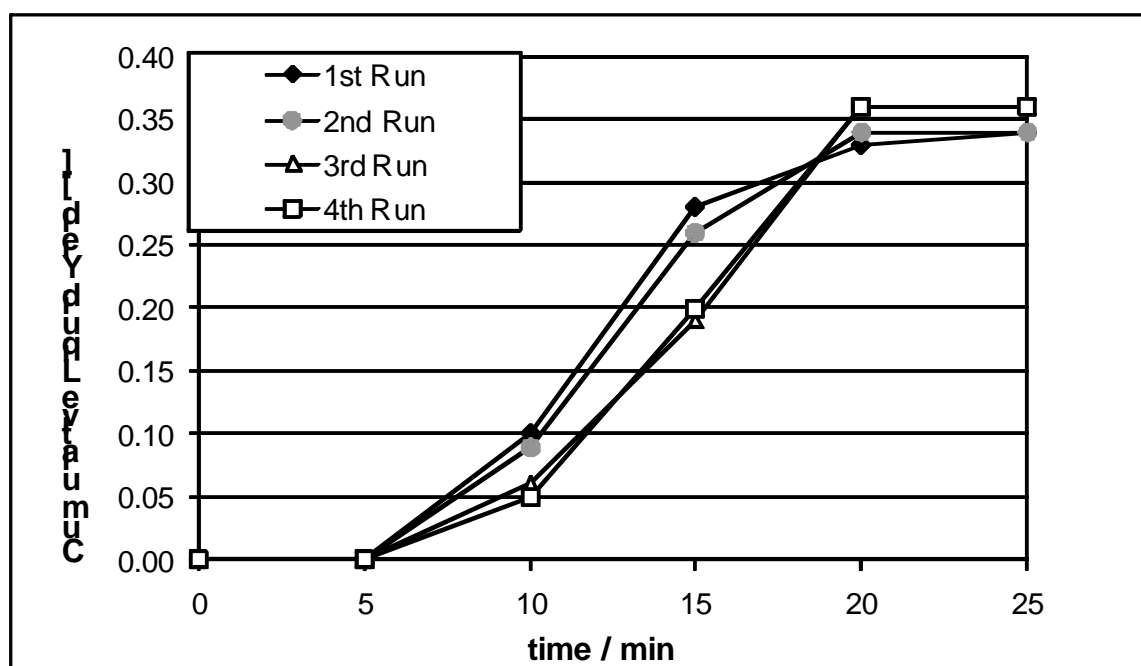


Figure 35: Cumulative liquid yield over HZSM-5 catalyst samples fresh and deactivated against time during catalytic degradation of lldPE

The cumulative yield supports this trend, but is less obvious as the slopes of conversion with respect to time remain relatively constant across the different reactions (Figure 34). With the similar temperature profiles this demonstrates the

catalyst's resistance to deactivation. The boiling point distributions indicate different performance trends of HZSM-5 catalyst compared to those with US-Y. There was only one sample collected for the first reaction, but this and the second reaction indicates that there are more, heavy than light hydrocarbons produced earlier in the reaction time (Appendix 2, Table A2.4). The boiling point distribution of the third and fourth reaction remains relatively constant across samples. The average boiling point distributions calculated from the sample mass fractions, in Figure 36, indicate that a similar trend takes place with successive reactions. The fresh catalyst produces the most, higher weight hydrocarbons and the following reactions all produce more of the lower weight hydrocarbons. This suggests that rather than being deactivated by the process of coking, HZSM-5 is actually better able to reduce polymer into smaller hydrocarbons with successive reactions. The amount of total coke accumulated was found to be 0.008 grams, yielding a total accumulated coke concentration of 2.12 %. This is consistent with measured data.

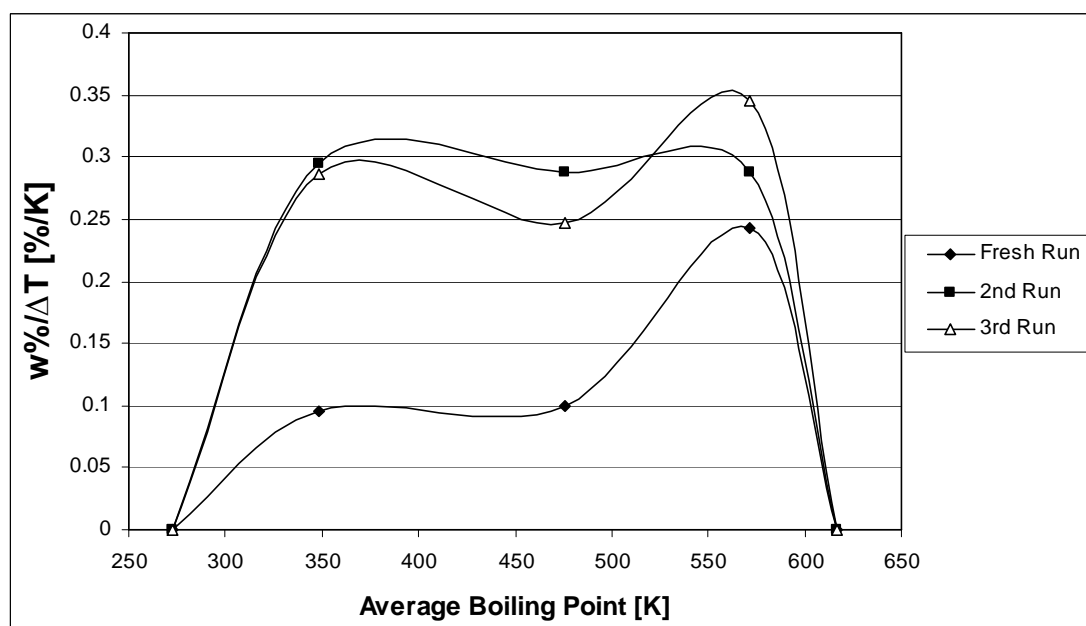


Figure 36: Boiling point distribution curves for HZSM-5 catalyst samples

## 5.2 Discussion

Coking through continued use affected the performance of all catalyst tested in different ways. US-Y catalyst was the most affected with severe progressive decreases in conversion rates and increasing percentages of coke yield and concentration. Boiling point distributions clearly indicated deactivation by the process of coking with

fewer and fewer light hydrocarbons formed as products with successive reactions. However, liquid yield and selectivity increased on the order of 1-6 %, indicating that coking results in slight increase of desired products.

Cracking Catalyst 1 (20 % US-Y) was less affected, having greater conversion rates that remained relatively constant through deactivation. Also, coke yield remained low. This was probably because of its smaller percentage of US-Y which makes the catalyst itself less acidic. The cumulative yield and boiling point distributions also remained relatively constant over the continued catalyst use. Liquids product yield and selectivity both increased over reaction, about a 1-7 % difference, although it appeared that this trend may reach a maximum at the third reaction.

Cracking Catalyst 2 (40 % US-Y) to the process of coking fell between the behavior of US-Y and Cracking Catalyst 1. The conversion of the Commercial Cracking Catalyst 2 was high and the coke yield and concentration was low like its Cracking Catalyst 1 (20 % US-Y) counterpart. However, cumulative yield and boiling point distributions indicate that Cracking Catalyst 2 (40 % US-Y) did suffer some amount of deactivation, with increasing amounts of heavy hydrocarbon-based liquid product formed at higher temperatures. This catalyst also experienced higher liquid product yield and selectivity as a result of coking, to the order of 4-6 %, with an apparent maximum at the third reaction. It's therefore important to note that the increase in liquid yield with each consecutive process cycle is due to the reduction in catalytic acidity. HZSM-5 showed the least deterioration, with nearly constant high rates of conversion and low coke yields and concentrations, there was a slight shift in cumulative yield to production at higher temperatures and there appeared to be a slight increase in the number of light hydrocarbons produced after successive reactions, but overall the composition of these products remained mostly constant. HZSM-5 also showed the most dramatic increase in liquid yield and selectivity, about 4-7 %. These results indicate that if a catalyst were to be deliberately deactivated by coking in order to produce more liquid products (largely considered as being the most valuable of this type of reaction), the best choice would be probably be Cracking Catalyst 1 (20 % US-Y). Although this catalyst was more affected than HZSM-5 after continued use, its superior initial liquid yield and selectivity clearly makes it a better option than HZSM-5, which produces mostly gas. However, since both catalysts have low amounts coke build-up, it would be interesting



to continue the deliberate third reaction. Eventually this could make HZSM-5 the better option, although it is enough to make it cost-prohibitive. In addition, it would be useful to carry out similar studies with more advanced techniques to examine the location and nature of coke formation on the surface of the catalyst; this would yield more results that could identify specifically how each individual catalyst is deactivated by coke formation.

## 5.3 Conclusion

In this part of the work the catalyst reusability was tested through experiments where the used catalyst samples were reused without regeneration for degradation of further polymer batches. The catalysts tested were US-Y, two commercial cracking catalysts containing 20 % (Cracking Catalyst 1) and 40 % (Cracking Catalyst 2) US-Y and ZSM-5. All catalysts showed a good reusability potential, which is encouraging for any future commercial polymer degradation process. From all samples tested US-Y showed the strongest deterioration from batch to batch with the highest additional coke amount formed. The commercial cracking catalysts showed excellent reusability with relatively little extra coke formed and little loss of activity due obviously to their lower acidity than US-Y. A positive side effect was a slight increase of the yield to liquid products in every subsequent cycle of reused catalysts accompanied by a matching slight decrease of their volatility.

In general, deactivation of catalysts in polymer catalytic degradation by the process of coking results in greater liquid product yield and selectivity, a desired result for those searching for valuable products of plastics recycling. However, the compositions of these products may not fall as easily within a specified range of hydrocarbons weights as can be done with fresh catalysts. Also, coking obviously results in increased coke yield and concentration and decreased conversion (although these changes may be negligible for certain catalysts). These results indicate that deliberate deactivation is probably not a good strategy for industrial processes, at least not without much more research and modification. However, these results do demonstrate that coking is not necessarily a negative end result on a catalyst as small amounts of deactivation in certain processes would not result in a significant hindrance in the production of varied products.

## Chapter Six

# Temperature Effects

---

*This chapter summarises the main findings of the temperature effects on polymer catalytic degradation by the study of the results of applying different final set point temperatures as well as different heating rates. The discussion of results focuses on the effect on conversion, liquid yield and product distribution.*

## 6.1 Introduction

The experiments belonging to this section of this research investigate the effect of changing the final set point temperatures of the heating controller and/or the heating rates for each experiment, on overall polymer catalytic degradation. The discussion of results derived focuses on the amount and composition of liquid product yield as a result of using these different conditions. In a similar manner as in previous chapters a boiling point distribution of the liquid products is carried out using gas chromatography. The chromatograph has the exact same settings as that already stated in Table 1, Chapter 3.

In this set of experiment Ultra-Stable Y zeolite (US-Y) is used, while the polymer was linear low-density polyethylene (lIdPE). The main objective was to quantify the temperature influence on the degradation product results by changing different set-point controller parameters of the heating unit. Therefore, the experimental results comprise of the total amount of liquid, gaseous and coke yield as well as time profiles

via different sampling times during the experiment. The experimental procedure was identical to that previously discussed in detail in Chapter 3.

## 6.2 Experiment results discussion

In the presentation of results of this set of experiments a slight change is introduced to the starting point of the experimental run and thus the time when product sampling is initiated. The start of each experiment was considered to be the time when the reactor temperature reached 50°C. This was done for the practical reason of speeding the overall experimental procedure cycle and thus facilitating more frequent experimentation. There was no need to wait for the heater to cool down to ambient temperature for the next experimental run to follow. As the final cooling period was the longest, starting the experiment even at 20 – 25°C higher saved a lot of time. In addition to this change, sampling started at 150°C (2.5 min) as no products were formed below this temperature. The sampling intervals were 2.5 – 7.5 min, 7.5 – 12.5 min, 12.5 – 17.5 min and 17.5 – 22.5 min.

The profiles for four set point temperatures (613 K, 663 K, 713 K, and 763 K) are shown in Figure 37. These four set point controller values applied to four polymer degradation reaction experiments.

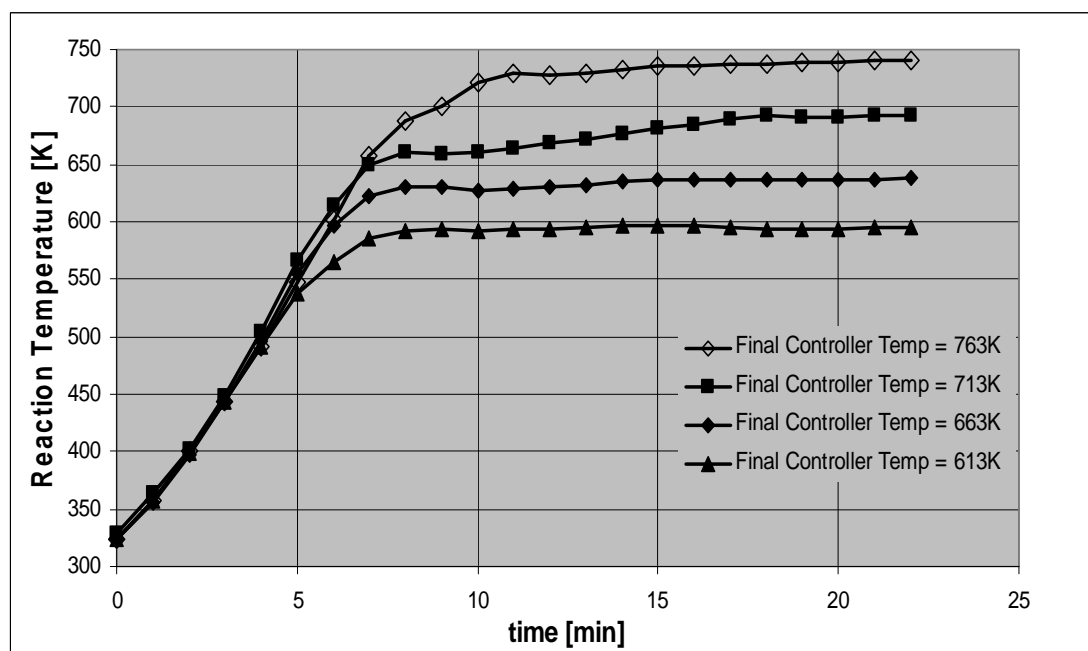


Figure 37: Reactor temperature against time at different controller set-point temperatures.

It can be observed that the time period between 5 – 10 minutes was where the significant deviation in temperature profiles of all four set point limits begins to take place. This trend was just as expected and should provide some guidance as to when the influence on the rate of degradation would begin to occur in the experimental results in which, the temperature set point analysis is applied.

In the other set of experiments, this chapter examines the results of temperature influence on polymer degradation as a function of heating rate. The reactor temperature profiles for three heating rates against time are shown in Figure 38.

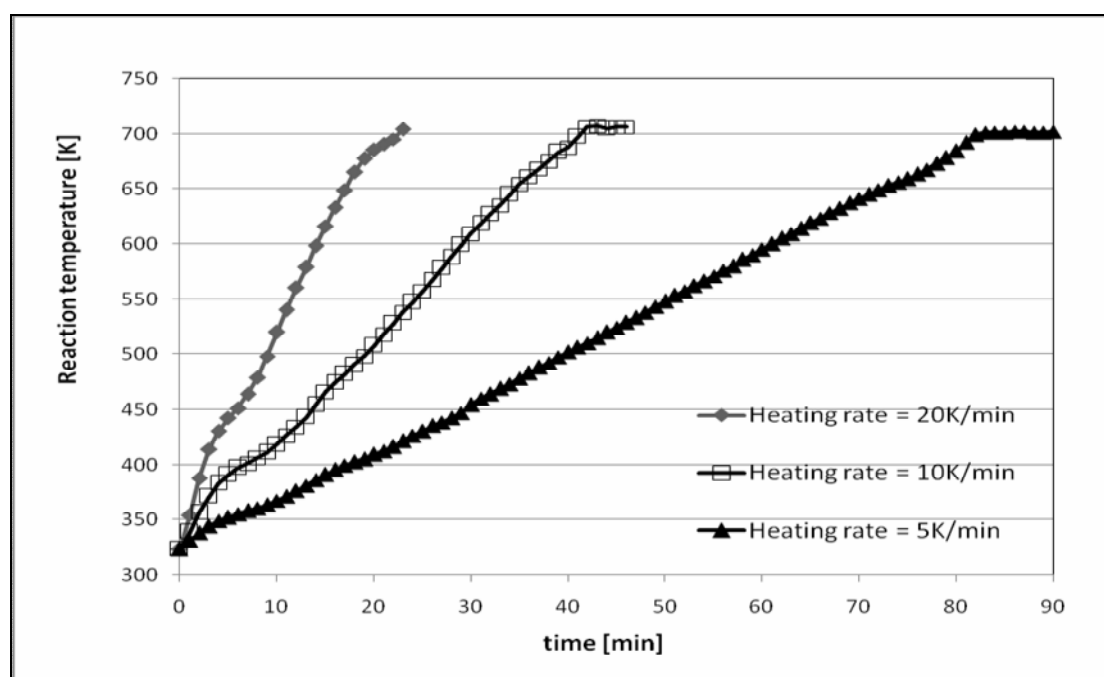


Figure 38: Reactor Temperature against time at different heating rates (Final controller set-point temperature: 713 K)

All three experiments had a maximum constant set-point temperature of 713 K and after this was reached a segment of constant temperature followed. As expected, there was a lag time between the controller temperature and reaction temperature which was reduced with decreasing heating rate.

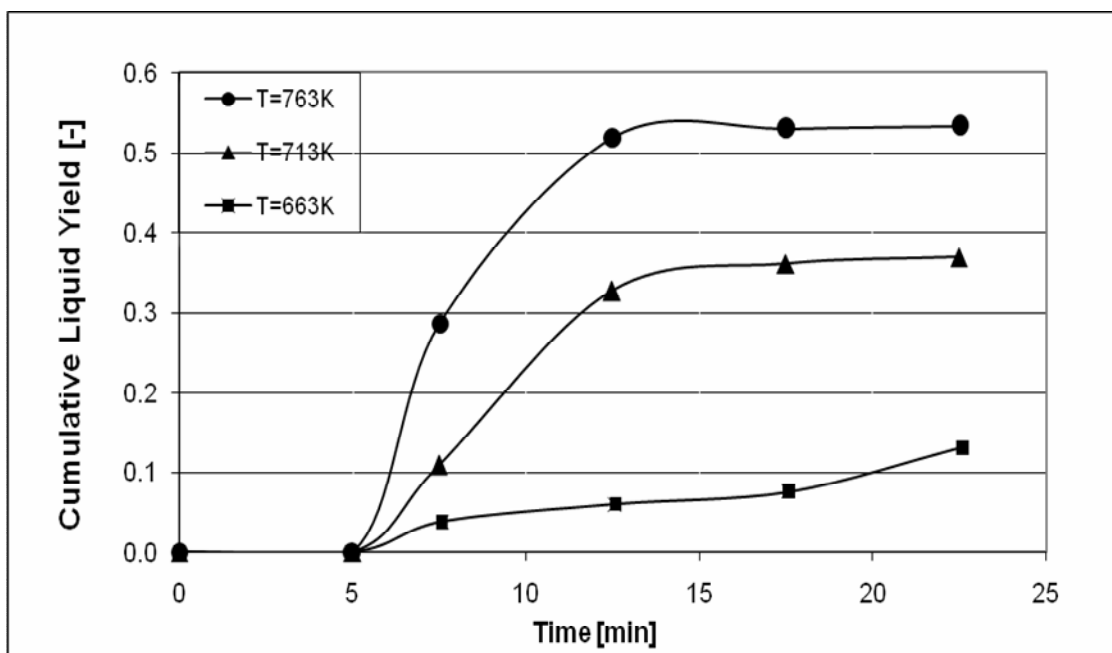


Figure 39: Time profiles of cumulative liquid yield during degradation of lldPE over US-Y at different controller temperature set points (heating rate = 20 K/min)

The results of the experiments that involve utilisation of different set-point controller temperatures on overall liquid yield are presented in Figure 39. In this chart it can be observed that there is an increase in liquid yield with higher controller set point temperature which also corresponds to higher temperature reactor temperature (Figure 37). As shown in Figure 39, in the time period between 2.5 – 7.5 minutes it is easy to observe that the liquid yield is highest when the set-point controller temperature is at 763 K and lowest at 663 K. The experiment with set-point controller temperature of 613 K produced even lower liquid amount. It is not presented in the graph as it failed to produce enough liquid to produce an accurate time profile of the liquid yield. Only the results of 663 K, 713 K and 763 K are compared. In the comparison, there is a strong relationship with the trend seen in this chart (Figure 39) and that observed in the reaction set point chart against time in Figure 38. The change in liquid yield of each experiment coincides with the difference in the reaction set point chart especially between the 2.5 – 7.5 minutes sampling time period.

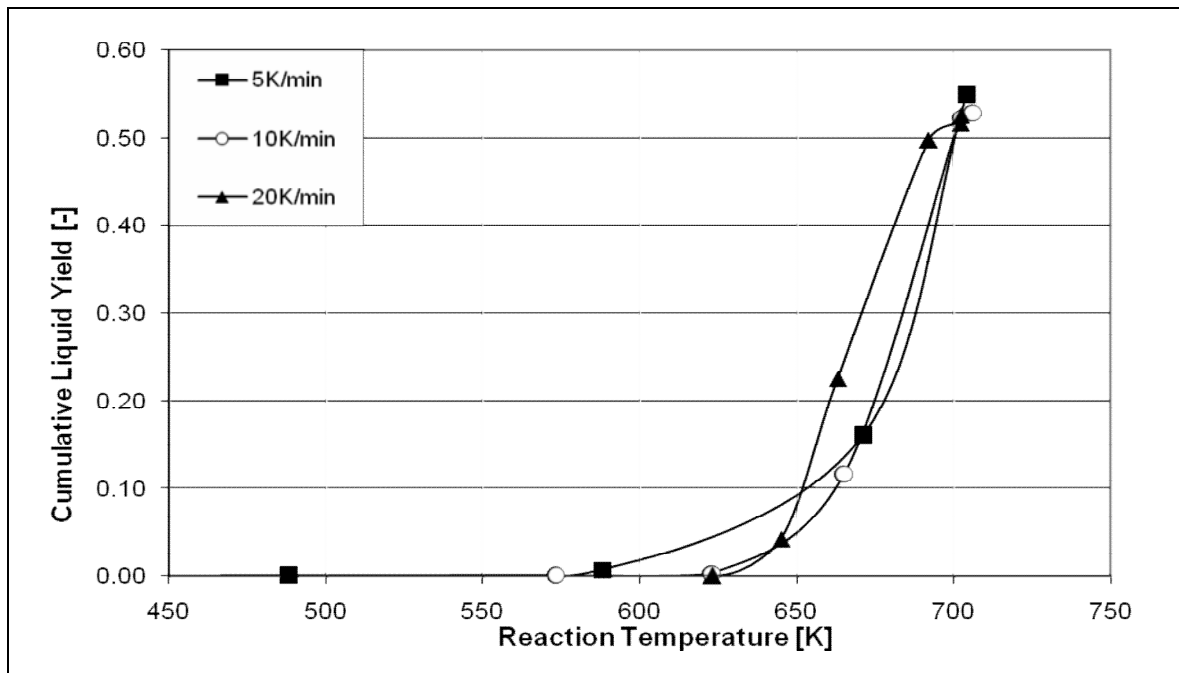


Figure 40: Cumulative liquid yield as a function of reaction temperature during catalytic degradation of lldPE at different heating rates. (Final temperature – 713 K)

The cumulative liquid yield as a function of different reaction heating rates is depicted in Figure 40. These results illustrate no major difference in the rate of liquid yield produced with temperature. The experimental procedure utilised in testing the effect of different heating rates is possibly not efficient enough to produce distinct results. The result is not entirely conclusive, as it was expected that the larger rate should have produced a greater liquid yield. This is not clearly demonstrated in the above exercise.

### 6.3 Boiling point distribution of liquid yield

The application of different final controller temperatures on the catalytic degradation experiment should produce more conclusive results. This test examines the influence of a change in controller and thus reactor final temperature will have on the reaction liquid yields. The following results show the boiling point distribution profiles derived from the products of the experiment when different final controller set-point temperature profiles are applied. As previously mentioned, catalytic degradation with maximum constant final set-point temperature of 613 K proved to be too low with

product yield being only approximately 5 %. Thus, the amount of liquid produced was too small to be analysed by a GC. The other set point temperatures of 663 K, 713 K and 763 K are presented in Figures 41, 42 and 43 below respectively. The boiling point distribution curves in Figure 41 are derived from the first condensers (2.5 – 7.5 minutes) of each experiment. Subsequent graphs in Figures 42 and 43 are derived from GC analysis of products analysed from second (7.5 – 12.5 minutes) and third (12.5 – 17.5 minutes) condensers of each experiment respectively.

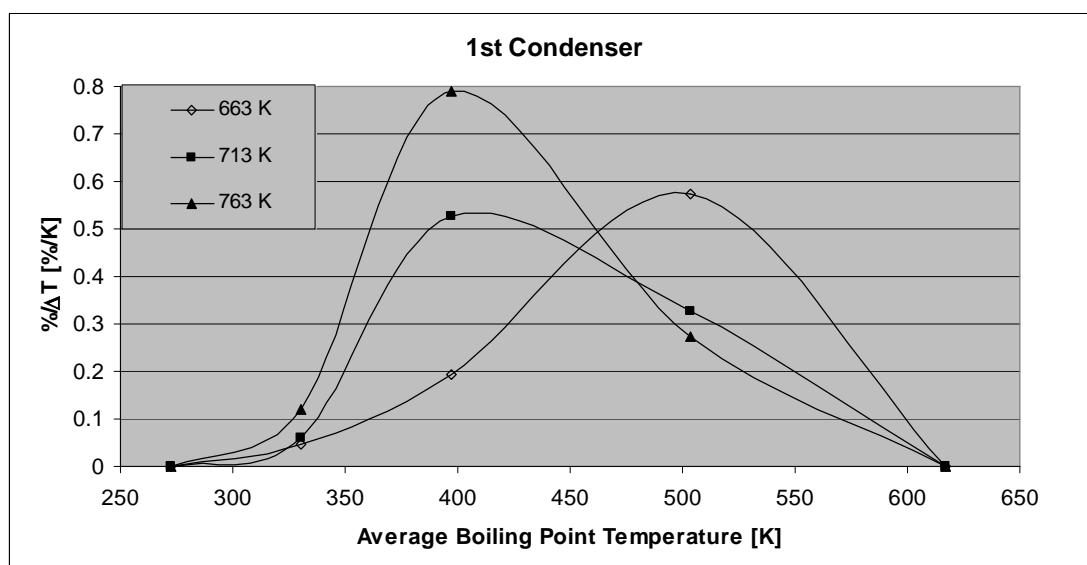


*Figure 41: Boiling point distribution of liquid products formed between 2.5 – 7.5 minutes (condenser 1), during catalytic degradation of lldPE over US-Y for all final set point temperatures*

The product spread shown in the boiling point temperature chart (Figure 42), demonstrates a simple trend. It can be observed that the higher the final reactor set point temperature, the faster the reaction and thus the more secondary reactions take place that lead to the increased production of lower weight hydrocarbon products.

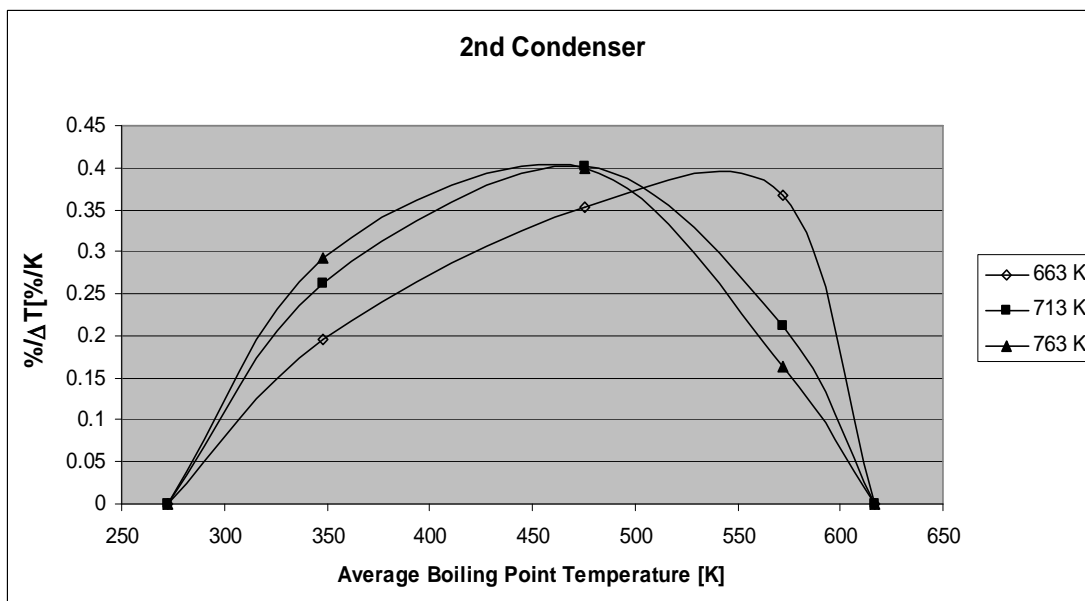


Figure 42: Boiling point distribution of liquid products formed between 7.5 – 12.5 minutes (condenser 2) during the catalytic degradation of lldPE over US-Y for all final set point temperatures

In Figure 42 the boiling point temperature of product yield contained in the second condensers of each set point experiment is shown. Similarly to the results found in the first condenser test, it is observed that there is a shift in yield towards higher hydrocarbons production as the final set point temperature of the reaction increases.



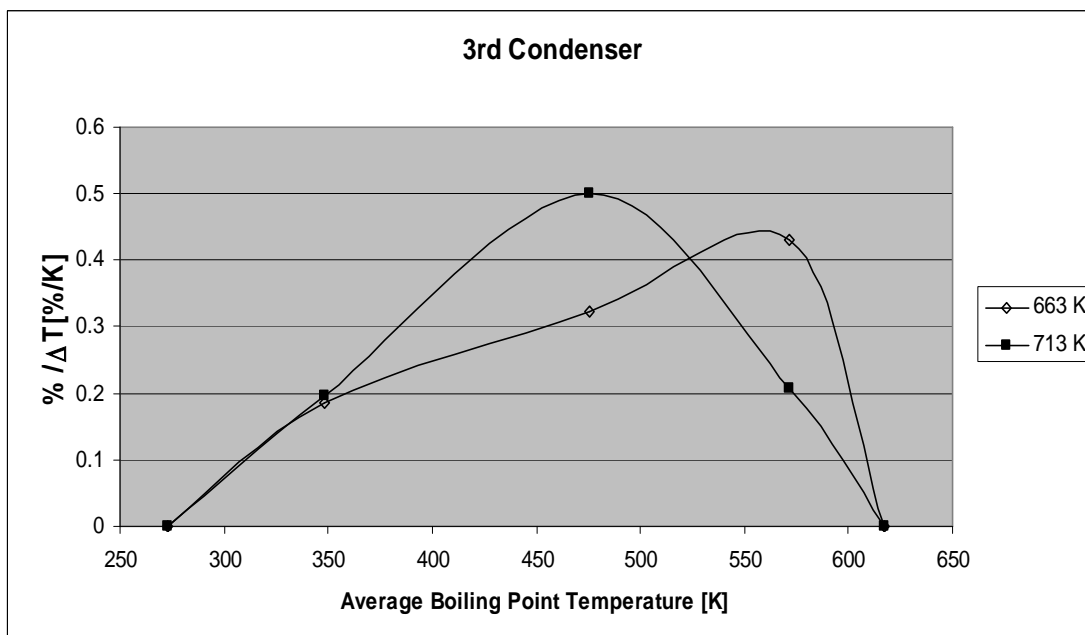


Figure 43: Boiling point distribution of liquid products formed between 12.5 – 17.5 minutes (condenser 3) during catalytic degradation of lldPE for all final set point temperatures

In Figure 43 a boiling point temperature of just the two final set point temperatures of 663 K and 713 K are illustrated. The reason a result for the third temperature of 763 K isn't shown is due to the lack of liquid product in this condenser as all the yield is produced in the

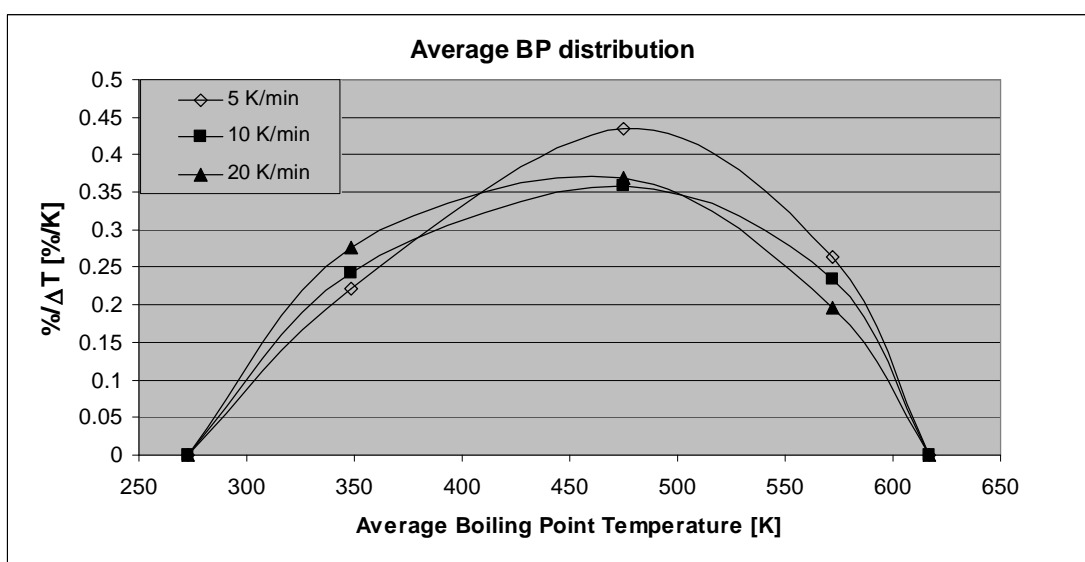


Figure 44: Average boiling point distribution of liquid products formed during catalytic degradation of lldPE over US-Y at different heating rates.

In Figure 44, the boiling point distribution derived from the products of the catalytic degradation of lldPE is presented. The chart demonstrates the effects of the application of the three different heating rates of 5, 10 and 20 K/min on catalytic degradation. It was necessary to take an average because each experiment, particularly the 5 K/min and 20 K/min experiments, yielded liquid products at different stages in the degradation cycle. It was thus necessary to use the yielded products produced during a similar temperature range. As a result, in the case of this set of experimental tests, products from the third condenser of 5 K/min experiment and the fourth condensers from both the 10 K/min and 20 K/min were used and their results compared. This is because the condensers used, contained yielded products derived within a similar temperature range in order to make it a more suitable comparison. Thus, it is from this that an average results profile demonstrated in Figure 44 is formulated.

## 6.4 Conclusion

In conclusion, it can be observed that the results with regards to selectivity were inconclusive due to the temperature rate of increase method. Therefore, it is worth suggesting that future work be conducted with the application of a continuous flow – reactor where the reaction temperature of the catalyst can be independently adjusted to different constants at which optimum catalytic reaction takes place. It is at these temperatures that each polymer would then be allowed to flow into the reactor. In all the experiments of this section of the study it can be observed that polymer is exposed (at least initially) to the same T-profile which most probably determines selectivity.

## Chapter Seven

# Effect of Polymer to Catalyst Ratio

---

*This chapter describes the experimental findings regarding the effect of the ratio of polymer to catalyst*

## 7.1 Introduction

The main goal in the last section of this research project is to observe the effects of using a non-active zeolite as a filling material, in order to embed the polymer homogeneously into active sites - even with an increasing Polymer-Catalyst-ratio (and thereby a relatively decreasing number of active sites). The focus is to study the effect of the fraction of active catalyst, i.e. acidic sites, on its performance in the system. The purpose of choosing to add an inactive inorganic zeolite as filling material and effectively decrease the amount of active catalyst was to enable better contact between polymer and active surface area of catalyst. In addition, direct investigation is carried out on the effect of the different amounts of filling in-active material and the possibility of contact improvements.

In order to evaluate the impact of the filling material and the characteristics of other substances used in the experiments, three basic experiments were conducted initially as stated in Table 12. These three experiments are described as follows:

- Experiment 1 uses only 1 g of US-Y-zeolite as a catalyst.
- Experiment 2 uses only 3-A-zeolite as an inactive filling material.

- Experiment 3 is conducted as a thermal degradation process without any inorganic solids added.

Four further experiments were conducted with catalytic mixtures of US-Y and 3-A-zeolite: three of them (experiments 4, 5 and 6) utilise a total mass of the catalyst mixture of 1 g at different US-Y: 3-A ratios, after which the catalytic mixture in experiment 7 takes into account that 3-A-zeolite has a higher density than US-Y-zeolite. To cater for the higher density, 1.125 g of 3-A-zeolite is added to 0.5 g of US-Y-zeolite. These ratios create a zeolite mixture with equal volumetric amounts.

**Table 12: Overview of experimental conditions and participating substances for all experiments**

	lIdPE	US-Y	3-A-zeolite	Cracking Catalyst 1	US-Y content of catalyst-mixture	Overall US-Y content
Exp. 1	2g	1g	-	-	100%	33.3%
Exp. 2	2g	-	-		0%	0%
Exp. 3	2g	-	1g		0%	0%
Exp. 4	2g	0.5g	0.5g		50%	16.7%
Exp. 5	2g	0.25g	0.75g		25%	8.3%
Exp. 6	2g	0.1g	0.9g		10%	4.2%
Exp. 7	2g	0.5g	1.125g		30.8%	13.8%
Exp. 8	2g	-	-	1g	20%	12%
Exp. 9	2g	-	0.5g	0.5g	10%	6%

In experiments 8 and 9, Commercial Cracking Catalyst 1 was used as an active catalyst. While experiment 8 was conducted with Cracking Catalyst 1 only, experiment 9 utilises a mixture of Cracking Catalyst 1 and 3-A-zeolite in equal amounts of 0.5 g.

The overall results with regards to yields, conversion, and selectivity are listed in Table 13. A detailed discussion of the results of each experiment and their interrelations is given in this chapter.

**Table 13: Summary of Results regarding Yield, Conversion, and Selectivity**

	Liquid yield	Gas yield	Conversion	Selectivity to liquids	Coke yield
Exp. 1	34%	59%	92%	36%	7.5%
Exp. 2	3.8%	8.6%	12%	31%	88%
Exp. 3	3%	10%	13%	23%	86%
Exp. 4	40%	52%	92%	44%	7.9%
Exp. 5	46%	42%	88%	52%	13%
Exp. 6	42%	42%	85%	50%	15%
Exp. 7	41%	53%	94%	44%	5.9%
Exp. 8	61%	34%	95%	64%	4.7%
Exp. 9	64%	32%	95%	67%	4.9%

## 7.2 Basic Experiments

### 7.2.1 Experiment 1

Experiment 1 was conducted with US-Y. It was used as a base experiment to compare against further experiments and the mass ratio of lldPE to US-Y-zeolite was 2:1. Based on results of former studies [Manos G et al (2000a)], the increase of the polymer degradation rate over smaller ratios, i.e. adding more catalyst is negligible. This is a consequence of the molecular structures of both reaction participants. The macromolecules of the un-reacted polymer are only able to access the outer surface of the US-Y cages. For small ratios all macromolecules of the melted polymer are in contact with acidic sites. Hence, more zeolite only offers redundant acidic sites which are not in contact with polymers and do not accelerate the reaction further in a noticeable way.

Figure 45 shows the liquid and gas yield collected over different time periods. It also illustrates the temperature profile of this experiment. Results are only plotted from minute 5 on because the degradation process initiates only from a temperature higher than 420 K [Gobin K et. al. (2001)]. Gases and liquids could only be collected after this temperature is passed. Due to relatively low temperatures, the conversion was less than 20 % in the first heating step (5 – 10 minutes). More liquids than gaseous products were formed because temperature in heating periods 2 and 3, the rate of

conversion rises. However, mainly gaseous products were formed due to overcracking of hydrocarbons in the liquid range.

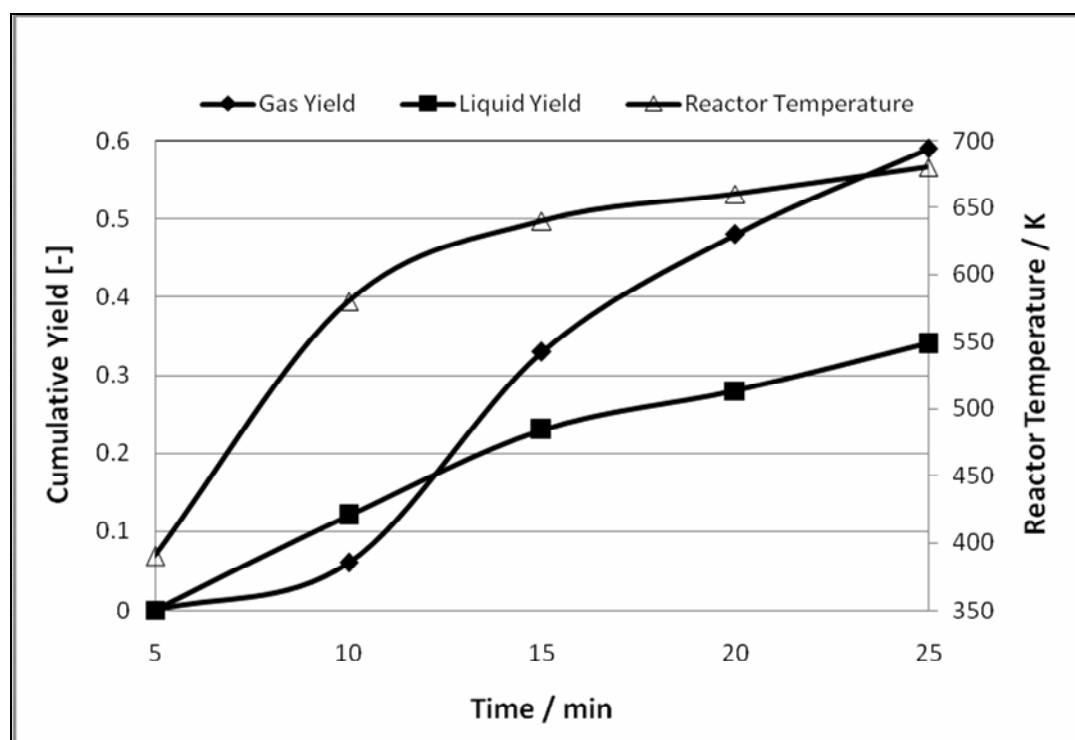


Figure 45: Gas Yield, Liquid Yield and Temperature Profile of Experiment 1.  
Polymer: lldPE, Catalyst: US-Y, ratio: 2:1(mass ratio)

On completion of the experiment the polymer had almost completely reacted: 92.5 % of the original polymer had turned into volatile products, while the residual amount formed coke fractions on the catalyst surface. Due to the high acidity of US-Y and the consequential overcracking at higher temperatures, the amount of gaseous products was significantly higher than the amount of liquids.

The composition of the liquid yield after catalytic degradation via US-Y is presented in Figure 46. Due to the insufficient amount of liquids collected over the first and fourth heating steps, only the samples from minute 10 to 15 and 15 to 20 could be analysed. The degradation over US-Y zeolite has mostly formed products of high molecular weight, while the products formed over the highest temperatures are the heaviest. Besides the formation of products in the gaseous range due to overcracking, at higher temperatures US-Y favours mechanisms of molecular restructuring like cross-linking of molecules as well [Kaminsky W., et al.,(1995), Manos G et al.(2001)].

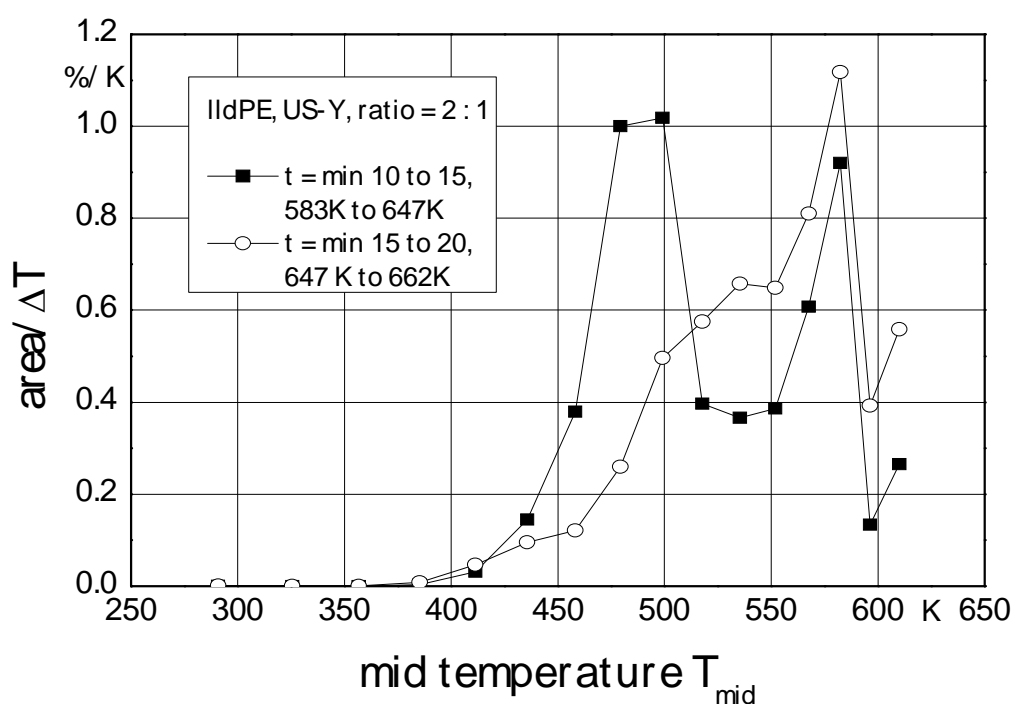


Figure 46: Boiling Point Distribution: Composition of the Liquid Yield of Experiment 1. Polymer: lldPE, Catalyst: US-Y, Ratio: 2:1

This explains the high appearance of gaseous products and heavy liquid products at the same time with almost no light liquid products being formed.

Experiments with US-Y in previous work [Bond G.C., (1987), Gates B.C., (1992), Sadeghbeigi R., (1995)] have shown that liquid products formed at lower temperatures have boiling points even in the low-molecular range. With increasing temperatures, the boiling points are increasingly shifted to products of higher molecular weight. This leads to the assumption that the boiling point distribution of the liquid products

collected from minute 5 to 10 must mainly consist of compounds of low or medium molecular weight, due to possible evaporation of light components during sampling.

### 7.2.2 Experiments 2 and 3

One problem resulting from a higher polymer to catalyst ratio is a heterogeneous mixture caused by different particle sizes. The powdery particles of the catalyst are much smaller than the granular particles of the polymer and therefore the small catalyst particles fall through the voids in the network of the polymer particles and remain in the bottom part of the reactor. While there is a homogenous mixture between catalyst and polymer in the bottom of the reactor with an oversupply of active sites, the polymer in the top layers does not have any access to acidic sites of the catalyst. Heating experiments in a similar reactor that only tended to melt the polymer in the presence of solid inactive 3-A-zeolite (heating duration: 20 minutes; maximum temperature: 200°C) have shown that the re-solidified sample kept its two-layered structure (bottom layer: polymer / catalyst; top layer: polymer only) for polymer-catalyst ratios of 1.5: 1 and higher. From visual observations, the melting of the polymer does not have any mixing effect. Thus, the number of polymer particles adjacent to active sites decreases with a decreasing amount of catalyst. This has two possible effects; it may lead to an unbalanced reaction and a large amount of unconverted polymer over lower temperatures. To avoid these problems, some experiments with inactive 3-A-zeolite as a filling material have been conducted. A homogeneous mixture of 3-A- and US-Y-zeolite assures that even the polymer particle in the top layers get in contact with acidic US-Y sites. To make sure that the used 3-A-zeolite is completely inactive and does not have any reactive influence on the degradation process, the degradation over 3-A-zeolite is compared with a thermal degradation without any catalyst over the standard temperature settings. Figure 47 illustrates the characteristics of a heating process of 2 g lldPE without any catalyst (experiment 2). The temperatures in this experiment were higher than the temperatures of experiment 1 (catalyst: US-Y, ratio: 2:1) throughout the whole run. Despite the higher temperatures nearly no reaction was taking place because temperatures were too low to initiate a degradation process without a catalyst. Less than 13 % converted to volatile – mostly gaseous – products. An analysis of the boiling point distribution was not possible due to the minimal liquid yield. The heating process with 2 g lldPE



and 1 g of inactive 3-A-zeolite yielded very similar results (Figure 48). Over a marginally lower temperature profile a conversion was achieved of 13.5 % of the original polymer, with mostly gaseous products.

The high gas yield in both experiments was not a consequence of overcracking. It was rather, an effect caused by the molecule structure of lldPE. The branches diverging from the main carbon chain are medium sized and easily split from the main chain at relatively low temperatures. The broken off hydrocarbons are short enough to be in the liquid range and are collected in the gas fraction.

These results prove that the 3-A-zeolite used in this and other experiments was inactive, i.e. it did not have any catalytic effect on the degradation process. For this reason 3-A-zeolite could be employed as a filling material in other experiments to achieve the effects explained above.

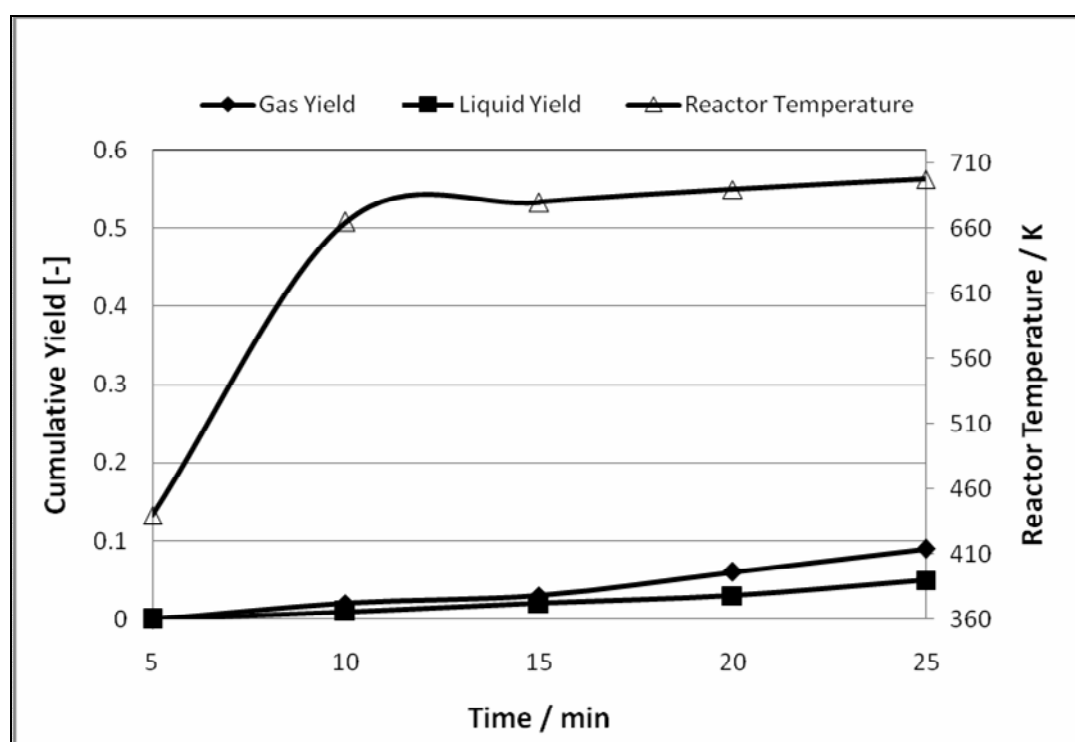


Figure 47: Gas Yield, Liquid Yield and Temperature Profile of Experiment 2.  
Polymer: lldPE, no Catalyst

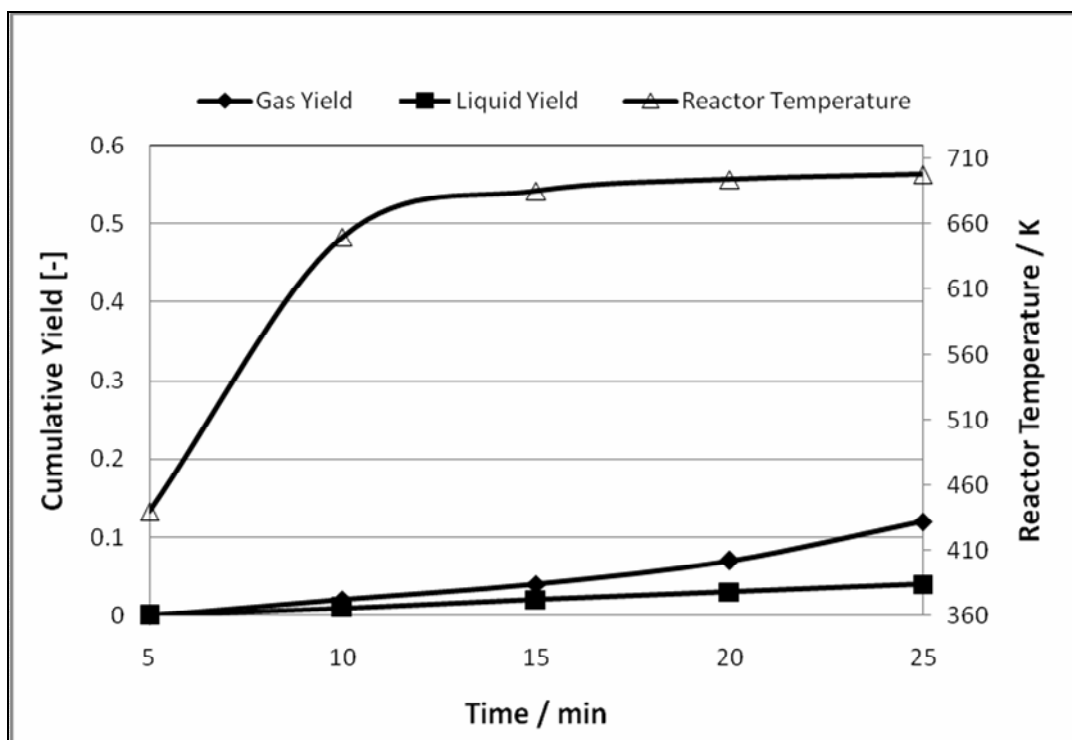


Figure 48: Gas Yield, Liquid Yield and Temperature Profile of Experiment 3.  
 Polymer: lldPE; zeolite: inactive 3-A- zeolite

## 7.3 Experiments involving mixtures of US-Y and 3-A-zeolite

Several experiments with different Polymer – US-Y ratios have been carried out. In order to provide a homogeneous mixture throughout the whole reactor inactive 3-A-zeolite is added until the overall zeolite amount equals 1 g.

### 7.3.1 Results of Single Experiments

Experiment 4 has been conducted with 0.5 g of US-Y and 0.5 g of 3-A-zeolite. The results of experiment 4 are shown in Figure 49. The conversion was with 92.2 % in the same range of experiment 1 (degradation with 1 g of US-Y). However, the liquid yield was 7 % higher due to a smaller number of active sites. Although less over-cracking was taking place, this zeolite mixture was active enough to form more gaseous products than liquid products.

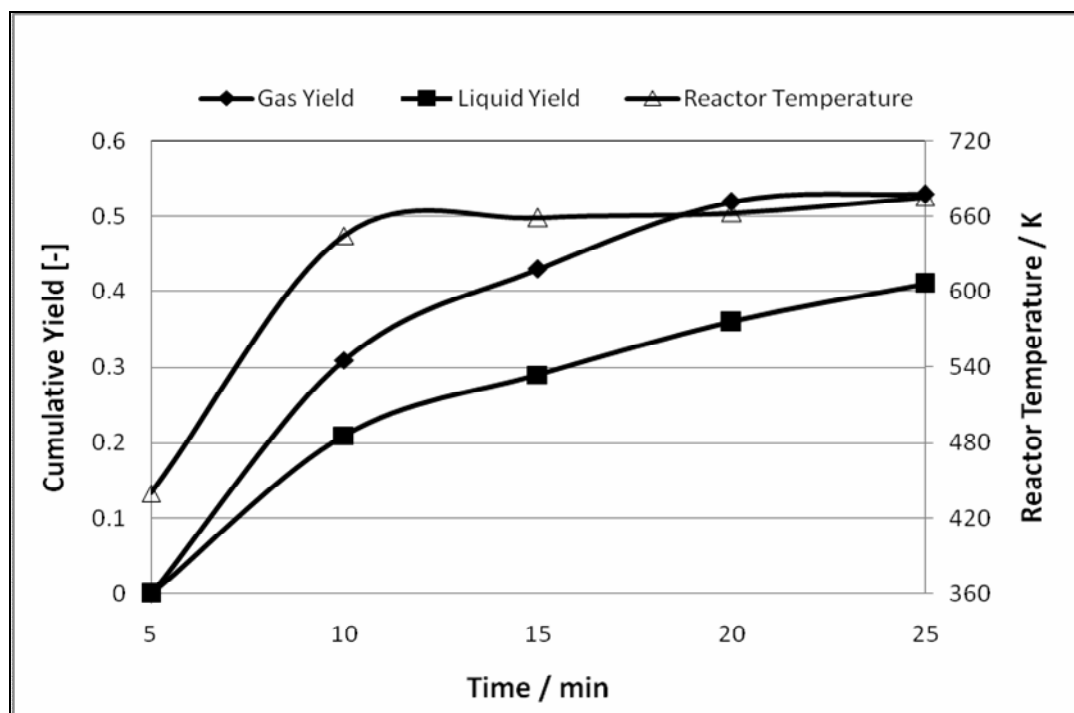


Figure 49: Gas Yield, Liquid Yield and Temperature Profile of Experiment 4. Polymer: lldPE; zeolite: 0.5 g of US-Y, 0.5 g of 3-A-zeolite

It is obvious that more than 50 % of lldPE was converted during the first heating step (5 – 10 minutes). This effect might have been caused by a higher temperature profile compared to Experiment 1. From 5 to 20 minutes the formation of gaseous products was consistently higher than the formation of liquid products. Only from 20 to 25 minutes more volatile products in the liquid range than gaseous products were formed.

The boiling point distribution of liquid formed in Experiment 4 (Figure 50) shows that the formed products are mainly hydrocarbons of medium molecular weight. All curves are very similar and have a peak in the range of C<sub>9</sub>- to C<sub>12</sub>-hydrocarbons. The lightest products are collected during the first heating step (5 – 10 minutes). The boiling point distribution curves of the second and third condenser were almost identical and slightly shifted to heavier products. The products with the highest boiling points were collected in the last time interval of the experiment.

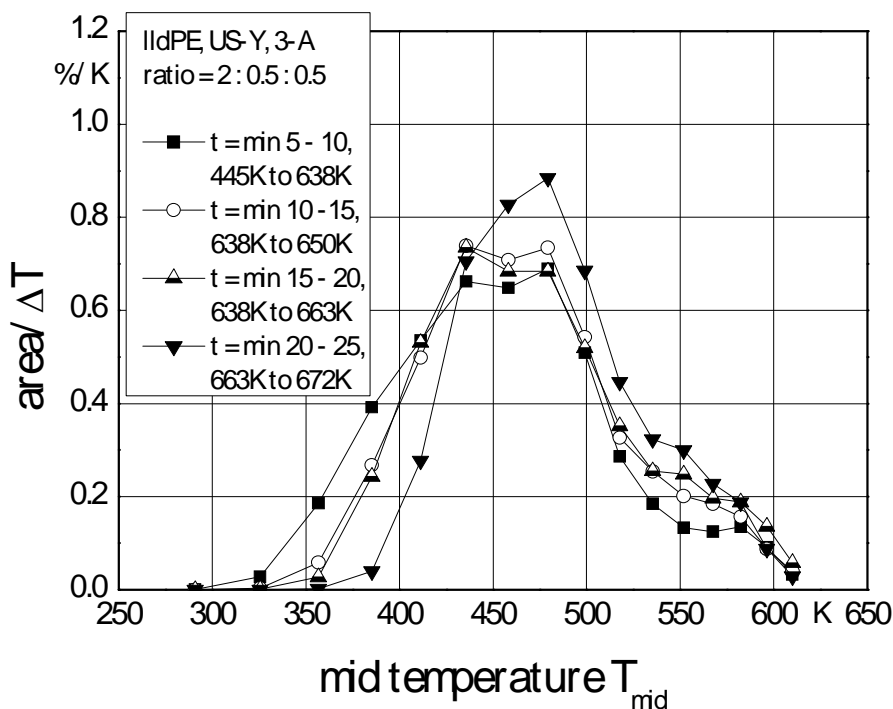


Figure 50: Boiling Point Distribution: Composition of the Liquid Yield of Experiment 4. Polymer: lldPE; zeolite: US-Y, 3-A; Ratio: 2 : 0.5 : 0.5

In general this experiment confirmed the results of Experiment 1 - that cracking with US-Y leads to heavier products over higher temperatures; this is possibly due to cross-linking of molecules taking place. This effect was not so obvious here due to a smaller amount of US-Y in this experiment. The products were generally lighter and even the curve with the heaviest products had most of its products in the range of medium molecular weight hydrocarbons.

The amount of US-Y-zeolite used in **Experiment 5** (results plotted in Figure 51) was 0.25 g, while 0.75 g of 3-A-zeolite was used as a filling material. This experiment achieved the highest liquid yield (45.5 %) compared to the other experiments US-Y-based catalyst mixtures. After 25 minutes of heating, more of the polymer has been converted to liquid than to gaseous (42 %) products.

Due to a low number of acid sites, less over-cracking takes place than in experiments 1 and 4. Another effect caused by the low number of active sites is a delayed reaction.

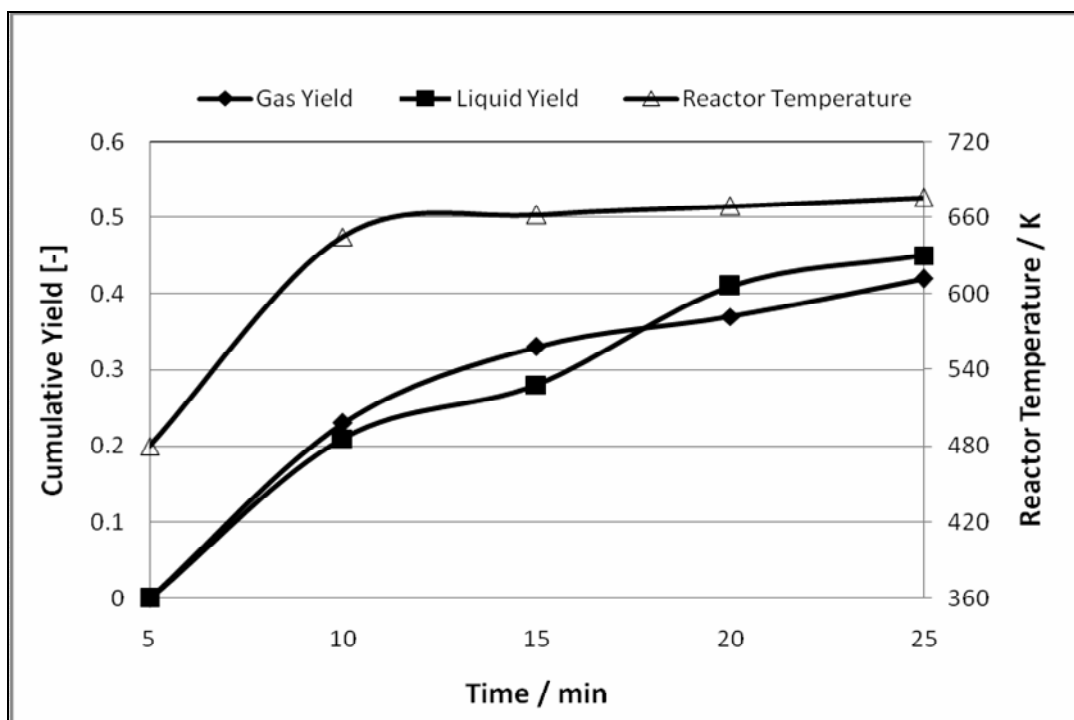


Figure 51: Gas Yield, Liquid Yield and Temperature Profile of Experiment 5.  
 Polymer: lldPE, zeolite: 0.25 g of US-Y, 0.75 g of 3-A-zeolite

Although the temperatures at the beginning of the experiment are even higher than those at the beginning of experiment 4, less than 50 % of lldPE are converted to volatiles during the first heating step.

The conversion rate between 20 and 25 minutes is still at 10 %, which means that some of the coke yield can be unconverted polymer.

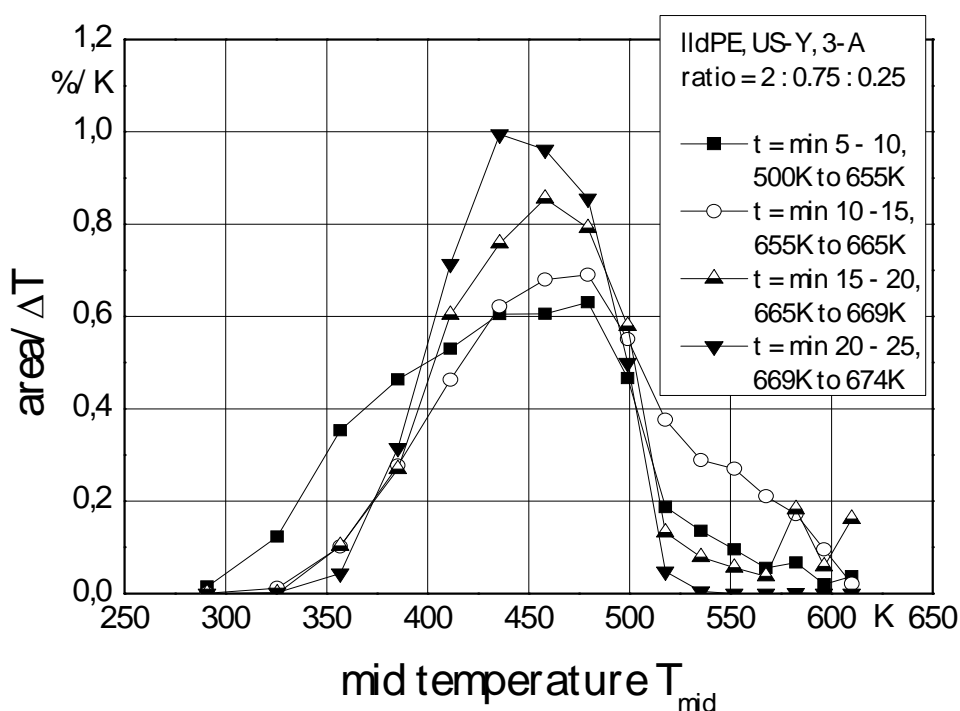


Figure 52: Boiling Point Distribution: Composition of the Liquid Yield of Experiment 5. Polymer: IldPE; zeolite: US-Y, 3-A; Ratio: 2 : 0.25 : 0.75

The products formed in Experiment 5 (Figure 52) were mainly in the range of hydrocarbons of medium molecular weight ( $C_8$  to  $C_{13}$ ). The narrowest boiling point distribution is achieved over the last heating step. The curve of the products collected from 15 to 20 minutes was fairly similar except for small peaks in the range of heavy hydrocarbons. The boiling point distribution of the products collected in the second condenser offers a wider spectrum of resulting products: besides the products of medium molecular weight the GC was able to detect heavy hydrocarbons as well. The lightest hydrocarbons are collected in the first heating step of the experiment.

A tendency to heavier products due to cross-linking at higher temperatures (see experiments 1 and 4) was not clearly noticeable in this experiment. Only the curve of the products of the first condenser's was slightly shifted to lighter hydrocarbons. The other curves are not displaying an obvious drift. This may be caused by a slightly increasing temperature from minute 10 to 25 ( $\Delta T = 19$  K). Furthermore, this was a consequence of a relatively low US-Y-acidity and associated with this a low number of active sites.

**Experiment 6** has been carried out with 0.1 g of US-Y and 0.9 g of 3-A-zeolite. Over these parameters the amount of liquid products formed is equal to the amount of gases formed (liquid yield = gas yield = 42.4 %). Although the beginning of the experiment yielded more gaseous products, more lldPE was converted to liquid products over higher temperatures (Figure 53).

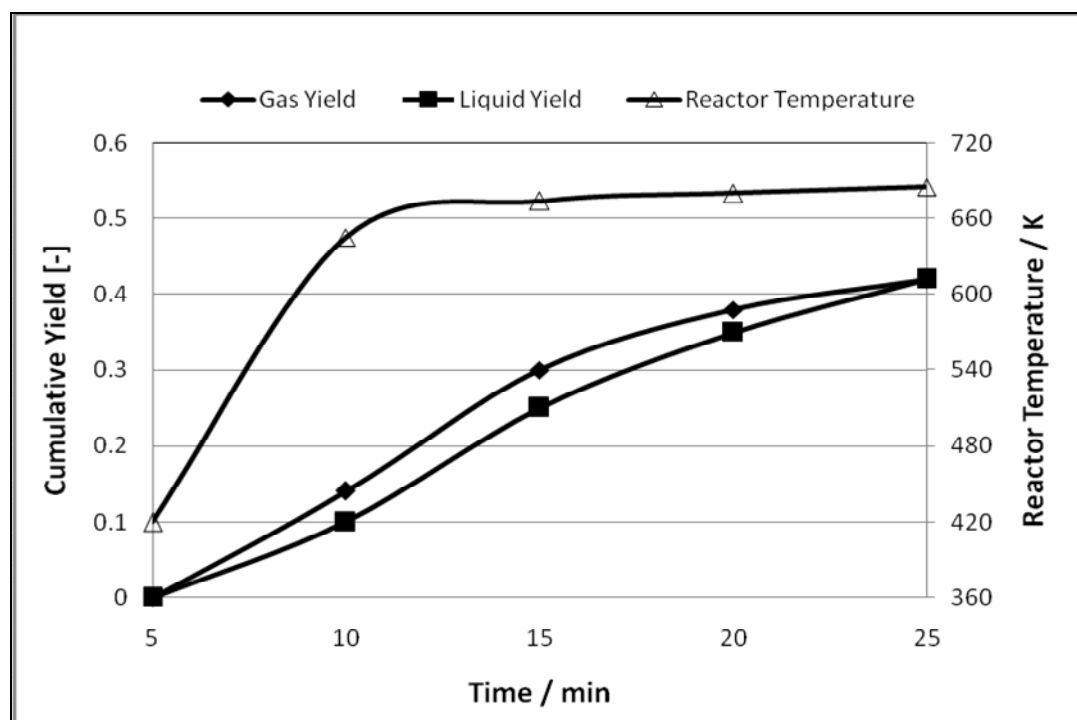


Figure 53: Gas Yield, Liquid Yield and Temperature Profile of experiment 6. 2 g lldPE, 0.1g of US-Y, 0.9g of inactive 3-A-zeolite

Due to a low US-Y-acidity the conversion rate during the first heating step was very low compared to other experiments with higher US-Y-ratios. While in experiment 4 and 5 far more than 40 % was converted during the first heating step, the conversion rate was lower than 25 % in the beginning step of this experiment. Although the conversion rate was higher over the following heating steps, only 84 % of polymer was converted to volatile products overall. The dark colour of the residues in the reactor indicated the possibility that coke could have been formed at the limited available active sites. The fairly high coke concentration to active catalyst implies that a certain amount of the original polymer must have stayed unreacted or only

fragmentarily cracked due to the low acidity of the zeolite mixture and thus remained in a solid polymer state.

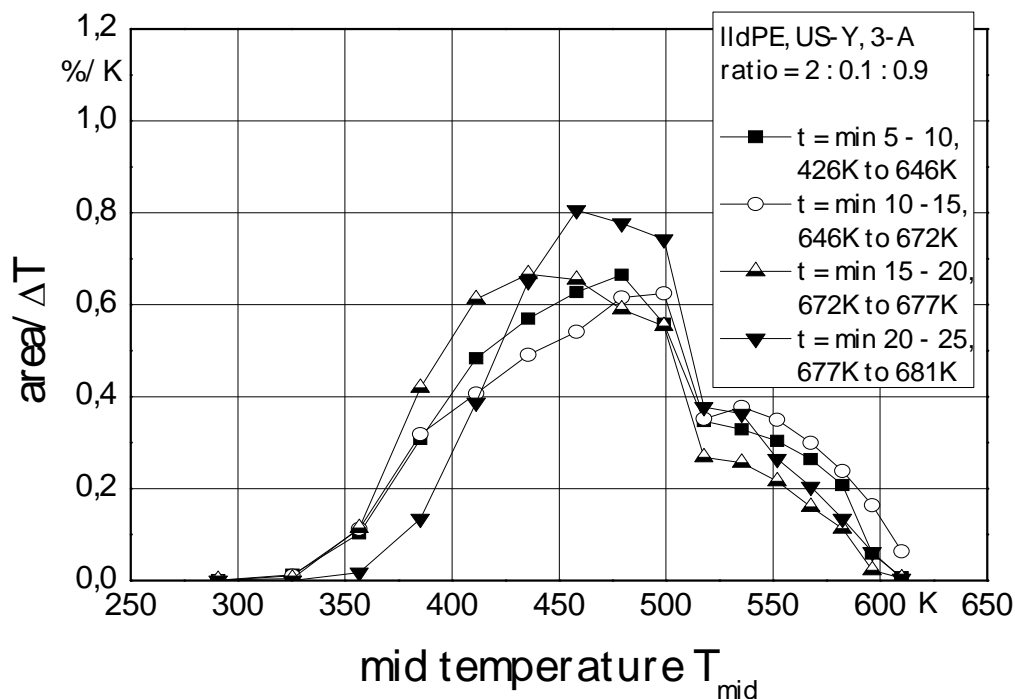


Figure 54: Boiling Point Distribution: Composition of Liquid Yield of Experiment 6. Polymer: lldPE; zeolites: US-Y, 3-A-zeolite; Ratio: 2: 0.1: 0.9

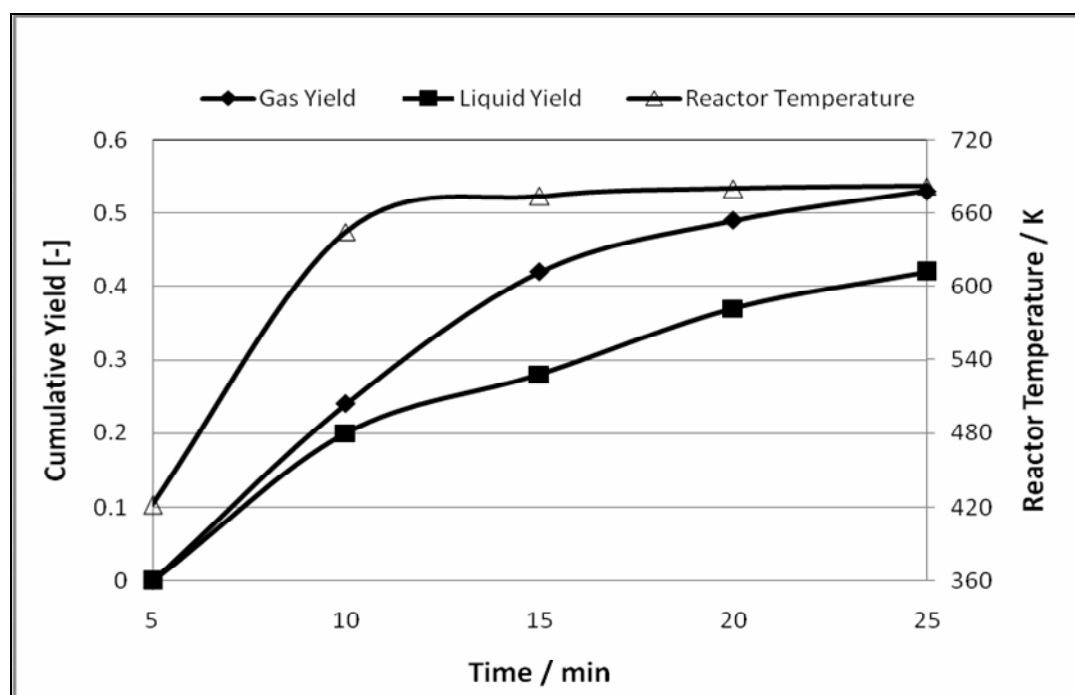
Most of the products formed over a US-Y-percentage of only 5 % were in the range of heavier light and medium molecular weight hydrocarbons ( $C_8$  to  $C_{13}$ ). However, some heavy products were formed in every heating step of the experiment.

The products formed at the beginning of the experiment (5 to 10 minutes; 10 to 15 minutes) showed the widest boiling point distributions. Both curves were very similar; however, the curve of the second condenser was slightly shifted to heavier products. The lightest hydrocarbons were formed during the third heating step. The narrowest boiling point distribution was obtained over the highest temperatures. However, with peaks in the  $C_{10} - C_{13}$  range the products formed over the last heating step were the heaviest.

Yet, a tendency of heavier products and narrower boiling point distributions over higher temperatures was not clearly noticeable in this experiment.



**Experiment 7** regards the different densities of US-Y and 3-A-zeolite. In order to provide a zeolite mixture with the same volume rather than the same mass, the mass of 3-A-zeolite needs to be 2.25 times as high as the conjugated US-Y mass. In order to gain reference results to Experiment 4, the zeolite mixture was calculated on the base of 0.5 g of US-Y. This required an additional amount of 3-A-zeolite of 1.125 g. The results of experiment 7 are plotted in Figure 56.



*M, Figure 55: Gas Yield, Liquid Yield and Temperature Profile of experiment 7. Polymer: lldPE; zeolites: 50 Vol.-% (=0.5 g) of US-Y, 50 Vol.-% (=1.125 g) of 3-A*

In general the curves look similar to those of experiment 4. Although more polymer was supposed to be in close contact to the active sites of the catalyst mixture in Experiment 7, the conversion was 43 % lower during the first heating step than in Experiment 4. The higher conversion was mainly based on a higher gas yield of the first sample of Experiment 4, which was a consequence of the more concentrated active sites. Nonetheless, with time cumulative yields and conversion of Experiment 7 were increasingly stronger than those of Experiment 4.

The conversion after 15 minutes was with 70.5 % (27.8 % liquid, 42.7 % gas) in the same range of Experiment 4. The total conversion was with 94.2 % (41.2 % liquid, 52.9 % gas), 2 % higher than the total conversion of Experiment 4. This is the highest

conversion of all experiments employing US-Y based catalyst mixtures - going along with the lowest coke yield. Although the reaction was not sped up by the more balanced availability of active sites in Experiment 7, it can be stated that degradation over zeolite mixtures with the same amount of US-Y, yet a lower relative acidity, could constrict coking tendencies.

Due to only small differences in selectivity to liquids compared to experiment 4 and time restrictions for this research project, no boiling point distribution was calculated for this experiment.

### 7.3.2 Discussion of Results regarding US-Y-Acidity of the Catalyst

In the following two sub-chapters the results of the experiments discussed before are integrated into single graphs to obtain a better comparability of results. In the first part, conversions and yields will be discussed in depth. In the second part of this chapter differences in the composition of products are observed over several boiling point distributions. In order to be able to estimate the plotted results in a proper way, any inconsistencies in experimental conditions should be noted.

Due to the reasons explained in Chapter 3 the temperature curves are partially deviating from each other. Whereas the influence of differing temperatures may be negligible to the overall results, an effect on the conversions, yields and boiling point distributions must be considered when comparing the individual heating steps of the experiments. Particularly at the beginning of the heating process (0 to 10 minutes) temperatures could widely differ. This might have resulted in the degradation process being initiated at different times. Figure 56 shows the temperature curves of the four experiments (1, 4, 5, 6) whose results are discussed in this chapter. The yield performances of experiments 4 and 6 (50 % and 10 % US-Y) were found to be very similar. Both temperature profiles were ascending steeply until 11 minutes and reached temperatures of 646 K and 670 K respectively. From that point on, both temperature curves increase very slowly and reach their maximums after 25 minutes of 672 K and 681 K respectively. The highest temperature profile was found in experiment 5 (25 % US-Y). Experiment 1 (degradation over pure US-Y) had the lowest temperatures during the heating-up and it took more than 15 minutes to reach 650 K. Regarding the temperatures from 5 to 10 minutes, the heating-up in this experiment was delayed by

60 – 80 s compared to Experiments 4 and 6 and by 100 – 130 s compared to experiment 5.

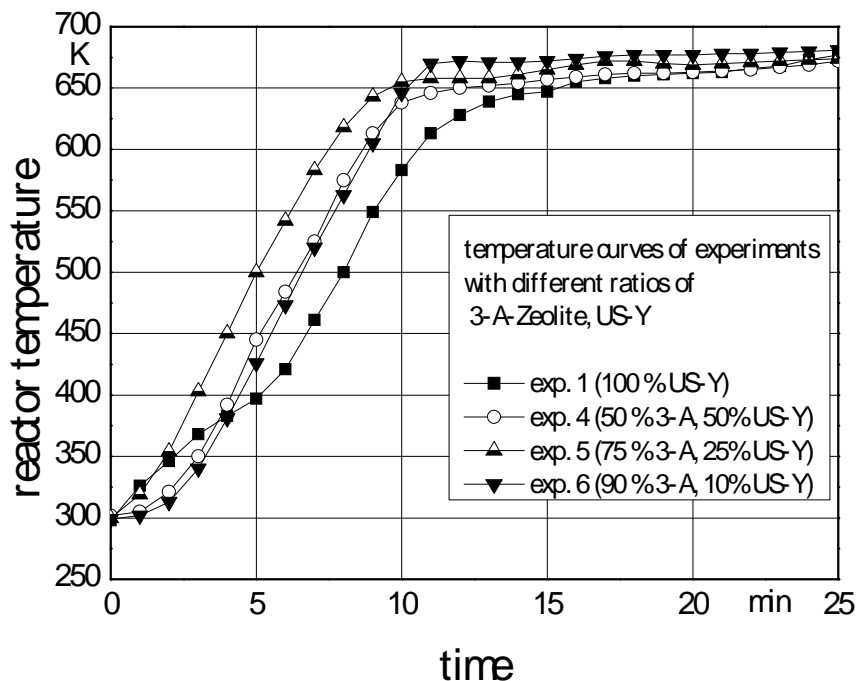


Figure 56: Temperature Curves vs. Time of Experiments 1,4,5,6

Interpreting the results by comparing yields and distributions of individual heating steps, deviations in the heating curves need to be considered.

### 7.3.2.1 Conversions / Yields over Different Acidities

Figure 57 shows the conversions of different experimental time intervals over the acidity of the zeolite mixture expressed as US-Y percentage. The values for the conversion of US-Y-acidity are calculated as the arithmetical average of the results of experiments 2 and 3. The highest conversion in the first time interval was realised in experiment 4 (50 % US-Y). Although the temperatures are lower than those of experiment 5 (25 % US-Y), more lldPE was converted into volatile products in experiment 4 (50 %) than in experiment 5 (44.6 %). Caused by a higher acidity the

degradation process was initiated at lower temperatures resulting to more converted polymers during the first heating step.

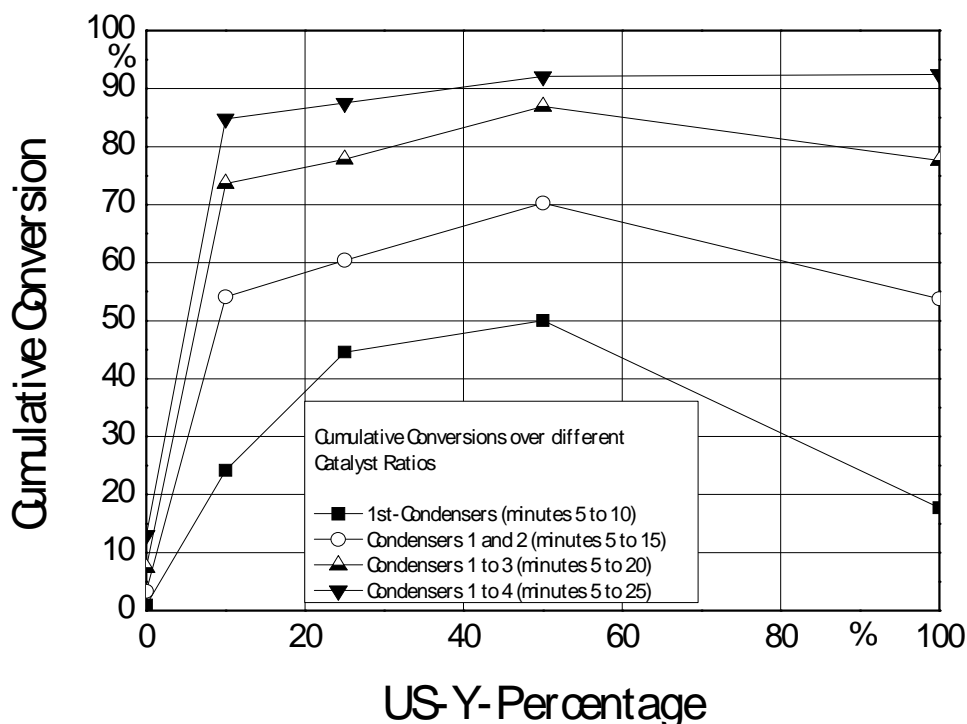


Figure 57: Cumulative Conversions vs. US-Y percentage at different heating steps i.e. time intervals.

Though the temperature profile of experiment 6 (10 % US-Y) was almost identical to that of experiment 4, the conversion during the first heating step was much lower due to the higher activation energy required over fewer numbers of active sites. The conversion in the first time step of experiment 1 was also low. This was a result of the low temperatures in the beginning of the experiment. The degradation process initiated only in the middle of the first time interval, (despite the acidity being the highest in this case). The curves of condensers 2 and 3 show a similar image. The conversion increases rapidly with a higher amount of US-Y. Due obviously to a delayed reaction in experiment 1 the conversion over pure US-Y was lower again. With proceeding length of the experiment, temperature effects become more and more negligible. The overall conversion could be seen as a result of experiments conducted over similar

heating conditions. The conversion over 50 % US-Y and 100 % US-Y is almost equally high, 92.1 % and 92.5 % respectively. With a decreasing amount of US-Y, conversion reduces as well. Over a US-Y-percentage being lower than 50 % less polymers get degraded, which results in a decreasing overall conversion.

The gas yield showed a similar picture to the conversion (Figure 58). During the first heating step most gaseous products are produced over 50 % of US-Y (30.3 % overall content). The experiments with a lower acidity were not producing as many gaseous products due to higher activation needed. Over 100 % US-Y lower temperatures delay the reaction and only 6.9 % of the original polymer was converted to gaseous products so far. With proceeding reaction, the trend changed. While most gaseous products were produced over 50 % of US-Y until 20 minutes (51 %), a more equally distributed picture was shown overall. After 15 minutes more than 30 % gaseous products was formed in every experiment with US-Y catalyst present. After 20 minutes over US-Y, almost the same gas yield as with 50 % US-Y was achieved (48 %). The gas yields in experiments 5 & 6 after 20 minutes were similar (both 38 %).

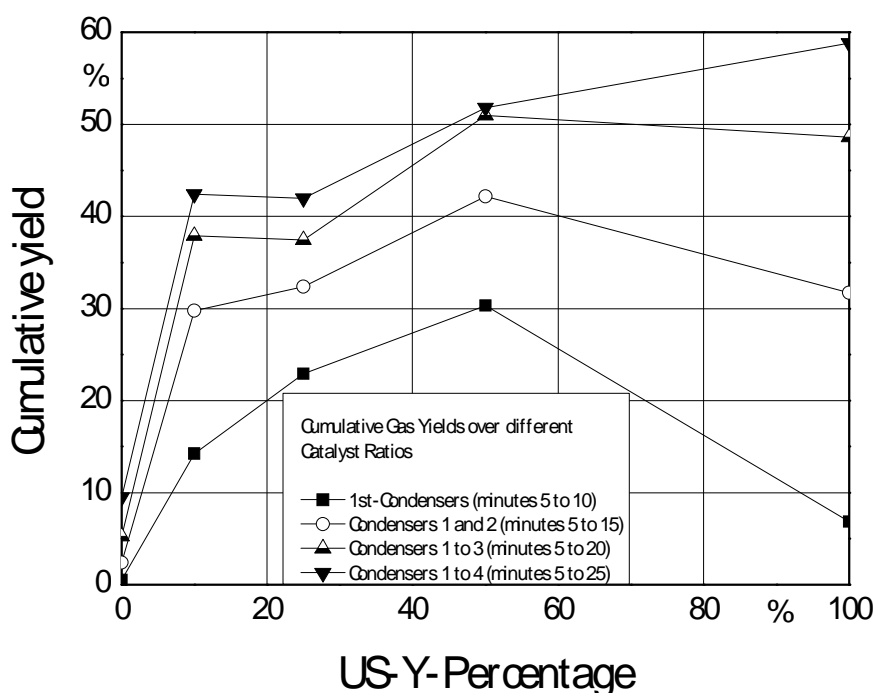
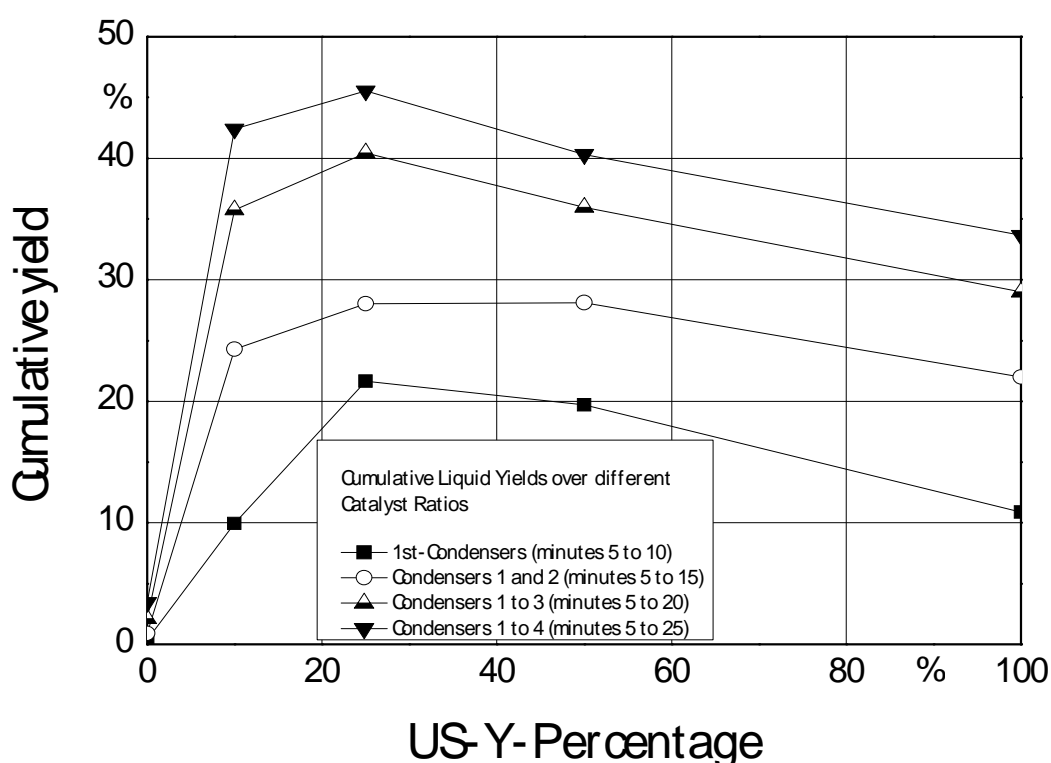


Figure 57: Cumulative Gas Yields vs. US-Y-Acidity divided by different Heating Steps.

The overall gas yield (after 25 minutes) displayed a tendency for more gaseous products to be formed over more acidic catalyst compositions. Without catalyst there were only 9.5 % of the polymers cracked to gaseous products. Over 10 %, with 25 % of US-Y while the yields of gaseous products were almost equal 42 %. When the ratio of the reaction mixture is over 50 % of US-Y, more gaseous products are formed than the lower catalyst ratios (51.8 %). The highest amount of gaseous products resulted from degradation over the catalyst with pure US-Y. This was as consequence of overcracking due to the presence of a higher number of acidic sites.

The curve of the overall liquid yield Figure 59 shows a different behaviour compared to the gas yield (higher yield over higher acidities). The liquid yield reached a maximum of 45.6 % during degradation over 25 % of US-Y. With only small fractions of an active catalyst, the liquid yield already increases steeply until a US-Y acidity of 10 %. After the maximum liquid yield over 25 % of US-Y more added active catalyst has a negative effect onto the liquid yield of the reaction, obviously due to secondary cracking reactions of primary products initially formed.



*Figure 58: Cumulative Liquid Yields vs. US-Y-Acidity divided by different Heating intervals.*

Over 50 % US-Y only 40.3 % liquid yield can be achieved and only 33.67 % over pure US-Y. The liquid yield after 20 minutes shows a similar distribution with liquid yields being about 5 % less than the overall liquid yields. The cumulative yields after 10 and 15 minutes are more influenced by effects of different temperatures in the heating processes. Although having a lower conversion, the degradation over 25 % of US-Y has a higher liquid yield after 10 minutes than degradation over 50 % of US-Y. High temperatures in the beginning of degradation over 25 % of US-Y favour high conversion rates although the relatively low acidity does not cause too much overcracking. This causes the higher liquid yield compared to cracking via a US-Y-percentage of 50 %. After 15 minutes, the liquid yields of both experiments are similar due to a higher conversion to volatile products in the higher acidic experiment from 10 to 15 minutes. Since one goal of catalytic cracking of polymers is to degrade predominantly to liquid products, the reaction over a US-Y-acidity of 25 % seems to be the most recommendable for a potential, industrial process. Although degradation processes with higher acidity achieve higher overall conversions, the acidity with 25 % of US-Y is still high enough to convert almost 90 % of the original polymer. The beneficial effect of using a less acidic catalyst is the less over-cracking it causes. Despite the lower overall conversion using a catalyst of 25 % US-Y-acidity, the highest liquid yield is obtained using these experimental parameters. As a final aspect the liquid yield is observed in dependency of the acidity content of the overall mixture. In Figure 60 the overall liquid yield of all US-Y/3-A experiments is plotted vs. the acidity content. As a parallel curve the liquid yield of degradation experiments of lldPE with 2 different Cracking Catalyst 1 and several polymer-catalyst ratios over similar heating conditions is plotted as well. Due to a synthetic composition especially designed for catalytic cracking of polymer, the liquid yield of Commercial Cracking catalyst 1 and 2 catalyst ranges over the curve of these experiments' results at all acidity contents.

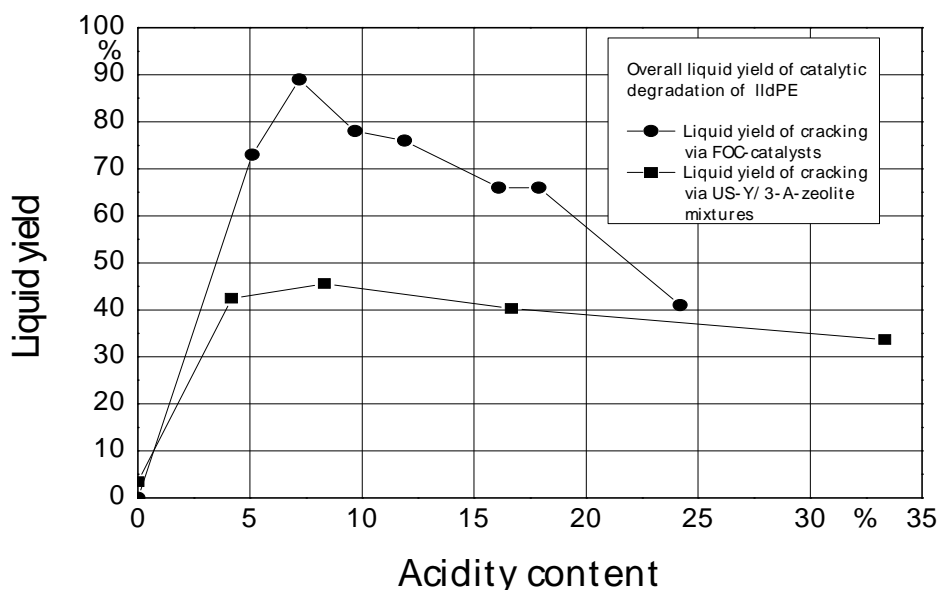


Figure 59: Overall liquid yield vs. Acidity content of catalytic degradations of lldPE via 1<sup>st</sup> Cracking catalysts 1 (according to [Gobin K. et al (2001)]) and 2<sup>nd</sup> US-Y / 3-A zeolite mixtures

Yet, one similarity can be observed between both catalysts. While the Commercial Cracking Catalyst 1-curve has its peak at an acidity content of 7.2 %, the US-Y/3-A-zeolite curve has its highest yield in the same range - at an acidity content of 8.3 %. Apparently, catalytic cracking over zeolite-based catalyst follows a regularity which causes a steeply increasing curve at low acidity contents to a maximum liquid yield in between the range of 5 to 10 % acidity content. From this point on, the liquid yield decreases smoothly with an increasing acidity. Due to the special properties of industrially used Cracking Catalyst 1, the increase and decrease of this curve is more distinctive compared to the shape of the liquid yield from catalytic cracking with the “self-made” zeolite mixture.

### 7.3.2.2 Boiling Point Distributions over Different Acidities

In the previous chapter conversion rates of the experiments and its distribution in liquid and gaseous products were discussed. This chapter focuses on analysing the



liquid products. The goal was to find interdependencies between the acidity of the catalyst used and the molecular range of the liquid products being formed.

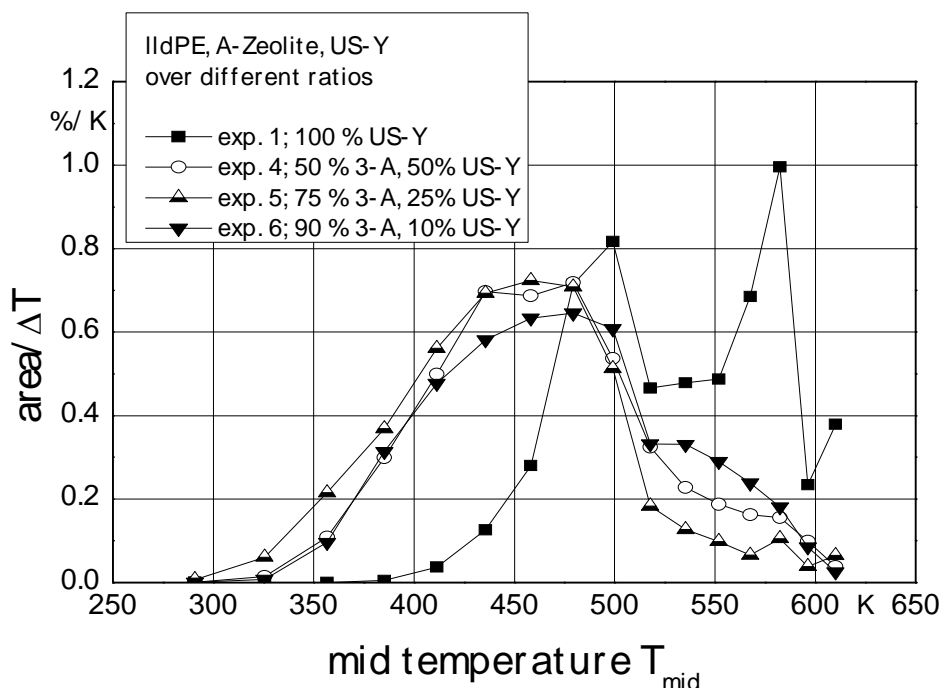


Figure 60: Overall Averaged Boiling Point Distribution: Compositions of the Liquid Yields of Experiments 1, 4, 5, 6. Polymer: lldPE; different ratios of zeolites

Figure 61 shows the overall averaged boiling point distributions of experiments 1, 4, 5 and 6. The heaviest products are resulted from the catalyst combination of experiment 1, which are mostly ranging in the dimension of alkanes having a boiling point temperature above 450 K ( $C_{11}$  to  $C_{17}$ ). As already mentioned, this is a consequence of overcracking due to high acidity in combination with high temperatures. In the other experiments products of boiling point temperatures of 400 K to 500 K ( $C_8$  to  $C_{12}$ ) were mainly produced. Thus the products of experiment with a high acidity were observed to be slightly lighter. A clear relationship concerning lighter products over a lower or higher acidity cannot be observed in this case.

In the following, the results of the single condensers are compared. In order to find an adequate way of displaying the results despite the differing temperature profiles of the experiments, two aggregations have been made:

- In the following charts the 16 product ranges of the boiling point distributions are concentrated to 3 categories of products.
- Instead of comparing boiling point distributions for all four condensers, results are averaged over condensers 1 and 2 as well as over condensers 3 and 4.

During the first two heating intervals (Figure 62) the lightest products were produced over a US-Y acidity of 25 %. Over 50 % and 10 % there was lower but still mentionable amounts of light products produced. Only over 100 % (only the liquids of the 2<sup>nd</sup> condenser could be analysed here) of US-Y there were hardly any products of low molecular weight produced.

Most products formed, no matter the experimental settings, were in the range of hydrocarbons of medium molecular weight. Comparing the settings with one another most medium weighed products were formed over 50 % US-Y acidity, the least over 100 % of US-Y.

Regarding the heavy products the image was diversified: While over 100 % of US-Y a big number of heavy products was formed, the number of heavy products over 50 % and 25 % was relatively low. Over 10 % of US-Y the number of heavy products is still noticeably high. Due to the low acidity, the temperatures in the beginning of this experiment were not high enough to crack as many heavy hydrocarbons like in the experiments with catalyst mixtures of a higher acidity.

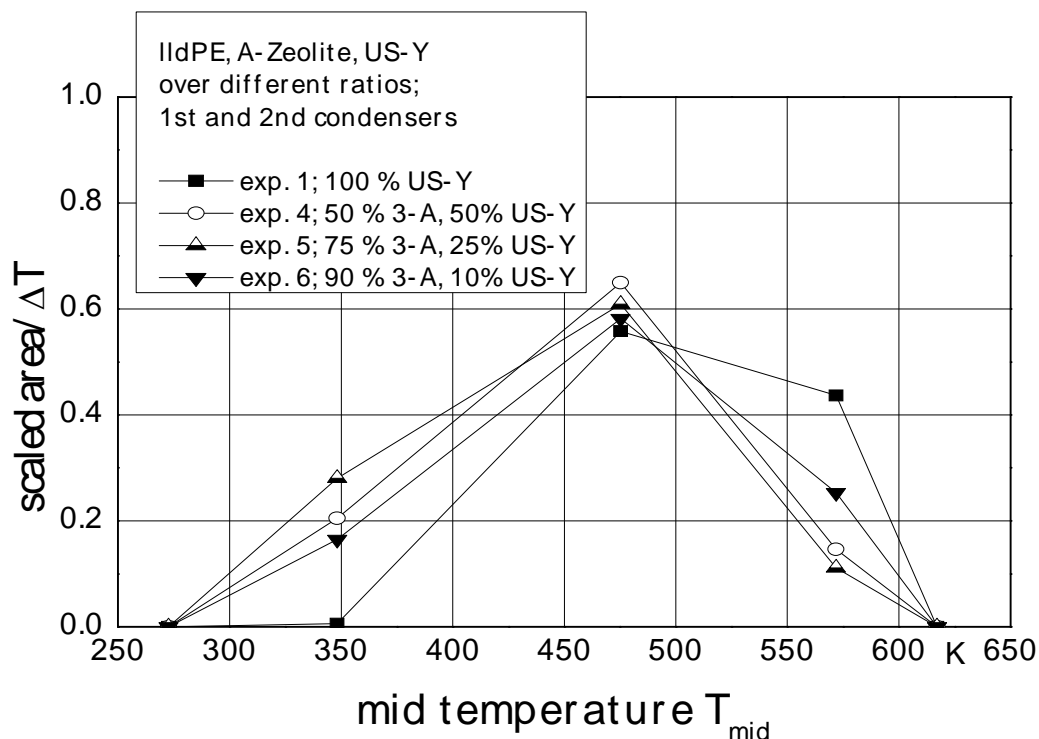


Figure 61: Averaged Boiling Point Distribution of 1<sup>st</sup> and 2<sup>nd</sup> Condensers: Compositions of the Liquid Yields of Experiments 1, 4, 5, 6. Polymer: lldPE; different ratios of zeolite

In Figure 63 the product distribution during the 3<sup>rd</sup> and 4<sup>th</sup> heating steps is plotted. In experiments 4 and 5 the number of light products was now lower than in the initial heating steps, while the number of light products in experiment 6 was almost the same. The number of light products formed over 100 % of US-Y (only the results of condenser 3 were analysed) is still negligible. All experiments involving mixtures with A-zeolite formed most of their products in the range of medium weighed hydrocarbons, whereby most medium weighed products are formed in experiment 5. The amount of medium weighed products in experiments 4 and 6 is only a little lower.

In the range of the heavy products the lowest amount was formed in experiment 5. Due to the already mentioned reasons the amount of heavy products in experiment 6 is smaller now than during the first two heating steps.

The number of heavy hydrocarbons produced in experiment 4 was higher in the second half of the experimental run with higher temperatures. This can be a

consequence of cross-linking effects which are already mentioned in the beginning of this chapter.

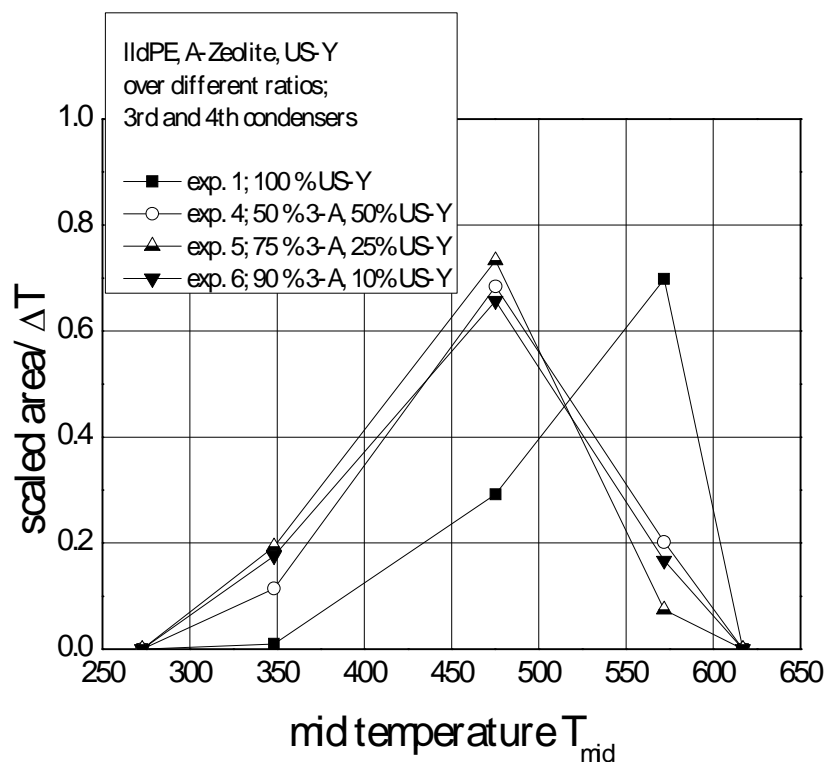


Figure 62: Averaged Boiling Point Distribution of 3<sup>rd</sup> and 4<sup>th</sup> Condensers: Compositions of the Liquid Yields of Experiments 1, 4, 5, 6. Polymer: lldPE; different ratios of zeolites

Cross-linking seemed to be the only rational explanation for the boiling point distribution of experiment 1. This is concluded from the second half of the experiment, where the formed hydrocarbons are even heavier than in the first part of the experiment.

In general, the results of the experiments involving 3A-/US-Y zeolite-mixtures showed an obvious tendency to forming medium-weighted hydrocarbons. This trend was favoured by higher temperatures: While more of the light products were over-cracking to gaseous products, the heavy products were cracked down to medium weighed products. Nevertheless, these effects could only be observed for catalyst mixtures with acidities lower than 50 %, since higher acidities favour undesirable side reactions like

cross-linking. The results of this chapter is summarised in Figure 64. The catalyst and filling 3-A zeolite mixture with 25 % US-Y-acidity has a minimum in heavy products as well as a maximum in light products as well as a maximum in light products. The reaction to medium products was in the same range with the other experiments employing a US-Y/3-A catalyst mixture. The product distributions over 10 % and 50 % US-Y acidity were almost equal.

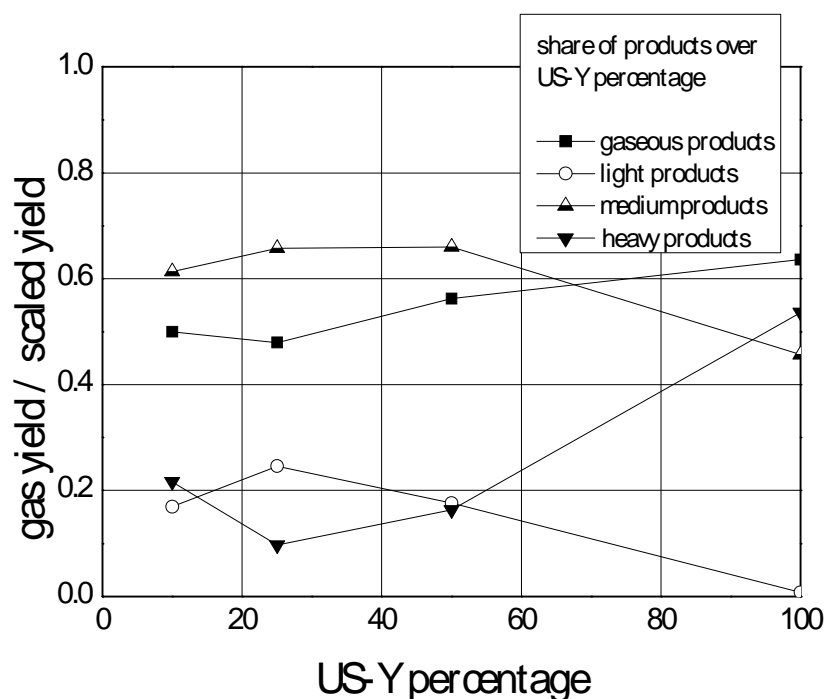


Figure 63: Share of different product ranges and gas yield against US-Y percentage of catalyst for experiments 1,4,5,6.

While the share of light hydrocarbons is the same, the number of heavy hydrocarbons is slightly higher over 10 % US-Y acidity. Thus, the product range is a little more shifted to heavier products over 50 % US-Y acidity. Over pure US-Y the number of heavy products is significantly higher than in all the other experiments with a lower US-Y acidity with almost no light products.

In addition to the product distribution, Figure 64 includes the number of gaseous products formed in relation to the liquid products. This curve has a relevance to the product distribution insofar, that gaseous products result as a consequence of over-cracking of light products and are therefore the next step in the hydrocarbon cracking chain. As it can be seen easily, the curve of the gaseous yield runs anti-parallel to the

curve of light products. The more gaseous products are formed over higher acidities the less light products can be detected during the analysis of the boiling point distribution. Another distinctive result is that the curve of gaseous products shows a parallel run to the curve of heavy products. This directs one to the result that too high acidity levels cause undesirable effects. Firstly, the amount of gaseous products is increasing over higher acidities. Secondly, the number of heavy products is increasing as well (if certain temperatures are passed). These two effects have the consequence that products in the range of medium and light hydrocarbons - these are the products which are most useful in industrial applications - can only be collected by an unsatisfying amount.

## 7.4 Conclusions

The main conclusion of this part of the work is that the dependence of the performance of the system on the acidity of the content was realised by using mixtures of active (US-Y) and inactive catalyst (3-A-zeolite). The result of this chapter of the study confirmed previously identified trends of a maximum in the yield of liquid products formed. At acidity contents near to zero the catalytic activity is very low, resulting in low liquid yield; while at high acidity content the opposite catalytic acidity is found to be true. Although catalytic acidity is higher in the second scenario, over-cracking causes increased gas production and thus resulted in lower liquid yield. However the shape of this dependence is not as clear as in previous studies and thus would require further research.

## Chapter Eight

# Conclusion and Directions for Future Work

---

*This chapter summarises the main findings of this thesis with regards to the experimental results and draws conclusions on them. It also outlines some possible directions for future work.*

## 8.1 Conclusions

### 8.1.1 Role of external sites on degradation

The main conclusion that is drawn from establishing the role of the external sites on catalytic polymer degradation performance is as follows:

The silylation procedure proved to be an effective method for poisoning the external active sites of the catalyst. The level of poisoning that occurred on those active sites was further clarified via utilising a TPD. With the TPD, a reduction in the strength of the signal produced could be attributed to the greater number of silylation cycles applied.

As a result of blocking the external active sites through the process of silylation the degradation of the polymer is significantly reduced depending on the degree of silylation. It could be said that this reduction is proportional to the number of silylation cycles carried out on the catalyst and thus the number of external active sites available. Though it was not possible to completely poison the active sites on the external catalyst surface the research confirmed that the initial catalytic decomposition of the

polymer macromolecules occurs as a result of the external acid sites and the reaction is unable to rely on the internal active sites of the catalyst.

### 8.1.2 Catalytic reusability

The main conclusions drawn from when catalyst reusability was tested through experiments where the used catalyst samples were reused for degradation without regeneration are as follows:

It can be concluded that the deactivation of catalysts in polymer catalytic degradation by the process of coking results in greater liquid product yield and selectivity, a desired result for those searching for valuable products of plastics recycling.

However, the compositions of these products may not fall as easily within a specified range of hydrocarbon weights as can be done with fresh catalysts. The results demonstrate that coking is not necessarily a negative end result on a catalyst as small amounts of deactivation in certain processes lead to the production of varied products which could be of potential value.

### 8.1.3 Effect of Polymer and Catalyst Ratio

The conclusion drawn from varying the polymer and catalyst ratio and thus the acidity of the reaction mixture on the degradation performance is as follows:

There is an enhancement of product yield with increased homogeneity of the reaction mixture for polymer degradation.

The dependence of the performance of the reaction system on the acidity of the content was realised by using mixtures of active (US-Y) and inactive catalyst (3-A-zeolite). This was found to have an optimum trend in liquid yield as a result of a balance in acidity content and over cracking reactions.



## 8.2 General Conclusions

In the past, simplified batch reactors systems may have played a primary role in investigations to do with performance of polymer degradation. But the inconclusive results on yields and selectivity during the study in Chapter 6 of the effects of different final set point temperatures and heating rates expose the limitations of a batch system. The use of a continuous flow reactor would have better suited the experiment for the reasons already mention, and is a closer replication of the current direction of trends industry today caused by the growing demand for recycling of polymer waste as discussed in previous chapters.

The polymer catalytic degradation reaction begins at the external active sites and the manipulation of these sites would create valued products.

## 8.3 Future Work

In this section, some of the limitations of the work are highlighted and recommendations for future work are outlined.

### 8.2.1 Experimental Work

In view of the significant theoretical progress reported in this thesis and other recent literature, perhaps the application of a continuous reaction system that would enable the catalyst to remain at optimum reaction temperature would enhance the efficiency of the system as oppose to the use of batch reactor system.

In addition there are areas in which future work could be pursued and these included the following:

- Industrial polymer recycle utilizes waste polymer raw material containing a mixture of various types of different polymers; an investigation of the performance of the modified catalyst through silylation in comparison to unmodified catalyst could be carried out using other polymers, such as; a mixed stream of plastics thus creating a more accurate simulation of the conditions in an industrial recycling process.

- The study could also be extended to investigate polymer mixtures as well as other common municipal waste such as paper, food and refuse.
- An assessment of the viability of scaling up of the silylation process in an industrial recycling plant could be carried out but this would require a systematic study of the influence of all system and process variables such as polymer and catalytic type and sizes, temperature, inert gas flow rate etc.
- The application of a continuous flow reactor system could aid in dramatically improving the system as it would mean that the polymer-catalytic reaction would be more efficient. As the catalyst would remain consistently remain at optimum reaction temperature. This would also eliminate errors due to irregularity of temperature changes in the heating rates.

## Bibliography

---

- Abbot J., Wojciechowski B.W., Hydrogen Transfer Reactions in the catalytic cracking of paraffins, *Journal of Catalysis*, 107, (1987), p.451.
- Abbot J., Wojciechowski B.W., The Effect of Temperature on the product Distribution and Kinetics of Reactions of Normal-Hexadecane on H-Y Zeolites, *Journal of Catalysis*, 109, (1988), p.274-283.
- Aguado J., Sotelo L., Serrano D.P., Calles J.A., and Escola J.M., Catalytic Conversion of Polyolefin's into Liquid fuels over MCM-41: Comparison with ZSM-5 and Amorphous SiO<sub>2</sub>-Al<sub>2</sub>O<sub>3</sub>, *Energy and Fuels*, 11, (1997), 1225-1231, American Chemical Society.
- Al-Khattaf S., The Influence of Alumina on the Performance of FCC Catalysis during Hydro-treated VGO Catalytic Cracking, *Energy and fuels*, 7, (2002), American Chemical Society.
- Arandes J.M., Abajo I., Lopez-Valerio D., Fernandez I., Azkoiti J.M., Olazar M., and Bilbao J., Transformation of Several Plastic Wastes into Fuels by Catalytic Cracking, *Ind. Eng. Chem. Res.*, 36, (1997), 4523-5429, American Chemical Society.
- Audisio G., Bertini F., Beltrame P.I., Carniti P., Catalytic Degradation of – Polyolefin's Macromolecular Chemie-Macromolecular Symposia 57, (1992), p.191.

- Bagri R., Williams P.T., *Journal of Analytical and Applied Pyrolysis*, 63, (2002), 29-41.
- Barrer R.M., Macleod D.M., *Trans. Faraday Soc.*, 51, (1955), 1290.
- Beltrame P.L., Cartini P., Audisio G., Bertini F., *Polym Degrad. Stabil*, 26, (1989), p.209.
- Bhatia B.S., *Zeolite Catalysts: Principles & Applications*, CRC Press Inc, Boca Raton Florida (1990), p.67
- Bond G.C., *Heterogeneous Catalysis – Principles and Applications*, 2<sup>nd</sup> Edition, Clarendon Press, Oxford, New York, Toronto, Singapore, Hong Kong, Tokyo, Nairobi, Melbourne, Dar- Es –Salaam, Cape Town, Delhi, Bombay, Calcutta, Madras, Karachi, (1987), p.29
- Brillis A. A., Manos G., *Coke Formation during Catalytic Cracking of C8 Aliphatic Hydrocarbons over Ultra-stable Y Zeolite.*, *Ind. Eng. Chem. Res.* 42, (2003), p.2292-2298.
- Brindley G.W., Semple R.E., *Clay Min.* 23 (1977), p.229-237.
- Buchanan J. S., *The chemistry of olefins production by ZSM-5 addition to catalytic cracking units*, *Catalysis Today*, 55, (2000), p.207-212, Elsevier Science Ltd.
- Burch R. (Ed), *Catal. Today* 2, (1988). p.12
- Butt, J.B., E.E. Petersen, *Activation, Deactivation, and Poisoning of Catalysts*, Academic Press, 1988.p.3-9.

- Cheng S., From Layer compounds to catalytic materials, *Catalysis Today*, (1999), p.303-312.
- Chiu S.J., Cheng W.H., Thermal Degradation and Catalytic Cracking of polyethylene terephthalate, *Polymer Degradation and Stability*, 63, (1999), p.407-412.
- Conesa J., Font A., Marcilla R., Garcia A., Pyrolysis of polyethylene in a fluidized reactor, *Energy Fuels*, 8, (1994), p.1238-1346.
- Consultation paper on Recovery and Recycling Targets for Packaging Waste in 2002, published jointly by DEFRA, Scottish Executive and the National Assembly for Wales, (2001), p.11.
- Cumming K.A., Wojciechowski B.W., Hydrogen Transfer, Coke Formation and Catalyst Decay and Their Role in the Chain Mechanism of Catalytic Cracking, *Catal. Rev.-Sci. Eng.*, 38, (1996), p.101.
- Curto D. – Italy, Basar Y. – Turkey, Regulations and Practices of Polymer Recycling in NATO countries A-European Countries in *Frontiers in the Science and Technology of Polymer Recycling*, Edited by Akovali G., Bernado A.C., Liedner J., Utracki A.L., Xanthos M., Kluwer, Academic Publishers in co-operation with NATO Scientific Affairs Division, Series E: Applied Sciences – Vol. 351, (1997).
- De la Puente G., Klocker C., Sedran., Conversion of waste plastics into fuels – Recycling Polyethylene in FCC, *Applied Catalysis B: Environmental* 36, (2002), p.279-285.
- Dietz W.A., Response Factors for Gas Chromatographic Analyses, Esso Research and Engineering Company Analytical Research Division, Linden, New Jersey, J. of G.C. – February, (1967), p.68-71.

- DM Price, Institute of Polymer Thermogravimetric analysis TGA Oxidations Principles of Thermal Analysis and Calorimetry Professor David Dollimore 1927- 2000 Chairman of the TMG **1969** Huddersfield HDJ 3DH UK
- Dwyer J., Rawlence D.J., Fluid Catalytic Cracking: Chemistry, Catalysis Today 18, (**1993**), p.487-500.
- Edgecombe F.H.C. – Ontario, Canada, Regulations and Practices of Polymer Recycling in NATO countries B – Canada and United States of America in Frontiers in the Science and Technology of Polymer Recycling, Edited by Akivali G., Bernado A.C., Liedner J., Utracki A.L., Xanthos M., Kluwer Academic Publishers in co-operation with NATO Scientific Affairs Division, Series @: Applied Sciences – Vol.351, (**1997**).
- European Packaging Waste Management Systems, Report by ARGUS for European Commission, (**2000**), p.29.
- Figueras F., Catal. Rev. Sci. Eng, 30, (**1988**), p.457.
- Fowles I.A., Gas Chromatography, 2<sup>nd</sup> Edition, John Wiley and Sons, Chichester, New York, Brisbane, Toronto, Singapore (**1995**).
- Garforth A.A., Lin H.Y., Sharrat P.N., Dwyer J., Production of Hydrocarbons by catalytic degradation of high density polyethylene in a laboratory fluidized-bed reactor, Applied Catalysis A: General, 169, (**1998**), p.331-342.
- Gates C.B., Catalytic Chemistry, John Wiley, Inc., New York, Chichester, Brisbane, Toronto, Singapore, 9, (**1992**). P.23.
- Gobin K., Manos G., Koumantaropoulos D., One Stage Catalytic cracking of plastic waste on zeolitic catalysts in: Studies in Surface Science and Catalysts Zeolites and Mesoporous Materials at the Dawn of the 21<sup>st</sup> Century.

Proceedings of the 13<sup>th</sup> International Zeolite Conference, Montpellier, France, 8-13 July 2001, vol. 135, (2001) edited by A. Galearneau, F. Di Reinzo and F. Fajula and J. Vedrine, p 323.

- Gobin K, Manos G. Polymer degradation to fuels over microporous catalysts as a novel tertiary plastic recycling method. *Polymer Degradation Stab* (2004); p. 83-273
- Gorte R.J., Perspectives in Catalysis: What do we know about the acidity of sold acids? *Catalysis letters*, 62, (1999), p.1-13.
- Guisnet M., Magnoux P., Coking and Deactivation of Zeolites, Influence of the Pore Structure, *Applied Catalysis*, 54, (1989), p.10.
- Hamid S.H., Mohamed B.A., Ali G.M., Handbook of Polymer Degradation, Research Institute, King Fahd University of Petroleum & Minerals, Dhahran, Saudi Arabia, p.335-344, Marcel Dekker, (1992), New York, Basel, Hong Kong.
- Hardman S., Leng S., Wilson D.C. (BP Chemicals Limited), Polymer Cracking, Eur Patent Appl. 567292, 91993).
- Herbst H., Hoffmann K., Pfaendner R. – Germany and Zweifel H. – Switzerland, Upgrading of Recycles – The Solution for High Value Applications: Restabilization and Repair in Fronitiers in the Science and Technology of Polymer Recycling, Edited by Akovali G., Bernado A.C., Liedner J., Utracki A.L., Xanthos M., Kluwer, Academic Publishers in co-operation with NATO Scientific Affairs Division, Series E: Applied Sciences – Vo.351 (1997).
- Igarashi M., et al., Pyrolysis of municipal solid waste in a fluidized reactor, *J. Energy Resour. Technol.*, 106, (1984), p.377-382.

- Ishihara Y., Nanbu H., Ikemura T., Takesue T., Fuel, 69, (1990), p.978.
- Ivanov, D.P., V.I. Sobolev, G.I.Panov, Deactivation by coking and regeneration of zeolite catalysts for benzene-to phenol oxidation, Applied Catalysis A: General, 241 (2003) p.113.
- Kagayama M., Thermal conversion of solid wastes and biomass, ACS Symp. Ser., 130, (1980), p.527-531.
- Kaloidas V., Koufapanos C.A., Gangas N.H., Papayannakos N., Scale Up studies for the preparation of pillared clays at 1kg per batch level, Microporous Materials 5, (1995), p.97.
- Kaminsky W., Olefins from polyolefin's and mixed plastics by pyrolysis, J. Anal. Appl. Pyrolysis., 32, (1995), p.19-27.
- Kaminsky W., Chemical recycling of mixed plastics by pyrolysis, Adv. Polym. Technol., 14, (1995), p.337-344.
- Kaminsky W., Polymerisation Catalysis, Catalysis Today, 62, (2000), p.23-34.
- Kikuch E., Matsuda T., Ueda J., Morita Y., Appl. Catal., 16, (1985), p.401.
- Kung H.H., Williams B.A., Babitz S.M., Miller J.T., Snurr R.Q., Towards understanding the enhanced cracking activity of steamed Y zeolites, Catalysis Today, 52, (1999), p.91-98.
- Lercher J. A., On the enhanced selectivity of HZSM-5 modified by chemical liquid deposition. Vol.22, Nos 1-2, January (2003).
- Liedner J., Introduction to Recycling, Ontario-Canada in Frontiers in the Science and Technology of Polymer Recycling, Edited by Akovali G., bernado A.C., Liedner J., Utracki A.L., Xanthos M., Kluwer, Academic Publishers in



co-operation with NATO Scientific Affairs Division, Series E: Applied Sciences – Vol. 351, (1997).

- Lourvanij K., Rorrer G.L., Appl. Catal., 109, (1994), p.147.
- Lourvanij K., Rorrer G.L., Ind. Eng. Chem. Res., 32, (1993), p.19.
- Magee J.S., Blazek J.J., ACS Monogr. 171, Zeolite Chem. Catl., (J.A Rabo, Ed.), p.615 (1976)
- Magee J.S., Letsch W.S., In Fluid catalytic Cracking III, Materials and Processes, Occelli M.L., O'Connor P., Eds., American Chemical Society, Washington DC, (1994).
- Manos G., Garforth A., Vertsonis K., Lin H-Y., Dwyer J., Sharratt P., Catalytic Degradation of High Density Polyethylene to Hydrocarbon Fuels on an Ultrastable Y Zeolite-Studies in a Semi-batch Reactor: Influence of Temperature and Heating Rate, AIChE spring National Meeting, (1996), paper Nr: 56b, N. Orleans.
- Manos G., Vertsonis K., Garforth A., Dwyer J., (1997), in: Proceedings of the 1997 Jubilee Research Event, ICHemE, p.1193.
- Manos G., Yusof I., Catalytic Degradation of Polymer Waste on Acid Catalysts with Bimodal Pore Size Distribution, (1998), ICHemE research Event.
- Manos G., Garforth A., dwyer J., Catalytic Degradation of High Density Polyethylene over different Zeolitic structures, American Chemical Society.Ind. Eng. Chem. Res., 39, (2000a), p.1198-1202.
- Manos G., Garforth A., Dwyer J., Catalytic Degradation of High Density Polyethylene on an Ultrastable Y Zeolite. Nature of Initial Polymer Reactions.

Pattern of formation of Gas and Liquid Products, Temperature Effects, *Ind. Eng. Chem. Res.*, 40, (2001), p.485-489.

- Matsuda T., Matsukata M., Kikuchi E., Morita Y., *Appl. Catal.*, 21, (1986), p.297.
- Matsuda T., Asanuma M., Kikuchi E., *Appl. Catal.*, 38, (1988), p.289.
- Menges G. – Aachen, PVC – Recycling with Chlorine Recovery in *Frontiers in the Science and Technology of Polymer Recycling*, Edited by Akovali G., Bernado A.C., Liedner J., Utracki A.L., Xanthos M., Kluwer, Academic Publishers in co-operation with NATO Scientific Affairs Division, Series E: Applied Sciences – Vol. 351, (1997).
- Ming-Yuan He, Zhonghui L., Enze M., Acidic and hydrocarbon catalytic properties of pillared clay, *Catalysis Today*, 2, (1988), p.321.
- Mokaya R., Jones W., Pillared Clays and Pillared Acid-Activated Clays: A Comparative Study of Physical, Acidic, and Catalytic Properties, *Journal of Catalysis*, 153, (1995), p.76-85.
- Mordi R.C., Fields R., Dwyer J., *J. Chem. Soc. Chem. Commun.* (1992), p.374.
- Morfis S., Philippopoulos C., Papayannakos N., Application of Al-pillared clay minerals as catalytic carriers for the reaction NO with CO, *Applied Clay Science*, 13, (1998), p.203-212.
- Occelli M.L., *Catal. Today* 2, (1998), p.339.
- Occelli M.L., Innes R.A., Hwu F.S.S., Hightower J.W., *Appl. Catal.*, 14, (1985), Ueno A., Namiki Y., Tanifuji S., Katoh H., Sunazyka H., Nakayama R., Kuroyanagi T., Acid Properties of Silica-Alumina Catalysts and Catalytic Degradation of Polyethylene, *Ind. Eng. Chem. Res.*, 32, (1993), p.3112.

- Park D.W., Hwang E.Y., Kim J.R., Choi Y.A., Woo H.C., Polym. Degrad. Stabil. 65, (1999), p.193.
- Paszun D., Szychaj T., Chemical Recycling of Polyethylene Terephthalate, Ind. Eng. Chem. Res., 36, (1997), p.1373.
- Paweewan, B., P.J. Barrie, L.F. Gladden, Coking and deactivation during n-hexane cracking in ultrastable zeolite Y, Applied Catalysis A: General, 185 (1999) p.259.
- Paweewan, B., P.J. Barrie, L.F. Gladden, Coking during ethane a conversion on ultrastable zeolite Y, Applied Catalysis A: General, 167 (1998) p.353.
- Plastic Waste Management Institute, Plastic Wastes: Disposal & Recycling, Past, Present, & Future in Japan, 88, (1991).
- Sakata Y., Uddin Md. A., Muto A., Koizumi K., Zaki, M.N., Murata K., Kaji M., Thermal and Catalytic Degradation of Municipal Waste Plastics into Fuel Oil, Polymer Recycling, Vol. 2, No. 4, (1996), p.309-315.
- Serrano, D.P., Aguado J. M., Orsi R., Feedstock recycling of agriculture plastic film waste by catalytic cracking, Applied Catalysis B: Environmental, 49 (2004) p.257.
- Uguina, M.A., D.P. Serrano, R. Van Grieken, S. Venes, Adsorption, acid and catalytic changes induce in ZSM-5 by coking with different hydrocarbons, Applied Catalysis A: General, 99 (1993) p.97
- Watson, J.S., Separation Methods for Waste and Environmental Applications, Marcel-Dekker, (1999).

- Weber, R.W., K.P. Moller, C.T. O'Connor, The chemical vapour and liquid deposition of tetraethoxysilane on ZSM-5, mordenite and beta, *Microporous and Mesoporous Materials* 35 – 36 (2000) p.533 – 543.
- Williams, B.A., S.M. Babitz, J.T. Miller, R.Q. Snurr, H.H. Kung, The roles of acid strength and pore diffusion in the enhanced cracking activity of steamed Y zeolites, *Applied Catalysis A: General*, 177 (1999) p.161.
- Williams, P.T., *Waste Treatment and Disposal*, Wiley, 1998.p.39-56.
- Xanthos M. – Newark, USA and Leidner, J.- Ontario,Canada, Thermolytic Process in “Frontiers in the Science and Technology of Polymer Recycling”, Edited by Akovali G.,Bernado A.C., Liedner J., Utracki A. L., *Applied Sciences – Vol.351, (1997)*.
- Zahavich A. T. P., Vlachopoulos J. – Ontario, Canada, Reprocessing of Polyolefins – Changes in Rheology and Reprocessing Case Studies, in “Frontiers in the Science and Technology of Polymer Recycling”,Edited by Akovali G., Bernado A.C., Liedner J., Utracki A.L., Xanthos M., Kluwer, Academic Publishers in cooperation with NATO Scientific Affairs Division, Series E: *Applied Sciences – Vol.351, (1997)*.

## Nomenclature

---

Symbol	Explanation	Unit
A	area underneath curve	%
$\dot{A}$	critical diameter	[m]
b	adsorption coefficient	$m^3/mol$
c	concentration	$mol/l$
C	constant (see equation (2.16))	[-]
E	power	$J/s = W$
hR	heating rate	$K/min$
k	reaction velocity constant	$l/s$
L	length of the reactor	$m$
LF	liquid weight fraction	[-]
m	mass	$kg$
q	heat flux density	$W/m^2$
r	radial coordinate	$m$
$\Delta d$	desorption change	[-]
$\dot{r}_v$	reaction flux density	$mol/s m^3$
R	universal gas constant	$J/mol K$
S	selectivity	[-]
t	time	$s$
T	temperature	$K$
u	generalised linear velocity	$m/s$
v	main linear velocity	$m/s$
V	flow rate	$m^3/s$
x	generalised linear coordinate	$m$

## APPENDIX

**Table: A2. 1 Cumulative yield for 100% US-Y**

cumulative yield for 100% US-Y <b>conversion</b>				cumulative yield for 100% US-Y <b>Liquid yield</b>				cumulative yield for 100% US-Y <b>Gas yield</b>			
time	1st Run	2nd Run	3rd Run	time	1st Run	2nd Run	3rd Run	time	1st Run	2nd Run	3rd Run
0	0	0	0	0	0	0	0	0	0	0	0
5	0	0	0	5	0	0	0	5	0	0	0
10	0.38	0.17	0	10	0.18	0.05	0	10	0.2	0.1	0
15	0.79	0.3	0.2	15	0.21	0.12	0.15	15	0.58	0.19	0.09
20	0.92	0.4	0.4	20	0.27	0.2	0.2	20	0.69	0.2	0.22
25	0.98	0.92	0.91	25	0.29	0.3	0.31	25	0.71	0.59	0.55

**Table: A2. 2 Cumulative yield for Cracking Catalyst 1**

cumulative yield for <b>Conversion</b>				cumulative yield for FOC 20% US-Y <b>Liquid yield</b>				cumulative yield for FOC 20% US-Y <b>Gas yield</b>			
time	1st Run	2nd Run	3rd Run	time	1st Run	2nd Run	3rd Run	time	1st Run	2nd Run	3rd Run
0	0	0	0	0	0	0	0	0	0	0	0
5	0	0	0	5	0	0	0	5	0	0	0
10	0.3	0.01	0.1	10	0.2	0.02	0.04	10	0.1	0.01	0.02
15	0.79	0.6	0.57	15	0.52	0.4	0.38	15	0.28	0.2	0.15
20	0.92	0.96	0.96	20	0.58	0.61	0.69	20	0.38	0.35	0.28
25	0.99	0.99	0.98	25	0.6	0.61	0.7	25	0.4	0.39	0.32

cumulative yield for FOC 20% US-Y <b>fourth run</b>			
time	conversion	liquid	gas
0	0	0	0
5	0	0	0
10	0.09	0	0.1
15	0.75	0.59	0.2
20	0.96	0.69	0.3
25	0.99	0.7	0.34

**Table: A2. 3. Cumulative yield for Cracking Catalyst 2**

cumulative yield for OVIS 40% US-Y <b>conversion</b>				cumulative yield for OVIS 40% US-Y <b>Liquid yield</b>				cumulative yield for OVIS 40% US-Y <b>Gas yield</b>			
time	1st Run	2nd Run	3rd Run	time	1st Run	2nd Run	3rd Run	time	1st Run	2nd Run	3rd Run
0	0	0	0	0	0	0	0	0	0	0	0
5	0	0	0	5	0	0	0	5	0	0	0
10	0.5	0.11	0.18	10	0.2	0.1	0.04	10	0.31	0.03	0.14
15	0.91	0.81	0.9	15	0.54	0.58	0.63	15	0.39	0.28	0.27
20	0.95	0.95	0.98	20	0.57	0.6	0.68	20	0.41	0.36	0.3
25	0.98	0.99	0.99	25	0.57	0.6	0.69	25	0.42	0.4	0.33

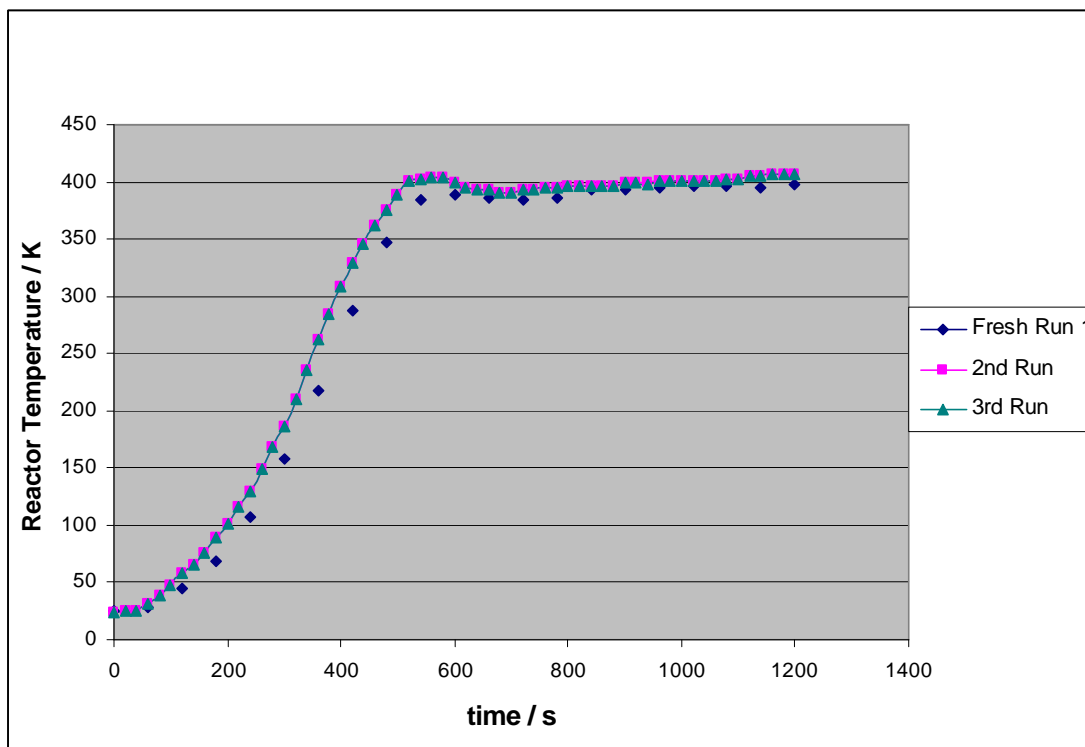
cumulative yield for OVIS 40% US-Y <b>fourth run</b>			
time	conversion	liquid	gas
0	0	0	0
5	0	0	0
10	0.08	0.05	0.05
15	0.76	0.59	0.2
20	0.96	0.62	0.35
25	0.99	0.62	0.37

**Table: A 2. 4 Cumulative yield for HMFI-90 (HZSM-5)**

cumulative yield for HMFI-90 (HZSM-5) <b>conversion</b>				cumulative yield for HMFI-90 (HZSM-5) <b>Liquid yield</b>				cumulative yield for HMFI-90 (HZSM-5) <b>Gas yield</b>			
time	1st Run	2nd Run	3rd Run	time	1st Run	2nd Run	3rd Run	time	1st Run	2nd Run	3rd Run
0	0	0	0	0	0	0	0	0	0	0	0
5	0	0	0	5	0	0	0	5	0	0	0
10	0.4	0.6	0.2	10	0.06	0.09	0.06	10	0.36	0.53	0.18
15	0.85	0.84	0.74	15	0.1	0.16	0.19	15	0.73	0.69	0.55
20	0.97	0.95	0.92	20	0.12	0.15	0.21	20	0.88	0.8	0.72
25	0.99	0.99	0.98	25	0.12	0.15	0.21	25	0.9	0.85	0.79

cumulative yield for HMFI-90 (HZSM-5) <b>fourth run</b>			
time	conversion	liquid	gas
0	0	0	0
5	0	0	0
10	0.35	0.09	0.28
15	0.83	0.2	0.61
20	0.98	0.21	0.76
25	0.99	0.21	0.8



A3.1. Reactor Temperature vs. time profile for 100% US-Y catalyst experiments